

POLITECNICO DI TORINO

Dipartimento di Ingegneria Meccanica e Aerospaziale

**Corso di Laurea Magistrale
in Ingegneria Biomedica – Classe LM-21 (DM270)**

Tesi di Laurea Magistrale

**Lab-on-a-Disc platform for cell
culture in flow and drug testing**



Relatore

Prof. Danilo Demarchi

Candidato

Giulia Zappalà

Dicembre 2020

*To my family,
my shining light in the darkest moments*

Preface

This Master thesis project was carried out at the Center of Intelligent Drug Delivery and Sensing Using Microcontainers and Nanomechanics (IDUN), Department of Health Technology at the Technical University of Denmark (DTU).

The project was supervised by Professor Danilo Demarchi (Politecnico di Torino), and Postdoc Laura Seriola (DTU). Part of the experiments were co-supervised by Senior Researcher Kinga Zór and PhD. Student Lina Gruzinskyte (DTU).



VILLUM FONDEN



Acknowledgements

First of all, I would like to acknowledge Professor Danilo Demarchi for giving me the opportunity to work on this amazing project.

My deepest gratitude goes to Postdoc Laura Seriola for her support and her constant encouragement during these past nine months. She taught me everything I know, and she was a role model for me in every way. She has been more than a supervisor, she has been my mentor and I could not have wished for a better guidance.

I would like to thank Senior Researcher Kinga Zór and PhD. Student Lina Gruzinskyte for trusting me and giving me the chance of improving myself in different fields.

Thanks to the IDUN group for welcoming me. A special thanks goes to the student office, Carl, Chrysillis, Carmen and Noline, for all the laughs and the good moments we have shared in and outside the office.

A heartfelt thanks goes to Carl. Thank you for being so kind and for supporting me during difficult months. You made me see Copenhagen in a new light through your eyes and I discovered a whole new enchanting world with you.

To my international family, Aida, Marta, Patri, Arnau, Krisz, Ximo, Ivan, Bence, Jose, Janak, Jitka, Dani, Richard, Marek, thank you for all the amazing adventures we lived, from going to the Deer Park at sunset to have a bath in the icy waters of Skodsborg. This period would not have been the same without you. A special thought goes to Alex, thank you for all the wonderful moments we have shared and for everything you gave me.

Un grazie di cuore va a tutti i miei amici, per avermi fatto sempre sentire la loro presenza a chilometri di distanza. Alle mie più che colleghe Letizia, Irene e Sara, per tutte le gioie e i dolori condivisi durante questi anni. Siete state fondamentali. A

Domenico, Michele, Mattia e Fabio per aver reso le lezioni più divertenti e per tutti i bei momenti vissuti in giro per l'Italia. Grazie anche a Giuliana e Alberto, con cui ho condiviso l'ultima parte del mio percorso e grazie ai quali sono arrivata a questo punto. Un sentito grazie alla famiglia del Secondo Piano del Collegio Einaudi, ai vecchi e ai nuovi, perché senza di voi questi anni universitari non sarebbero stati gli stessi. Un ringraziamento speciale va a Martina, mia vicina di camera e compagna di viaggi, ma soprattutto una delle persone che ammiro di più. Ne abbiamo passate tante insieme, ma sono certa che il meglio debba ancora venire.

Ringrazio gli amici di una vita, Bonti, Diego, Federica, Martina, perché so di poter sempre contare su di voi, a prescindere dalla distanza. Ringrazio anche Francesco, senza il quale forse non avrei mai avuto il coraggio di andare a Torino.

Un grazie alle mie cugine Ginni, Tiziana, Federica e Giorgia, per tutto l'affetto che ci lega. Grazie soprattutto a Francesca, con cui da sempre condivido tutto.

Il più grande grazie va alla mia stupenda famiglia, a cui devo tutto. Grazie a mia zia Ada e mio zio Guido per essere stati il mio punto di riferimento a Torino e per non avermi fatto sentire la mancanza del calore familiare. Grazie a mia zia Teta, per tutto l'amore che mi dimostra ogni giorno con i suoi piccoli grandi gesti. Grazie a mio cugino Daniele per essere sempre stato un fratello maggiore attento e affettuoso.

Grazie soprattutto a mia sorella Martina, la mia roccia. Sei il mio modello di forza, sei la mia persona e non importa quante migliaia di chilometri ci separino, so che potrò sempre contare su di te.

Grazie dal profondo del mio cuore a mia madre e a mio padre, siete e sarete sempre il mio porto sicuro. Vi ringrazio per tutto l'amore datomi ogni giorno, per aver sempre creduto in me e per avermi sostenuta quando io stessa pensavo di non farcela.

Infine, vorrei ringraziare mia nonna. Sei sempre accanto a me.

Abstract

The process of developing and bringing into market new drugs represents one of the fundamental activities which improves human health and quality of life. The preclinical phase of the Drug Development Process is considered a crucial step for the discovery of new potential pharmaceutical compounds. In fact, at this stage, screening of new molecules and essential pre-tests are carried out using *in vitro* models. In this view, *in vitro* systems are valuable tools to understand cell mechanisms and the effects of drugs on a culture.

A wide range of *in vitro* models have been created during the years, where the majority are based on static 2D cultures. Although traditional static cultures are still the most used in scientific research due to their simplicity, the need for better mimicking certain aspects of the *in vivo* microenvironment has led to the development of several new systems based on perfusion. Perfusion culture systems provide a continuous flow of nutrients and oxygen over the culture, which better reproduces the mechanisms found in a living organism. Among these systems, a key role is played by microfluidic devices, the so-called Lab-on-a-Chip (LoC). LoCs allow the integration of several operational units and lab protocols on a single chip where cells are grown using dynamic conditions over time. Despite their advantages, these systems still rely on expensive and complex pressure sources (e.g. pumps and tubing) and electronics.

Centrifugal microfluidics, the so-called Lab-on-a-Disc (LoD), is a possible solution to these problems. Various operational units (e.g. valving and mixing) can be implemented on LoD platforms, allowing to reduce size, complexity, volumes required and costs of these systems. These *in vitro* systems are mainly used for sample pre-treatment, analysis and detection of a specific compound, biochemical markers, etc. While Lab-on-a-Disc platforms are largely used for biological assays (e.g. immune-assays), they are rarely employed for cell-based assays.

In this thesis, a novel application of centrifugal microfluidics is presented. A compact and robust Lab-on-a-Disc device is used for long-term cell culture (up to 6 days) and drug testing. In particular, the LoD was used for culturing bacterial and mammal cells in two different applications. Once the cells were grown on the platform, different antibiotic treatments were tested on bacterial biofilm and cytotoxicity assays were carried out on mammalian cells where real time detection was also possible to achieve. The LoD platform provided relevant and reproducible results in both applications, proving to be a reliable tool.

The results obtained make this device highly relevant in the initial phase of drug screening, representing a possible alternative to traditional cell culture systems and *in vitro* models.

Contents

List of abbreviations	6
1. Introduction.....	9
1.1 Drug development	9
1.2 <i>In vitro</i> systems for cell culture.....	11
1.2.1 <i>In vitro</i> cell culture: 2D methods	12
1.2.2 <i>In vitro</i> cell culture: 3D static methods.....	13
1.2.3 <i>In vitro</i> cell culture: perfusion methods.....	15
1.3 Goal of the thesis: Lab-on-a-Disc platform for cell culture in flow and drug testing	20
2. Application 1: bacterial biofilm growth and test of antibiotic tolerance	22
2.1 Bacterial biofilms.....	22
2.2 Antibiotic tolerance in bacterial biofilms.....	25
2.3 <i>Pseudomonas aeruginosa</i> : a case of study.....	28
2.4 Bacterial Culture on disc (BCoD) microfluidic platform	30
3. Application 2: mammalian cell culture and cytotoxicity assays.....	32
3.1 Mammalian cells: Caco-2 and HeLa cells.....	32
3.1.1 Caco-2 cells	32
3.1.2 HeLa cells.....	34
3.2 Cytotoxicity assays.....	35
3.3 Mammalian Cell culture on disc (CoD) microfluidic platform.....	38
4. Centrifugal microfluidics: Bacterial Culture on Disc and Mammalian Cell Culture on Disc.....	40
4.1 Bacterial-Culture-on-Disc: theory and design	44
4.1.1 Mammalian-Cell-culture-on-Disc: design optimization	49

4.2 Bacterial-Culture-on-Disc: fabrication process.....	50
4.2.1 Mammalian-Cell-culture-on-Disc: fabrication optimization	54
4.3 Flow and shear stress characterization	55
4.3.1 BCoD and CoD flow characterization	55
4.3.2 BCoD and CoD shear stress characterization.....	57
4.4 BCoD and CoD sterilization process	58
4.5 Cell inoculation and growth	59
4.5.1 BCoD cell inoculation and growth	59
4.5.2 CoD cell inoculation and growth.....	60
4.6 BCoD and CoD treatment.....	62
4.6.1 BCoD antibiotic treatment	62
4.6.1 CoD doxorubicin treatment	63
4.7 Optical monitoring and data analysis.....	64
4.7.1 Bacterial biofilm biomass and viability monitoring and data analysis	64
4.7.2 Mammalian cells growth and viability monitoring and data analysis.....	67
5. Results and discussion	72
5.1 Bacterial Culture on Disc (BCoD) results	72
5.1.1 PAO1 biofilm development and growth	72
5.1.2 PAO1 biofilm treatments	73
5.2 Cell Culture on Disc (CoD) results.....	76
5.2.1 Long-term culture Caco-2 cells.....	76
5.2.2 HeLa cell cultures and cytotoxicity assays	78
6. Conclusions and future perspectives	85
References	87

List of abbreviations

ASM	Artificial sputum medium
ATP	Adenosine 5'-triphosphate
BAT	Biofilm antibiotic tolerance
BCoD	Bacterial Culture on Disc
CAD	Computer-aided design
CFD	Computational fluid dynamics
CHI	Chitosan
CIP	Ciprofloxacin
CLSM	Confocal laser scanning microscopy
CMOS	Complementary Metal-Oxide-Semiconductor
CNC	Computer numerical control
COC	Cyclic olefin copolymer
CoD	Cell on Disc
DMEM	Dulbecco's Modified Eagle Medium
DNA	Deoxyribonucleic acid
DOX	Doxorubicin
ECM	Extracellular matrix
e-DNA	Extracellular DNA
EMA	European Medicines Agency
EPS	Extracellular polymeric substance
ESC	Embryonic stem cell
FBS	Fetal bovine serum
FDA	Food and Drug Administration
GFP	Green fluorescent protein
GHz	Giga Hertz

GLP	Good Laboratory Practice
IND	Investigational New Drug
LB	Luria Bertani
LED	Light Emitting Diode
LoC	Lab-on-a-Chip
LoD	Lab-on-a-Disc
M	Molar concentration
MC	Microcontainers
MIC	Minimum inhibitory concentration
MoD	Microscope on disc
MSC	Mesenchymal stem cell
MTT	3-[4,5-dimethylthiazol-2-yl]-2,5 diphenyl tetrazolium bromide
NAC	N-acetylcysteine
NaOH	Sodium hydroxide
NDA	New Drug Application
NEAA	Non-essential amino acids
OoC	Organ-on-Chip
<i>P. aeruginosa</i>	<i>Pseudomonas aeruginosa</i>
PC	Polycarbonate
PDMS	Poly(dimethyl siloxane)
PDT	Population doubling time
PMMA	Poly(methyl methacrylate)
PP	Polypropylene
PS	Polystyrene
PSA	Pressure sensitive double adhesive tape
RSD	Relative standard deviation
SRB	Sulforhodamine B
WHO	World Health Organization

Δp_c	Centrifugal pressure
Δp_{cap}	Capillary pressure
ΔQ	Flow rate
ΔV	Volume
Δt	Time interval
$^{\circ}\text{C}$	Degree Celsius
μg	Microgram
μl	Microliter
μm	Micrometer
μM	Micromolar
cm	Centimetre
h	Hour
Hz	Hertz
mg	Milligram
min	Minute
ml	Milliliter
mM	Millimolar
rpm	Revolutions per minute
v/v	Volume per volume
A	Area of contact
F	Force
g	Acceleration due to gravity
h	Height of the column of liquid
p	Average pressure
r	Radial point
κ	Meniscus shape

1. Introduction

1.1 Drug development

Over the past few decades, the development of new drugs has become one of the essential activities capable to improve the human quality of life [1]. Several drugs, such as anticancer, autoimmune, antibacterial drugs and many others have been released into the pharmaceutical market [2]. The drug development process is the result of a synergic work within academic institutions, pharmaceutical industries and government agencies driven by medical needs and in certain cases also by business opportunities [3]. It consists of different stages (Figure 1.1): discovery of new compounds, preclinical research, clinical trials and a final review where all the findings are assessed and analysed by regulatory agencies [4].

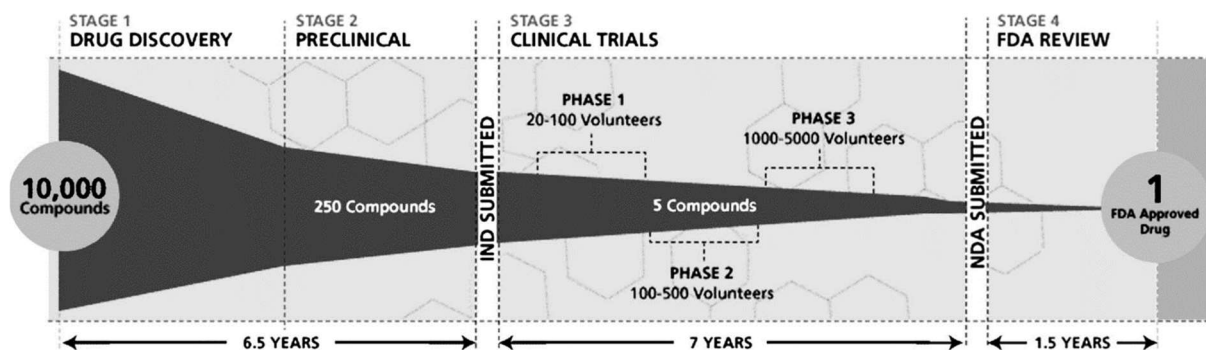


Figure 1.1 Drug development stages [3]

The first stage, the drug discovery phase, involves the identification and validation of new compounds. In here, thousands of compounds are screened to identify the ones that will eventually reach the market [3].

When the promising drug candidates are chosen, safety tests are conducted to study the drug's pharmacokinetics, such as drug absorption, distribution, metabolism and

excretion [5]. This phase can have an average duration of 3 years and it is followed by the second stage of preclinical research, which usually takes from 2 to 5 years [6].

In the preclinical phase, experiments are first conducted *in vitro*, using cellular models, and then *in vivo*, in animal models. During these experiments, researchers examine the drug's mechanism of action and its effects on the organism [3]. Drug toxicity and drug interaction with other treatments are the main focus at this stage [5]. These studies must follow the Good Laboratory Practice (GLP), defined by the Food and Drug Administration's (FDA) guidelines [7].

Once the testing has provided good results, all data are collected and included in an Investigational New Drug application (IND), which is submitted to FDA in order to start the trials in humans. Clinical trials are structured in three phases [3], [4], [8]:

- Phase I: trials are conducted in a small sample of volunteers (20-100) to prove the drug's safety and to give information about its metabolism and its pharmacokinetics. The results are fundamental to design Phase II protocol [8].
- Phase II: studies are carried out to assess the efficacy and the side effects of the treatment in patients with a certain disease. Phase II trials involve several hundred people for a period of treatment which has a duration of several months [3].
- Phase III: adverse reactions are monitored in larger trials that can involve thousands of patients and treatments are carried out for months or years. Participants are randomly divided in two groups: an investigational group, which receives the drug, and a control group, which receives a placebo or a standard treatment. Here, studies must prove the efficacy and the safety of the new drug in comparison with other standard treatments [4].

All the results and the information gathered during clinical trials are submitted to the regulatory agency through an application. In the United States, the New Drug Application (NDA) has to be approved by the FDA in order to obtain the authorization

to enter into the drug market. In the European Union, instead, the drug approval process can follow four different pathways depending on the type of drug: a centralized process (mandatory for some classes of drugs, such as drugs for oncology, diabetes, neurodegenerative disorders, autoimmune disease and viral diseases) controlled by the European Medicines Agency (EMA), a national process, a mutual recognition process that allows the manufacturer to obtain the drug release approval not only in its state but also in others, and a decentralized process for simultaneous approval in different states [9].

After the release into the market, the drug is still subjected to a postmarketing surveillance to report undesired effects and adverse events, in order to monitor how the product evolves over the months and years [10].

The entire development process can take around 12 years and can have an average cost of 1 billion USD [11]. It is a long and complex process, where the early preclinical stages are crucial since they increase the efficiency and effectiveness of the process [12]. The use of new *in vitro* technologies in preclinical testing can increase the success rate of drug development process. In fact, they enable cell and tissue physiology and pathophysiology investigation [13]. *In vitro* models are thus valuable tools to understand cells behaviour and the effects of potential new compounds on them [14]. In particular, *in vitro* systems recreating a disease state can give significant information about the drug's efficacy and can predict *in vivo* results [15]. Moreover, cell-based models are convenient because of their simplicity, high-throughput screening and predictive abilities, cost-effectiveness relationship and their lack of ethical implications [16].

1.2 *In vitro* systems for cell culture

In vitro cell cultures are essential devices to comprehend biophysical and biomolecular mechanisms of cells, such as differentiation, migration and growth [17]. The meaning

of the term *in vitro* is literally “in glass” and refers to a process conducted in a test tube or a culture dish outside a living organism [18]. These systems are widely used in biomedical research to simplify the complexity of an organisms and thus enable faster study developments [19]. Moreover, they are more cost-effective than *in vivo* systems, which are time consuming, resource-intensive and require advanced trained personnel and maintenance fees. In addition, regulatory and ethical concerns have to be considered when working with animal-based systems. In fact, the debate on the use of animals for medical research continues to evolve, particularly in recent years [19], [20], [21], [22].

Therefore, an extensive variety of *in vitro* models have been developed and used for cell cultures: traditional static 2D cultures, static and dynamic 3D cultures and perfusion cultures [17].

1.2.1 *In vitro* cell culture: 2D methods

In standard 2D cell cultures, cells grow in fluid suspension or adhere to a solid surface [23]. Traditionally, static cultures are performed in Petri dishes, multiwell plates, or culture flasks (Figure 1.2A) where cells can form a homogeneous monolayer [13]. However, other devices can be used either for attachment or cell suspension, such as roller bottles or spinner flasks (Figure 1.2B) [24].

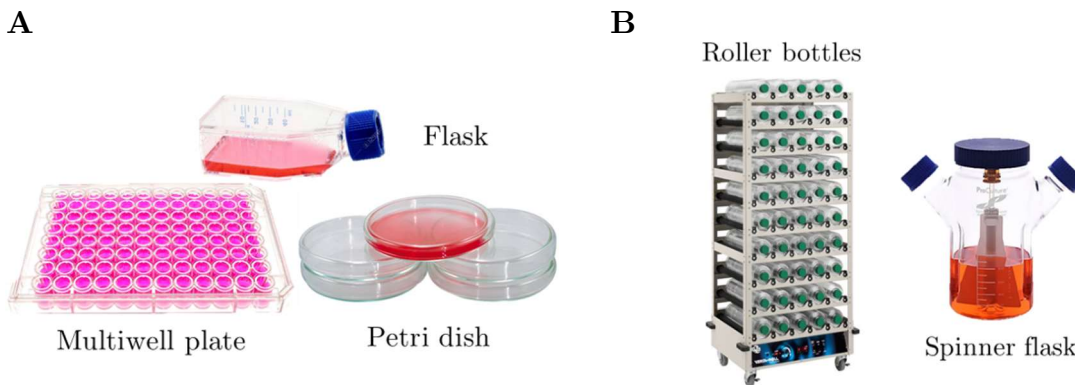


Figure 1.2 2D culture devices. (A) Flask, multiwell plate, Petri dish, (B) roller bottles, spinner flask

In all these devices, cells receive a similar amount of nutrients and growth factors present in the medium, which leads to a homogenous growth and proliferation [17].

However, traditional cell culture methods present some limitations. First of all, they do not recreate the environment conditions that are found *in vivo*: in fact, the amount of culture medium and the oxygen concentrations are higher than in a living tissue [25]. Moreover, 2D cultures do not provide natural mechanical stimuli, such as compression and strain [13]. Another drawback is the presence of a single type of cell in each culture, while different cell types coexist *in vivo*. However, the major limitation is the structure itself: a monolayer cannot mimic the complexity of a three-dimensional structure [24].

1.2.2 *In vitro* cell culture: 3D static methods

The cellular microenvironment [26] with its architecture, signalling mechanisms and mechanical stimuli, is too complex to be reproduced by standard 2D culture conditions. Therefore, 3D culture methods have been introduced to better model the *in vivo* cell's organization and interactions [13]. Three different techniques have been implemented to recreate 3D cells' structure: spheroid culture, biopolymer scaffolds and hydrogels [17].

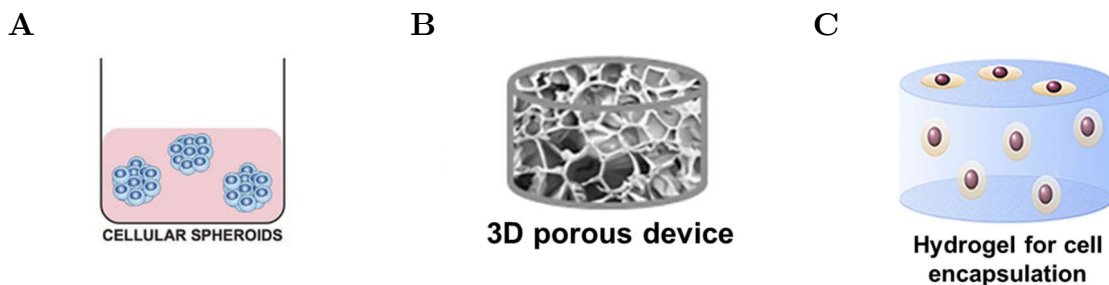


Figure 1.3 Materials and supports for 3D cell culture. (A) Spheroids [27], (B) biopolymer scaffold [28], (C) hydrogel [29]

Spheroid are aggregates of cells in suspension (Figure 1.3A), which are typically around 70-300 μm to prevent the core necrosis [25]. They can be created using different techniques: the most widely used method is *the hanging drop* method [30], in which the traditional culture setup is inverted, and cells spontaneously aggregate in drops in suspension. In spheroid cultures, the extracellular matrix (ECM) is secreted and mutual cell-cell and cell-matrix interactions are established [30]. The main applications of this type of culture are cancer research for modelling solid tumour masses [31], and differentiation studies of stem cells [32]. An advantage of this matrix-free cultures is that there is no need of any foreign material, which can cause unexpected biological effects. On the other hand, maintaining the proper conditions to provide cell aggregation and handling the spheroids are two significant issues of this culture method [25], [30].

Scaffolds can also be used to grow cells in three dimensions [17], (Figure 1.3B). These structures aim to reproduce the ECM architecture to promote adhesion, spreading, proliferation, differentiation, and maturation of cells [33]. Scaffolds are porous and degradable matrices developed from natural or synthetic polymers [28]. Moreover, the chosen biomaterial interacts with the cells and influences their functions and mechanism of differentiation [34]. Many techniques have been employed to fabricate scaffolds: 3D printing [35], stereo-lithography [36], polymer phase separation [37], lyophilizing [38], gas foaming [39]. After the fabrication, the surface can be functionalized with bioactive molecules, such as specific proteins or peptide sequences, to induce a specific cell response [33]. Nevertheless, the non-physiological conditions implemented during these fabrication and functionalization methods can damage cells and lead to a poor scaffold cellularization [28].

Similar to scaffolds, but made of other types of biomaterials, are the hydrogels (Figure 1.3C) [17]. Hydrogels are three-dimensional structures with hydrophilic chains able to supply tissue-like water content. These matrices have good properties, such as

biocompatibility, elasticity and the capability of reproduce the extracellular matrix, and they are thus employed in different biomedical fields, from regenerative medicine to tissue engineering [40]. However, hydrogels do not always provide the right mechanical properties: due to their small mesh, which often lacks microtopography, they cannot control and sustain cell shape and cell mobility, [29].

Although 3D cultures provide better conditions to mimic the *in vivo* environment, 2D cultures are often preferred due to their simplicity. Clearly, 3D methods are more technologically challenging and expensive to use than standard 2D cell culture systems [25]. Furthermore, either 2D or 3D cultures are often developed in static conditions, without mimicking the natural mechanism of continuous perfusion of liquid over cells as happens in a living organism [41].

1.2.3 *In vitro* cell culture: perfusion methods

Since nutrients depletion and accumulation of toxic metabolic waste over time on the culture, static *in vitro* cultures represent a poor choice in terms of mimicking *in vivo* conditions [13]. Instead, perfusion cultures, which allow a continuous flow of nutrients and oxygen over the culture, better reproduce the mechanisms found in a living organism and thus represent a significant improvement in cell culture strategy [42]. Additionally, perfusion *in vitro* systems provide certain stimuli such as shear stress, which has a considerable effect on the cellular morphology and on gene expression [43]. Perfusion systems are commonly represented by continuous bioreactors and microfluidic techniques (Figure 1.4) [44].

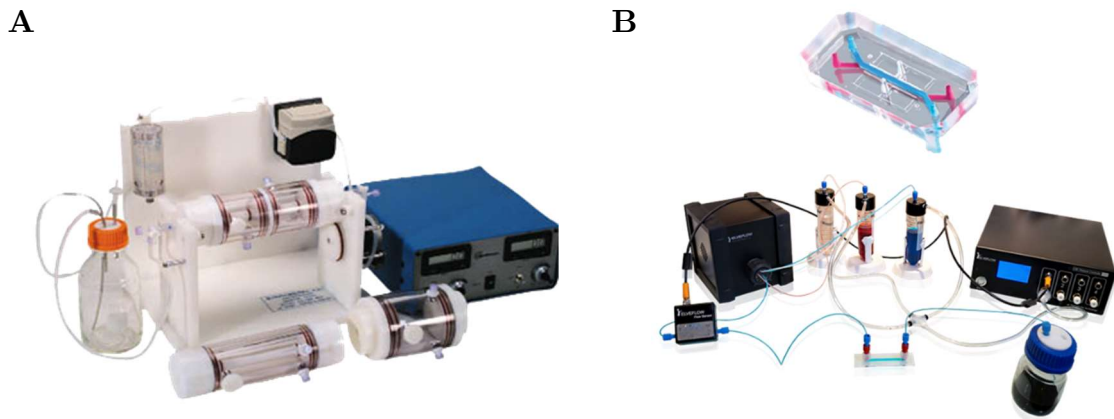
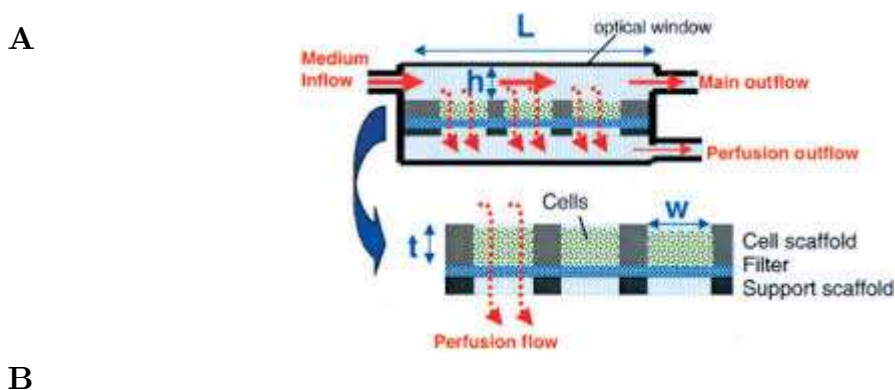


Figure 1.4 Perfusion systems for cell cultures. (A) Bioreactor, (B) microfluidic system

Bioreactors (Figure 1.4A) are tools in which all biological and biochemical processes are developed under monitored and controlled conditions [45]. There are different kind of bioreactors, depending on the mode of operation: batch, fed batch, or continuous reactors [46]. For instance, continuous bioreactors are open systems in which a mass flow rate moves into the chamber continuously, maintaining steady-state conditions [46]. These systems with perfusion pumps and dynamic stress-loading actuators are often used to transport gas, nutrients, and wastes through 3D cellular scaffolds [17]. Perfusion bioreactors can present different configurations (Figure 1.5): Parallel-Plate Bioreactors, Hollow-Fiber Bioreactors, Fixed (Packed) and Fluidized-Bed Bioreactors [47].



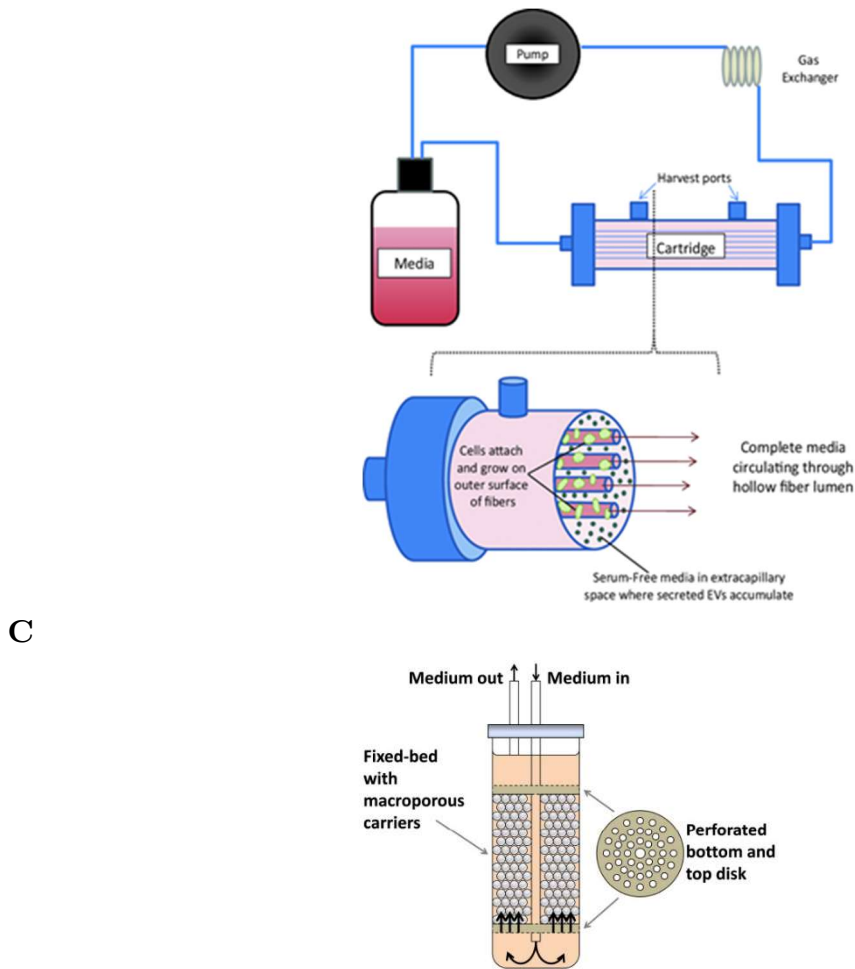


Figure 1.5 (A) Parallel-Plate Bioreactors [48], (B) Hollow-Fiber Bioreactors [49],
(C) Fluidized-Bed Bioreactors [50]

Parallel-plate bioreactors (Figure 1.5A) are composed of two compartments: one for culture medium and tissue culture surface (used for cell adhesion), and the other one for a mixture of gases. The two chambers are separated by a gas-permeable, liquid-impermeable membrane [47].

Hollow-Fiber Bioreactors (Figure 1.5B) are used to reproduce the capillary-type circulatory systems and provide good *in vivo* like conditions to grow cells, employing a high surface area for attachment and proliferation and a low level of shear stress [47]. These devices consist of a group of thousands of hollow fibers, which are permeable membranes placed into a tubular shell. Cells can grow on both the internal and the external surface of the fibers [51].

Fluidized-Bed Bioreactors (Figure 1.5C) are composed of a reservoir for medium and an immobilized scaffold in a column, in this last one cells are seeded with or without a carrier. These carrier particles can be packed or can be floating in the column [47].

Lately, micro-bioreactors have been introduced and developed to reproduce biomimetic properties for cellular application, and to create a microenvironment in which biological systems' interactions are monitored and controlled [52]. These systems require small amount of reagents, provide a large surface-area-to-volume ratio and they can be manufactured through soft-lithography techniques, making them cheaper than the conventional bioreactors [47]. Micro-bioreactors are mostly used to study the bioactivity of different cells, such as mesenchymal stem cells (MSCs) [26], embryonic stem cells (ESCs) [53] and tissue-specific cells [54]. Moreover, they are considered as valuable tools for screening therapeutic drugs and controlling cell microenvironment [17].

Bioreactors aside, recent technological developments have led to the creation of different kinds of microfluidic devices for cell studies (Figure 1.4B) [55]. The term “microfluidics” refers to the control and manipulation of fluids constrained in channels of the dimension from tens to hundreds micrometers [56]. Among the main microfluidic systems, the so-called Lab-on-a-Chip (LoC) devices are microsystems that integrate microfluidic channels and other active or passive components (filters, valves, mixers) in a single chip [57]. These systems have many advantages, such as the reduced amount of expensive reagents needed, the increased throughput, the advanced spatiotemporal control, and the enhanced physiologic relevance of the microenvironment in which cells are cultured [58], [59]. Therefore, *in vitro* systems based on microfluidic are found in a wide range of applications, especially chemistry [60], biology [61], medicine [62], and physical sciences [63]. Especially they have become fundamental tools in cancer detection [64], diagnostic [65], embryonic development [66] and drug screening [67].

Complex models whose aim is to mimic the structure and the functions of a specific organ have been also developed on chip [68]. Organ-on-Chip (OoC) devices create an *in vivo* like microenvironment, offering significant advantages especially in the drug development field [69].

Flow manipulation and control, perfusion of nutrients and oxygen together with waste removal and reproduction of *in vivo* like stimuli over a culture are the main advantages of the perfusion systems. However, some intrinsic limitations need to be highlighted. In perfusion devices, pressure sources (e.g. pumps, tubes), sensing units and electronics (e.g. high-voltage power supply, electrical circuits and sensors) are stand-alone units that increase the complexity and the costs of these systems [70]. Moreover, the use of expensive pumps and tubes can lead to the creation of bubbles, capable of obstructing channels, distorting the flow and damaging the cell culture [71].

A solution to these disadvantages can be found in Centrifugal microfluidics (Figure 1.6).

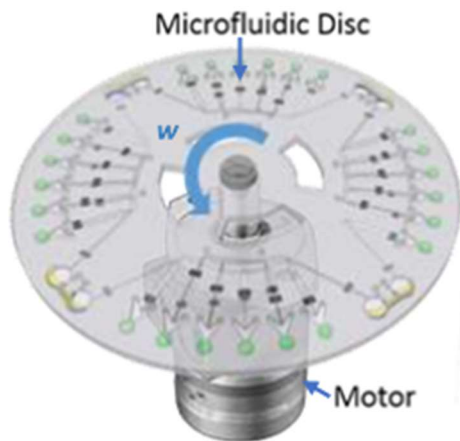


Figure 1.6 Schematic representation of a centrifugal microfluidic platform [72]

In centrifugal microfluidics, also called Lab-on-a-disc (LoD), fluids are moved in a network of microchannels engraved on a compact disc device due to the centrifugal forces [70]. LoDs are usually made of polymers and fabricated using rapid prototyping techniques, reducing the manufacturing costs [73]. Only a simple and compact motor

is required for fluid activation removing the use of external pumps and tubing [74]. Moreover, many other operational units (e.g. valving, mixing) can be implemented on these platforms, reducing the size, and the complexity of these *in vitro* systems [75]. Centrifugal microfluidic systems are mainly used for sample pre-treatment (cell lysis and homogenization) [76], analysis and detection of a specific compound [77], biochemical markers [78], etc.

1.3 Goal of the thesis: Lab-on-a-Disc platform for cell culture in flow and drug testing

Nowadays, Lab-on-a-Disc platforms are widely used for biological assays, such as immunoassays [74]. Instead, they are rarely employed for cell-based assays [79].

In this project, a centrifugal microfluidic platform is used for long-term cell culture and drug testing. In particular, the LoD is used for two different applications, which involve bacterial and mammalian cells.

In the first application the LoD is used to culture bacteria from single cells to mature biofilm for antibiotic testing. In this study, the bacterium *Pseudomonas Aeruginosa* was chosen as a case of study since often involved in chronic lung infections of cystic fibrosis patients. First, *Pseudomonas Aeruginosa* biofilm is grown on disc and then the effects of different antibiotic treatments are analysed.

In the second application, mammalian cancer cells are cultured for performing cytotoxicity assays using a chemotherapy drug. Two different cancer cell lines, Caco-2 cells and HeLa cells are used: the first cell line is used to prove the possibility of culturing mammalian cells for long-term culture on disc, while the second one for cytotoxicity assay to test the effects of doxorubicin.

In this view, the goal of the thesis is to assess the relevance of this platform in the initial phase of drug screening, showing that it can be used for long-term cultures and testing of drugs. Therefore, the purpose is also to present this LoD as a possible alternative to traditional *in vitro* cell culture systems.

2. Application 1: bacterial biofilm growth and test of antibiotic tolerance

The discovery of antibiotics represents one of the most significant medical achievements, which have provided many important advances in healthcare [80]. Unfortunately, the successful use of antibiotic was compromised by the appearance of resistance and tolerance strain of bacteria. Consequently, the efficacy of antibiotic treatments has decreased while drug-resistant strains of bacteria have increased, resulting as a threat for the public health [81]. Therefore, there is a significant need of new antibiotics, whose discovery represents a significant challenge [82]. In fact, many bacteria are refractory to antibiotic treatments, especially due to their ability of growing and forming biofilms, which play a critical role in the spread of antibiotic resistance [83].

2.1 Bacterial biofilms

A biofilm (Figure 2.1) is an organized community of microbial cells living within an extracellular polymeric matrix (EPS) [84]. Bacterial biofilms appear as microcolonies, often attached to a surface, where each bacterium adhere one to another [85].

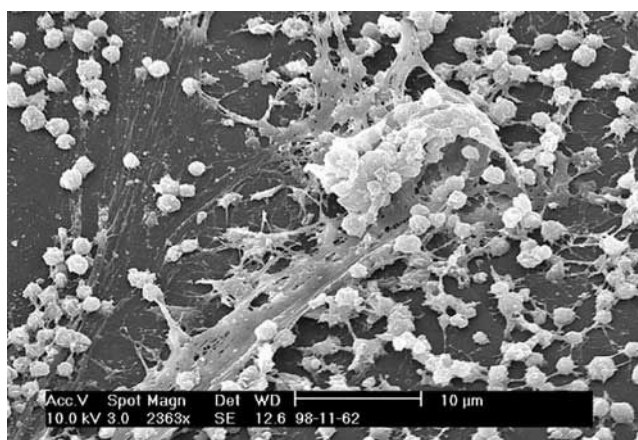


Figure 2.1 Scanning electron micrograph of a Staphylococcus biofilm [85]

In nature, biofilms can be found everywhere, especially on surfaces exposed to water, such as rocks or stones in rivers or lakes [86]. Biofilms are also found in industrial set-ups, for example in water distribution pipe-lines [87], and in food processing (e.g. liquid pipelines, pasteurizer plates, membranes, storage silos) [88]. Even more important, they are directly involved in several human disease (e.g. colitis, conjunctivitis, otitis) [84], and they colonize medical devices (e.g. arterial and central venous catheters) [89], artificial implants (e.g. artificial hip and knee joints) [90] and prostheses [91]. This bacterial biofilm colonization on device surfaces leads to pathological infections, which can spread through the dispersion of single cells (planktonic cells) [89].

In general, biofilms develop as layers of bacteria embedded in a matrix within which different cell phenotypes can be found. [92]. Usually microbial cells take between 5-35% of the entire volume of a biofilm, while the remaining part is taken by the EPS. The EPS is constituted of proteins, polysaccharides, extracellular DNA and channels for water and nutrients [93]. The EPS gives a structural support by holding together the bacterial microcolonies and plays an important role as a barrier against the host immune defences and antimicrobial treatments [94]. Moreover, cell-to-cell communication (quorum sensing) and exchange of genetic material take place inside the EPS [93], [95].

Biofilm development is a complex process that occurs in five main stages (Figure 2.2) [95]:

1. Initial contact, when the planktonic cells reach a surface and start to adhere through flagella or through physical forces (e.g. van der Waal's forces, electrostatic interactions) [93], [95].
2. Cell aggregation, when bacterial cells start to proliferate and consequently secrete the EPS [93], [95].
3. Development of biofilm architecture, when micro-colonies and water channels are developed [92], [95].

4. Maturation of biofilm architecture, when cell-cell signalling molecules are secreted and the communication between micro-communities is established in order to form a mature biofilm [92], [95].
5. Detachment and dispersion of the biofilm, when micro-colonies are released in order to spread the infection [95].

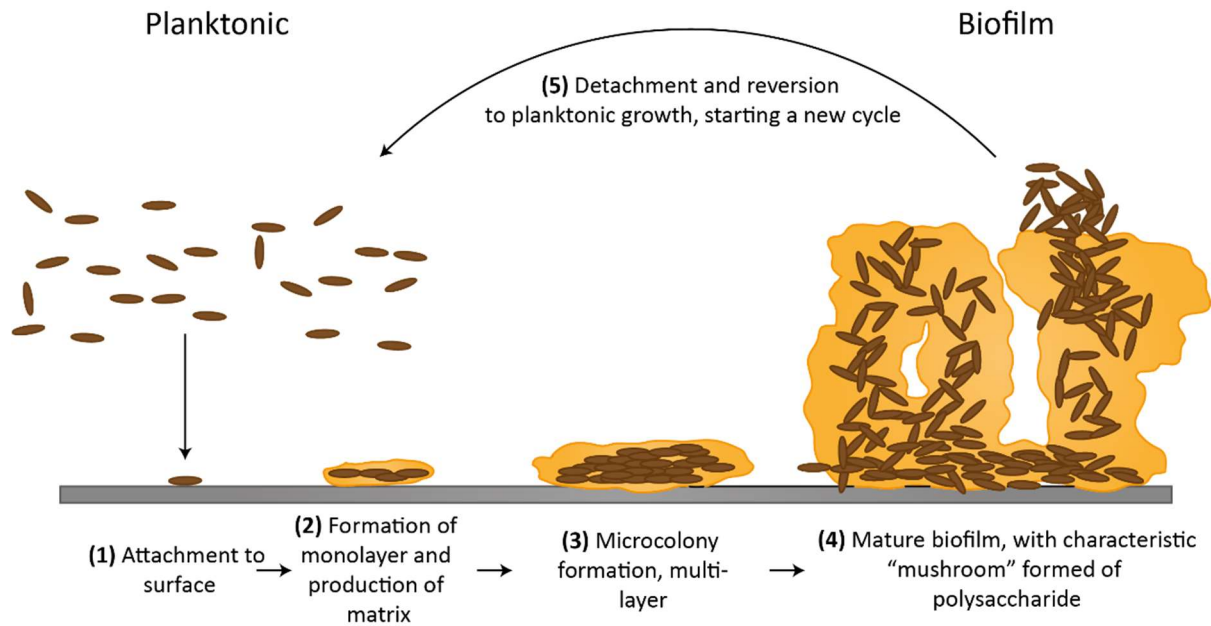


Figure 2.2 Steps of biofilm formation process [96]

This biofilm formation process is triggered by many environmental conditions, such as surface properties, shear stress and cell-cell signalling [97].

Surface composition, morphology and structure influence every step of a biofilm formation. In particular, rough [98] and hydrophobic surfaces [99] promote bacterial cells attachment. Moreover, porous materials enhance biofilm development, depending on the pore size and the degree of porosity [100].

Hydrodynamic conditions such as shear stress have a significant effect on biofilms structure. For example a high shear stress inhibits biofilm formation, leading to a thin monolayer biofilm [101]. However, shear stress can also have opposite positive influence.

In fact, a high flow rate helps the migration of detached bacterial cells, enabling the colonization of new niches [102]. Therefore, shear stress limits the maturation of a biofilm matrix, but promote new biofilm formation and spreading [97].

Another important factor in biofilm formation is quorum sensing, which is, as already mentioned, the process of communication between bacterial cells and it is responsible of gene expression regulation [97]. During quorum sensing, chemical signalling molecules, called autoinducer, are produced by microbial cells. Autoinducer molecules are fundamental since cell population density depends on their production [103]. Autoinducer receptors are capable of controlling the response of bacterial cells to some stimuli (e.g. environmental condition changes) by activating or repressing certain genes. For example, it was shown that biofilm size and bacterial cell phenotypes within the biofilm rely on the process mentioned above [104]. In addition, quorum sensing contributes to antibiotic tolerance [95].

The formation of a biofilm makes bacteria thousands of times more tolerant to antibiotic treatments compare to their counterparts [105]. The major challenge in treating biofilm infections is the lack of understanding of how a biofilm grows. Therefore, research studies where biofilms are modelled *in vitro* or *in vivo* are crucial to identify possible successful treatments for biofilm eradication [84].

2.2 Antibiotic tolerance in bacterial biofilms

Two mechanisms are involved in the failure of antibiotic treatments: antibiotic resistance and antibiotic tolerance [80]. Antibiotic resistance occurs due to a permanent change in bacterial cells, which allows cells to grow in the presence of an antibiotic agent [106]. The phenomenon of resistance is connected to an increase in the minimum inhibitory concentration (MIC) value, which is the lowest concentration of an antibiotic necessary to inhibit the visible growth of a microorganism [107], [108]. Instead,

antibiotic tolerance is due to a reversible phenotypic state that enables survival of bacteria during a treatment [107].

To understand these two phenomena, it is important to know the mechanism of action of antibiotics (Figure 2.3). Antibiotics use one of the following mechanisms to kill bacteria [109]:

- Cell wall synthesis inhibitors: in the presence of these agents, bacteria are deprived of peptidoglycan, the polysaccharide backbone present in bacterial cell walls [109], [110].
- Cell membrane function inhibitors: they prevent the cytoplasmatic membrane to work as a barrier, causing macromolecules and ions outflow and the consequent cell death [109], [110].
- Protein synthesis inhibitors: these inhibitors disturb protein synthesis stages, including initiation and elongation stages [109], [110].
- Nucleic acid synthesis inhibitors: they can be divided into DNA inhibitors and RNA inhibitors. Messenger RNA transcript of genetic material is hindered by RNA inhibitors, while DNA synthesis stages are prevented by DNA inhibitors [109], [110].

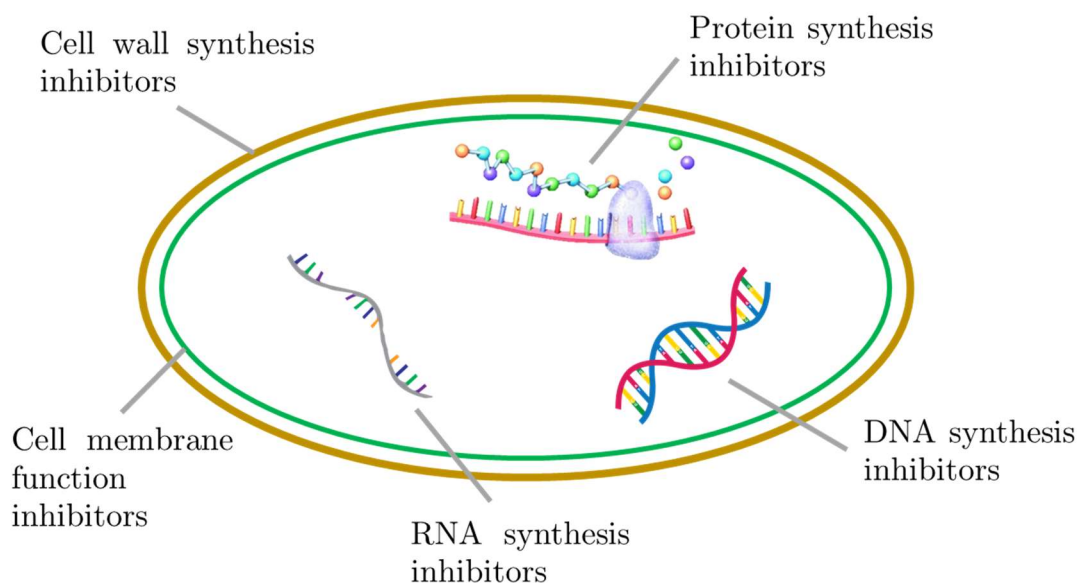


Figure 2.3 Antibiotic mechanisms of action

Since bacteria growth and reproduction are mainly determined by cell wall synthesis, cell membrane function, protein synthesis and nucleic acid synthesis, the inhibition of one or more of these functions causes the death of the cell [110].

Even though antibiotics can kill bacterial cells, they cannot entirely eradicate the whole biomass of a biofilm. This failure in the treatment is due to the tolerance presented by bacterial biofilm towards antibiotic treatment [111]. Biofilm antibiotic tolerance (BAT) is caused by several factors (Figure 2.4), such as [95]:

- Antibiotic restricted penetration: the EPS of several biofilm species have proved to act as a shield against antibiotic penetration [94]. The EPS matrix can absorb antimicrobial treatments, thereby minimizing the quantity of agent that can interact with bacterial cells [84]. However, this phenomenon is not universal in all biofilm-forming species and also seems to be antibiotic specific [95].
- Reduced growth rate: the complex internal structure of a biofilm produces gradients of oxygen and nutrients, which slowed bacterial growth in many species [112]. Since the targets of many antibiotics are active bacterial cells,

slow-growing or dormant cells are unaffected by these agents and thus increasing the level of antibiotic tolerance [95].

- Presence of persister cells: persister cells are a subcategory of bacterial cells in a dormant state, which are characterized by an extreme antimicrobial tolerance [95]. Several studies have shown that after antibiotic treatments, a small amount of persister cells will survive despite the antibiotic concentration utilized [113], [114]. These residual persister cells can start to reform the biofilm [115].

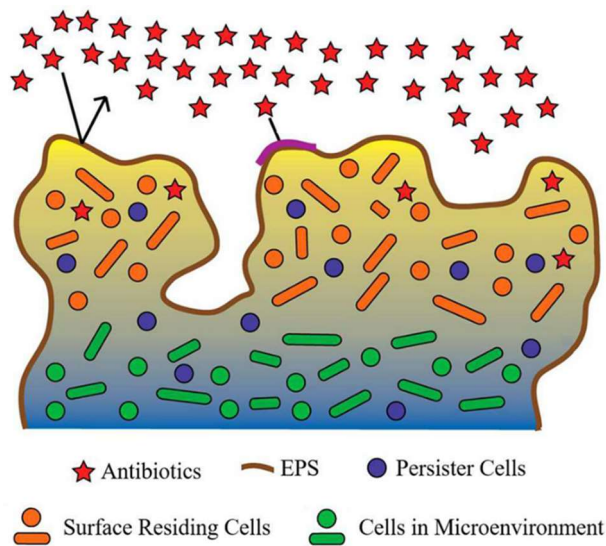


Figure 2.4 Mechanisms contributing to biofilm antibiotic tolerance

The above-mentioned mechanisms and the possibility of acquiring resistance through a mutation are among the cause of the reduced antibiotic susceptibility of bacterial cells in biofilm. The physiological status of bacteria within a biofilm needs to be studied more accurately in order to find new treatment methods and to understand when and how to treat biofilms infections [84].

2.3 *Pseudomonas aeruginosa*: a case of study

The World Health Organization (WHO) presented a list of “critical priority” pathogens, which represent a global threat for public health [116]. All the pathogens in

the list are Gram-negative bacteria, such as *E. coli*, *Salmonella typhimurium*, *Klebsiella pneumoniae*, *Enterobacter*, *Acinetobacter baumannii* and *Pseudomonas aeruginosa* [117]. One of the most resistant bacteria is *P. Aeruginosa* (Figure 2.5), which belong to the family Pseudomonadaceae [118].

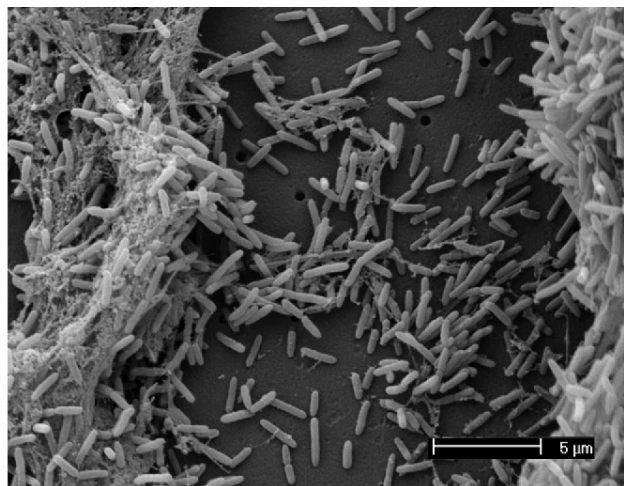


Figure 2.5 *Pseudomonas aeruginosa* biofilm [119]

This organism is 1–3 μm in length and typically is an aerobe bacterium [120]. It can be found in different environments, for example it can grow at 37°C as well as 42°C and can tolerate severe environmental conditions [121]. *P. aeruginosa* exists in water, soil, plants, animals and in human body such as in the throat, nasal mucosa and skin [122]. It can colonize hospital environment, such as hospital sinks, drains, bathtubs, ventilators [123]. *P. aeruginosa* is an opportunistic pathogen that can cause mild infections if the host is a healthy subject, or severe infections if the host is an immunocompromised patient [124]. A significant example is the effect that this pathogen has on cystic fibrosis patients, in which it infects the lower respiratory tract, becoming one of the main causes of mortality [118].

Treating *P. aeruginosa* infections is challenging due to its intrinsic tolerance, which can become resistance, to a wide range of antimicrobial agents [121]. *P. aeruginosa* tolerance is given mainly due to the synergic effect of two mechanisms: the restricted permeability of its outer membrane and the increased efflux and enzymatic antibiotic

modifications (e.g. β -lactamase) [125]. The outer membrane works as a selective barrier and limits the penetration of antimicrobial agents into the cells [125], [126]. Furthermore, *P. aeruginosa* can acquire resistance through the horizontal transfer of genetic elements and mutational resistance [118]. DNA elements, such as plasmids, transposons, integrons, which show antibiotic resistance genes, can be acquired by conjugation, transformation or transduction. All these factors increase antibiotic resistance and can also rise to the phenomenon of multidrug resistance [125].

Since *P. aeruginosa* still represents a significant cause of morbidity and mortality in biofilm-related infections [127], it raised the interest of the scientific and clinic research and thus it has been chosen as a case of study in this thesis.

2.4 Bacterial Culture on disc (BCoD) microfluidic platform

In this first application, a Lab-on-a-disc platform is optimized to culture bacteria from single cells to mature biofilm for antibiotic testing. The aim of the study is thus to analyse the effects of different types of treatments on *P. aeruginosa* biofilm grown on a centrifugal microfluidic system, described in detail in Chapter 4 “*Centrifugal microfluidics: Bacterial Culture on Disc (BCoD) and Mammalian Cell Culture on Disc (CoD)*”.

In order to mimic the biofilm present in cystic fibrosis patients and provide a microenvironment more similar to the *in vivo* habitat of the bacterium, *P. aeruginosa* (lab strain PAO1) was chosen and cultured under flow condition for 48 h in artificial sputum medium (ASM). The PAO1 strain was genetically modified: a gene encoding green fluorescent protein (GFP) was introduced in the chromosome at a neutral site using Tn7 tagging [44]. The bacteria acquired a green fluorescence visible under the microscope at 488 nm light source [128].

Ciprofloxacin (CIP) was the chosen antibiotic to treat *P. aeruginosa* biofilm. It belongs to a group of drugs called quinolone antibiotics, which act by inhibition of DNA replication [129]. Literature has shown that Ciprofloxacin has been extensively used to treat *P. aeruginosa* biofilm infections and thus, it was used in this experimental setup [130].

Once the biofilm was developed, different antibiotic treatments were administered:

- Bolus injection of ciprofloxacin: the antibiotic was introduced directly on the biofilm to mimic the intravenous injection.
- Microdevices, also called microcontainers (MCs), loaded with ciprofloxacin and coated with Chitosan (CHI), and MCs loaded with ciprofloxacin and coated with CHI together with N-acetylcysteine (NAC). MCs are reservoir-based microdevices for local drug delivery, in which the drug is loaded into the reservoir and protected by a polymeric lid [131]. The drug is released throughout the lid when this starts to dissolve and degrade. In a previous work MCs coated with CHI have shown promising results in the treatment of biofilm-related infections [132]. Also, in this case the microdevices were introduced in close proximity of the biofilm.

The antimicrobial activity of the CHI/NAC and CHI functionalized MCs was compared to bulk delivery (bolus injection) of ciprofloxacin.

In the Bacterial Culture on disc (BCoD) device, the biofilm was monitored, using confocal microscopy, during the entire process of development from single cells to mature biofilm and during the antibiotic treatment. Once the images were collected, they were treated and used as input to calculate the bacterial biomass.

Techniques, tools and experimental set-up used for this application are further analysed in Chapter 4.

3. Application 2: mammalian cell culture and cytotoxicity assays

Understanding the human body and its biological response to diseases and drug administration is one of the major challenges in pharmaceutical research and development [133]. Some cellular models have given valuable knowledge of *in vivo* mechanisms, while others have failed *in vitro/in vivo* correlation, especially when related to a disease [134]. Novel *in vitro* models capable of reproducing a disease are required in order to provide accurate clinical outcome predictions. Therefore, more reliable *in vitro* models have been developed and a particular attention is given to dynamic cell culture systems based on microfluidics often used to model cancer diseases [135]. Diseases are usually reproduced by single cell monolayer cultures, based on immortalised cancer cells [136].

3.1 Mammalian cells: Caco-2 and HeLa cells

3.1.1 Caco-2 cells

Over the last twenty years, the human colon adenocarcinoma cell line, Caco-2 cell line, has been used for *in vitro* cell models for high-throughput screening of drug permeability [137]. When cultured on a Petri dish, Caco-2 cells grow as a confluent cell monolayer, forming a cylindrical polarized structure with microvilli on the apical membrane and tight junctions between adjacent cells [138]. Upon differentiation, these cells can express certain morphological and biochemical characteristics similar to those found in the small intestinal epithelium [139].

The development of Caco-2 cells is highly influenced by culture conditions, such as time of culture and cell density used as inoculum in the *in vitro* system. Therefore,

culture conditions need to be strictly monitored and controlled in order to obtain reproducible results and to not compromise the cell culture [138]. Caco-2 cell line has a relevant characteristic: it is a slow-growth cell line. In fact, its population doubling time (PDT), the time interval calculated during the logarithmic phase of growth necessary for cells to double in number, is approximately 3 to 4 days [140], [141].

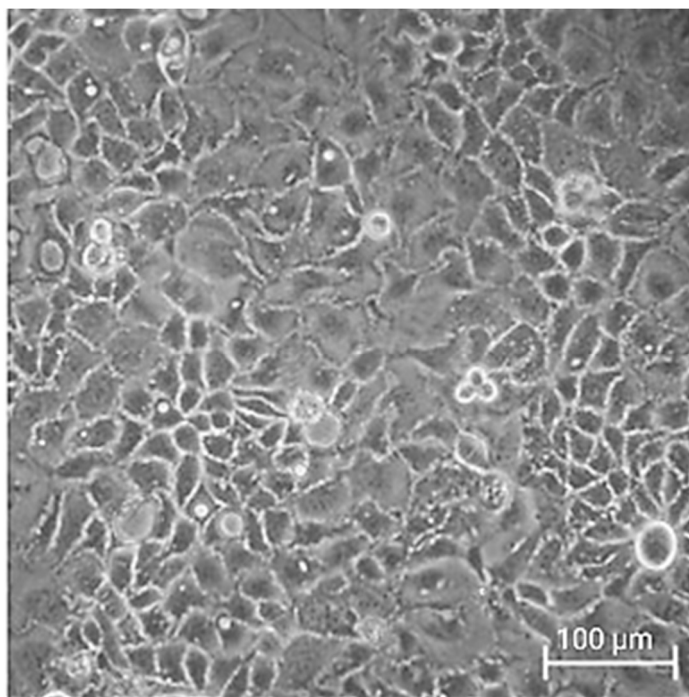


Figure 3.1 Optical microscope image of Caco-2 cells after 4 days of culture [142]

Caco-2 cells have been used for a wide range of applications, such as [143]:

- studying food-intestine interactions and the absorption of food substances at the barrier of the intestinal epithelium [144];
- studying the transport mechanism of compounds such as drugs or food across the intestinal epithelium [145];
- analysing possible toxic effects of drug molecules or food metabolites in the intestinal mucosa [146].

To carry out accurate studies using Caco-2 cells, it is fundamental to closely monitor the morphology of the culture and the growth rate. However, Caco-2 cells can represent valuable *in vitro* models for toxicity tests.

3.1.2 HeLa cells

Unexpectedly, in the 1950s, HeLa cells became very popular among the scientific community. These cells came from the cervical cancer of a woman named Henrietta Lacks, from which they took their name, and during the years they have demonstrated to be a valuable model for testing of new developed treatments in the biomedical field [147].

HeLa cells (Figure 3.2) have some characteristics that make them different from usual human cells. In fact, HeLa cells contain from 76 to 80 mutated chromosomes, while normal human cells karyotype (chromosomes features) contains 46 chromosomes [148]. Moreover, HeLa cells divide indefinitely when cultured, while normal human cells go through approximately 50 divisions depending on the age of the subject. For this reason, they are called “immortal”. [149].

HeLa cells are not only capable of endless division, but also of extraordinarily rapid division, even more than other cancer cells. In fact, these cells can double their number just after 24 h of cultivation. The telomerase enzyme is responsible of this activity [147]. When a normal cell divide, the activity of this enzyme reduces and consequently the telomeres (short repetitive DNA sequences at the end of a chromosome) become shorter [150]. This mechanism regulates the division number of cells through apoptosis and cell death when cells reach the maximum number of divisions. In contrast, HeLa cells can divide indefinitely due to high telomerase [151].

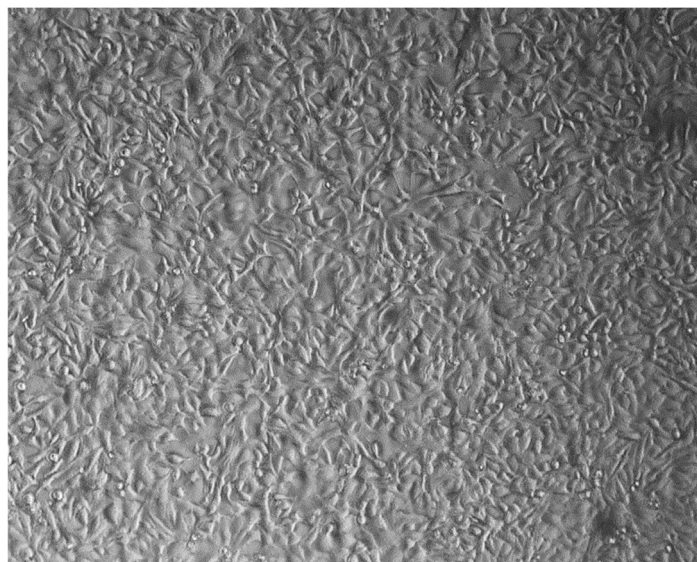


Figure 3.2 Optical microscope image of HeLa cells after 24 h of cultivation with a concentration of 0.75×10^5 cells/cm²

HeLa cells have been used in numerous applications in biomedical research [147][152][153]. One of the firsts was connected to the test of the vaccine against poliomyelitis where HeLa cell cultures were used as testing model [154]. Since the success with polio vaccine, HeLa cells turned into a fundamental cell culture model useful for the isolation and cultivation of several viruses [155], and also for the production and therefore testing of antibodies [156] and chemotherapy drugs [157].

Consequently, for more than sixty years HeLa cells contributed to scientific discovery of inestimable importance [158]. HeLa cells are even more important today since they are the most used cell line for cancer disease models [159].

3.2 Cytotoxicity assays

The term cell viability refers to the measure of the proportion of cells that are alive in a certain population [160]. During testing, the number of alive and proliferating cells is utilized as an indicator of cell response towards a drug or a substance [161]. Cell viability can be determined using either cell viability assays [162] or cell toxicity assays [163], which enable a quantification of dead and alive cells. In particular, cell toxicity

assays are used to determine the capability of a chemical agent to damage or kill cells and represent valuable techniques for estimating the number of survival cells to a treatment [160].

Cell cytotoxicity assays were one of the first *in vitro* methods used to predict the toxicity of a substance in relation to cells [164]. They have been employed in several applications, such as to analyse damages to specific organs due to a chemical agent (e.g. liver) [54], and to evaluate the pharmacological profile of anticancer drugs [165].

A wide range of procedures have been used for measuring cell viability and assessing cytotoxic effects. These techniques can be divided into different categories [161]:

- Dye exclusion methods: different dyes pass through the membrane of dead cells; an example is trypan blue dye exclusion assay [166].
- Metabolic activity: such as MTT assay, which measure cell viability through the variations of mitochondrial activity, responsible of the conversion of MTT (3-[4,5-dimethylthiazol-2-yl]-2,5 diphenyl tetrazolium bromide) into formazan crystals [167].
- Adenosine 5'-triphosphate (ATP) assay: ATP levels indicate cell viability and are monitored through bioluminescent detection. Firefly luciferase enzyme catalyses the reaction between firefly luciferin and ATP. Cell viability is directly proportional to the quantity of luminescent light [168].
- Sulforhodamine B (SRB) assay: cell viability is directly proportional to the quantity of SRB dye that binds to all protein components [169].

- Protease viability marker assay: method based on the detection of proteolytic activities associated with viable cells. In fact, protease enzymes are included in the process of protein degradation and cell division [170].
- Clonogenic assay or colony formation assay: method related to cell proliferation and colonies formation that evaluate the ability of cells to reproduce after the administration of a drug [171].
- Raman micro-spectroscopy: method based on the scattering of light occurring when a photon collides with a substance. It is used to analyse the different stages of cell cycle to observe *in situ* and in real-time biochemical changes in living cells [172].

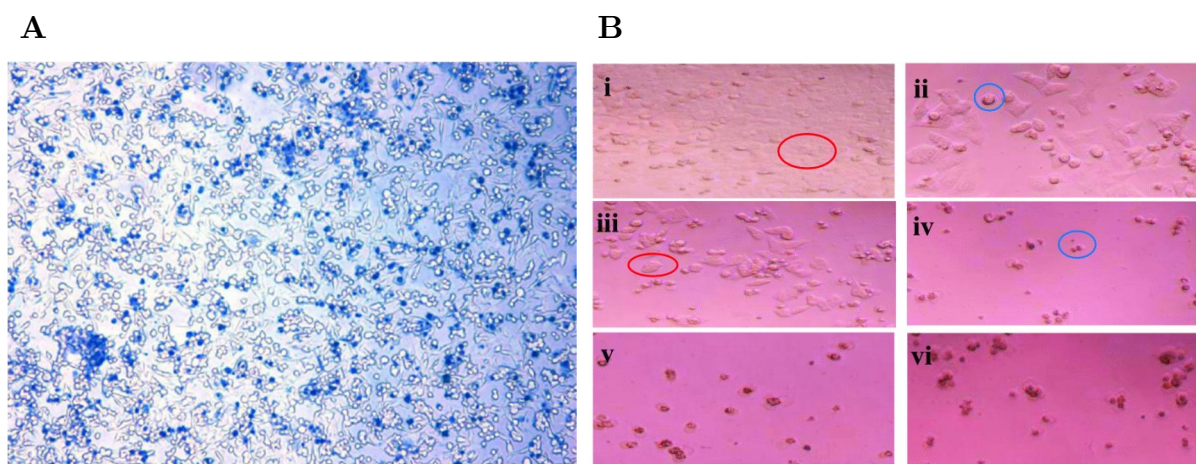


Figure 3.3 Examples of cytotoxicity assays. **(A)** Trypan blue dye exclusion assay [173], **(B)** SRB assay [174]

Cell viability measurement has an essential role in all cell culture studies because it represents one of the most valuable information in cell cultures [162]. Since different assays can be used, the most appropriate one needs to be chosen depending on the cell type and the culture conditions [161].

3.3 Mammalian Cell culture on disc (CoD) microfluidic platform

In this second application, a Lab-on-a-disc platform is optimized to culture mammalian cells for performing long-term culture and cytotoxicity assays. The aim of the study is to assess the possibility of long-term growing of mammalian cells on the platform and analysing in real-time the effects of a common chemotherapy drug.

In the first set of experiments, Caco-2 cell line was used for a long-term culture up to 6 days. Caco-2 cells were chosen since their PDT is approximately 3-4 days [140], which is a fundamental characteristic to test the platform reliability on a long time. The cell growth was monitored real-time with an integrated miniaturized microscope. A conventional optical microscope was used for comparison. At the end of the culture, confocal images were taken to assess Caco-2 cell viability.

To perform a cytotoxicity assay on the disc, HeLa cells were chosen. They were cultured for 24 h in flow in order to form a confluent monolayer. After 24 h of growing, different concentrations of doxorubicin (DOX) were added to the culture.

DOX is a common chemotherapy drug, which is used in several applications because effective in the treatment of different types of cancers [175], such as breast [176], prostate [177], uterus [178], stomach [179] and liver [180] tumours.

The two phases of growth and treatment were monitored real-time as explained in the previous paragraph. The images taken with the microscope on disc (MoD) were then used as input to calculate cell viability with a dedicated software called Cellari (<https://cellari.io/>).

Techniques, tools and experimental set-up used for this application are further analysed in Chapter 4 “*Centrifugal microfluidics: Bacterial Culture on Disc (BCoD) and Mammalian Cell Culture on Disc (CoD)*”.

4. Centrifugal microfluidics: Bacterial Culture on Disc and Mammalian Cell Culture on Disc

During the last decades, microfluidics has emerged within the different fluidic branches of research. It is based on the handling and processing of fluids in channels of the dimension of hundreds micrometers [56]. The miniaturization of different lab protocols on a small chip has several advantages, such as the reduced volume of reagents needed, the high level of automation and the number of experiments that can be performed at the same time [181]. These systems, called Lab-on-a-Chip devices (LoC), are found in a wide range of applications, especially diagnostics [182], genomics [183], biochemical assay [184], cell research [185], biosensor [186] and drug development [187].

However, as mentioned in chapter “1.2.3 *In vitro cell culture: perfusion methods*”, LoC devices, in order to work, require pressure sources (e.g. pumps, actuators and tubing) and sensing units and electronics (e.g. high-voltage power supply, electrical circuits and sensors) which increase the complexity and costs of these systems (Figure 4.1A) [70].

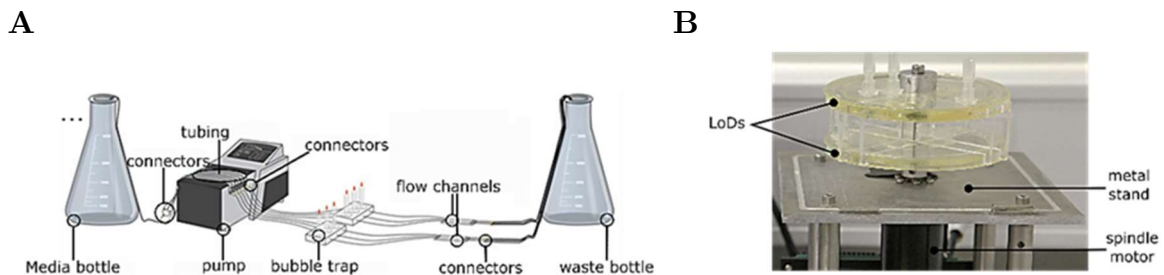


Figure 4.1 Lab-on-a-Chip(A) and Lab-on-a-Disc (B) set-up. Figure adapted with permission from [188].

A solution to the above listed disadvantages can be found in Centrifugal microfluidics (Figure 4.1B) [75]. Centrifugal microfluidic systems use the inertial pseudo forces to

move fluids through microchannels and chambers that are fabricated on a disc-shaped platform, also called Lab-on-a-disc (LoD) [189]. LoDs are commonly made of polymers (e.g. polycarbonate, polypropylene) and fabricated using rapid prototyping techniques (e.g. laser ablation) [73]. These platforms do not need external pumps and valves for actuating the liquid, since only a simple and compact motor is required to spin the disc [190].

Operational units, such as mixing, metering, pumping and valving can be implemented on centrifugal microfluidics [75]. Mixing (Figure 4.2A) is used to reach an adequate homogeneity of the sample and reagent molecules. It can be based on intrinsic forces, such as centrifugal force, the Coriolis force, and the Euler force, or on external perturbations, such as through the action of magnetic beads or gases [75], [191]. Metering (Figure 4.2B) is essential for applications that require exact volumes of liquids and it is often connected to the use of valves, which can control the liquid flow across the microfluidic channels [191].

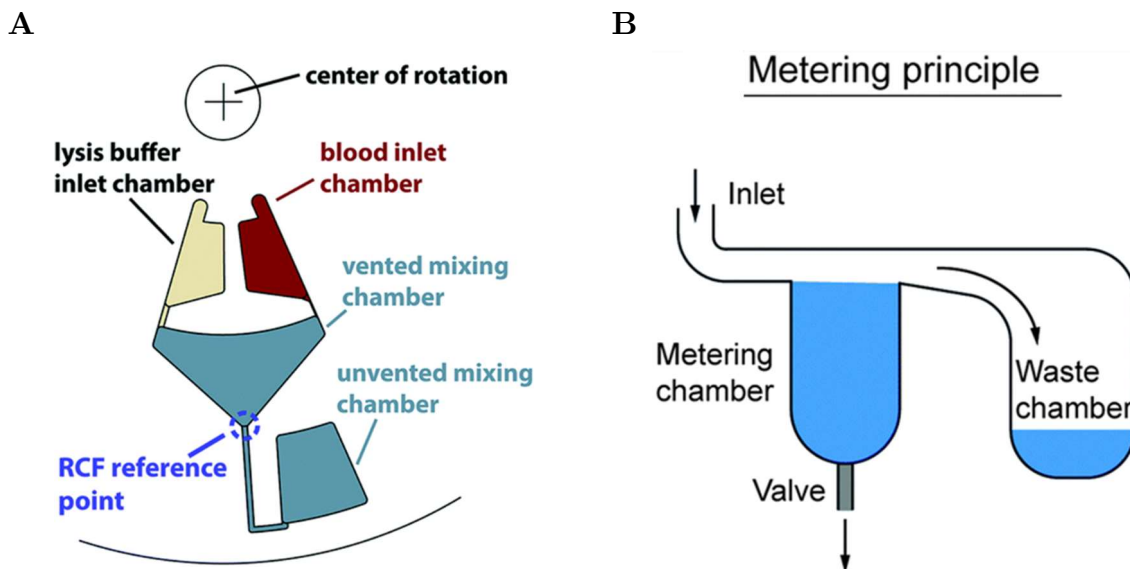


Figure 4.2 Examples of integrated operational units on a centrifugal microfluidic platform. (A) Mixing unit [192] and (B) metering unit [191].

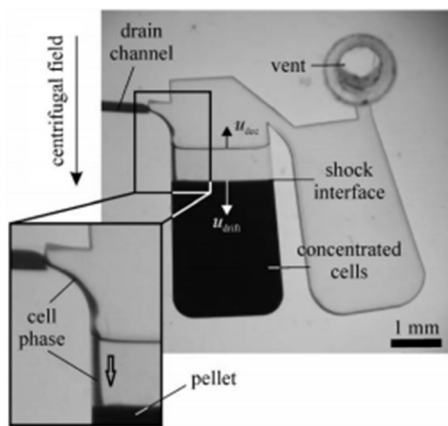
Centrifugal microfluidic platforms have been used for a wide range of applications, such as clinical chemistry testing [193] and immunoassays [194] based on absorption, agglutination or fluorescence detection [189]. They have also been employed for nucleic-acid analysis in relation to cell lysis, nucleic acid purification, and their amplification and detection [191].

Furthermore, centrifugal microfluidic systems are compatible with several detection methods [195]. The most used and successfully employed methods are based on fluorescence [196], absorbance [197], and scattering [198].

A new area of interest is represented by cell-based LoD applications [195]. In this area, LoDs are mainly employed for [199]:

- Cell separation, concentration, and purification.
- Cell capture and counting.

A



B

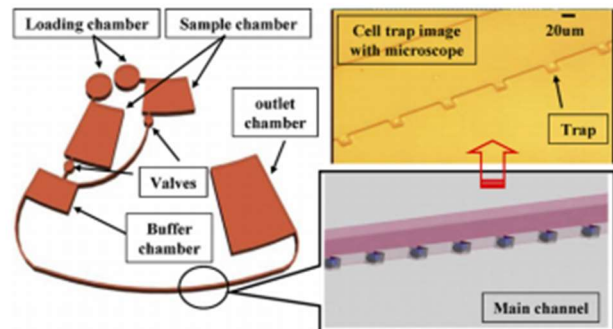


Figure 4.3 Examples of cell based LoD applications. **(A)** Blood cell separation from plasma for blood assays [200]. **(B)** Cell trapping for cytotoxicity assays [201].

One of the first steps in cell analysis processes is cell separation, used to separate a specific target from a complex matrix (Figure 4.3A). This process is extremely relevant in blood assays, in which centrifugal microfluidic devices have been used as blood

separation devices. In here, blood cellular components are extracted through centrifugal sedimentation and collected in a first chamber, while the cell free plasma is collected in an overflow chamber [200].

Another fundamental step is to perform an assay for cells identification and behaviour (Figure 4.3B). In particular, it is important to measure the response of cells when exposed to different environmental conditions or reagents. To do so, cells are captured in traps and cytotoxicity assays are performed [201].

The above-mentioned applications showed the implementation of cell assays and lab protocols on a centrifugal microfluidic platform, but they do not show the possibility of long-term cell culture in continuous perfusion. Only few applications about cell culture on LoD have been shown in the past [79], but in these studies and experiments cells were cultured in static while the disc was spun only in case of waste removal from the cell culture chamber and to add nutrients.

In fact, to establish a cell culture in perfusion on a LoD, certain requirements need to be satisfied, which are:

- sterile environment;
- constant low (below few $\mu\text{l}/\text{min}$) flow rate;
- adequate low (below few mPa) shear stress;
- possibility of culturing for multiple days without addition of medium.

This thesis presents a centrifugal microfluidic platform where cells can be cultured under constant perfusion of nutrients for multiple days and where antibiotic treatments, cytotoxicity assays and real-time monitoring can be performed.

4.1 Bacterial-Culture-on-Disc: theory and design

To develop a new LoD platform, the basic physical laws of centrifugal microfluidics needs to be considered.

In this paragraph, the design and the operational units (Figure 4.4) of the Bacterial-Culture-on-Disc (BCoD) are presented and explained in relation to the theoretical laws taken into account.

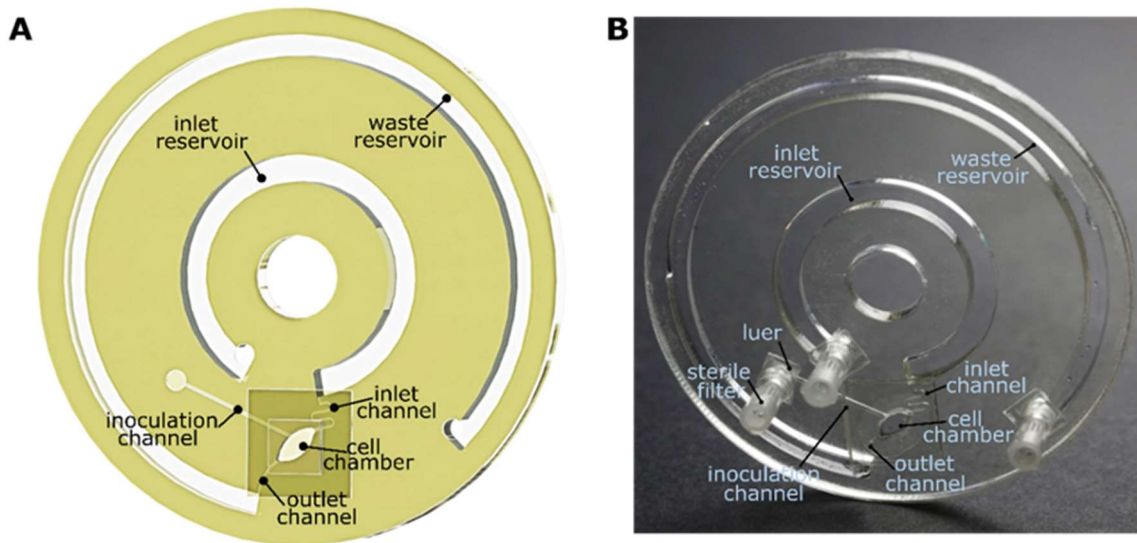


Figure 4.4 Design and operational units of the BCoD. **(A)** Computer-aided design (CAD) design with main operational units. **(B)** Photo of the disc with operational units highlighted. Figure reprinted with permission from [188].

The shape of the inlet and waste reservoirs is circular to keep the flow rate stable and constant over time during cell culture. In this design, the flow of the liquid from inlet to waste reservoir is determined by the centrifugal pressure, Δp_C , which is given by:

$$\Delta p_C = \frac{1}{2} \rho \omega^2 (r_2^2 - r_1^2) \quad \text{Eq. 1}$$

Eq.1 shows that Δp_C depends on:

- ρ , the liquid density (culture medium in our experimental set-up);
- ω , the angular rotational frequency set to spin the disc;
- r_1 and r_2 , the inner and the outer radial point of a liquid column.

In our case, r_1 is considered as the distance between the centre of rotation and a point positioned in the middle of the inlet reservoir, while r_2 as the distance between the centre of rotation and a point in the middle of the waste reservoir (Figure 4.5).

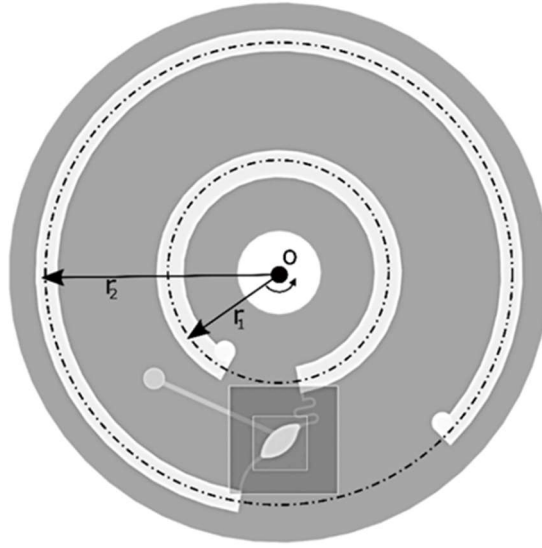


Figure 4.5 r_1 and r_2 representation on the disc. Figure reprinted with permission from [188].

In order to keep the flow rate stable and constant, the pressure between inlet and waste has to be the same over time. Δp_c (Eq.1) results to be constant when r_1 and r_2 are placed equidistant in a circular shape.

In the inlet reservoir, the liquid movement is also subjected to the capillary pressure, Δp_{cap} , given by:

$$\Delta p_{cap} = \sigma \kappa \tag{Eq. 2}$$

Where:

- σ is the surface tension of a liquid (culture medium surface tension in our experimental set-up);
- κ is the meniscus shape.

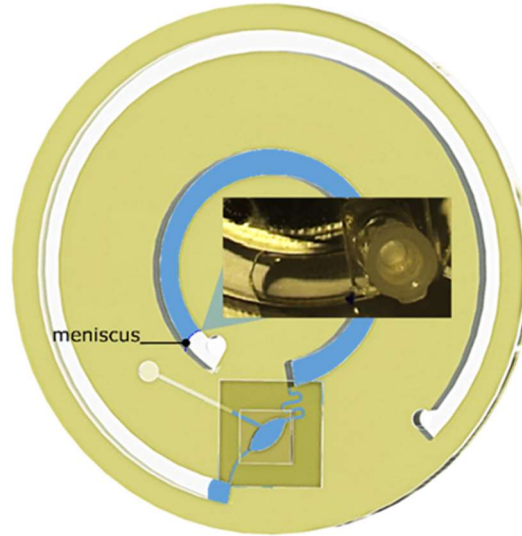


Figure 4.6 Illustration and photo of the meniscus created on disc. Figure reprinted with permission from [188].

The medium is pushed from the inlet to the outer units by the meniscus (Figure 4.6), the front of the liquid, mainly due to the Δp_c and together with the centrifugal force and Δp_{cap} . The capillary pressure equilibrium is established by the meniscus semi-circular shape. To maintain the equilibrium, it is necessary to ensure an adequate meniscus shape, which is possible if the inlet reservoir has a width of maximum 5 mm (the maximum width was chosen in this design). In fact, if the channel has a width bigger than 5 mm, the meniscus cannot be formed on this platform. On the contrary, widths less than 5 mm proved to be suitable: in fact, the waste reservoir has a width of 4 mm.

In order to design the inlet and waste reservoirs, two other factors have to be considered:

$$F = pA \tag{Eq. 3}$$

Where:

- p is the average pressure;
- A is the area of contact.

$$p(h) = \rho gh \quad \text{Eq. 4}$$

Where:

- ρ is the density of the fluid (culture medium in our experimental set-up);
- g is the gravitational acceleration;
- h is the height of the column of liquid (height of inlet/waste reservoir).

Eq. 3 expresses the force exerted on the meniscus by the liquid (culture medium) (Figure 4.7). It is shown that it depends on the average pressure, p , which is a function of h , the height of the column of liquid (height of inlet/waste reservoir). Therefore, the two equations (Eq. 3 and Eq. 4) show how changes in h have a significant effect on the pressure and consequently on the force exerted on the meniscus.

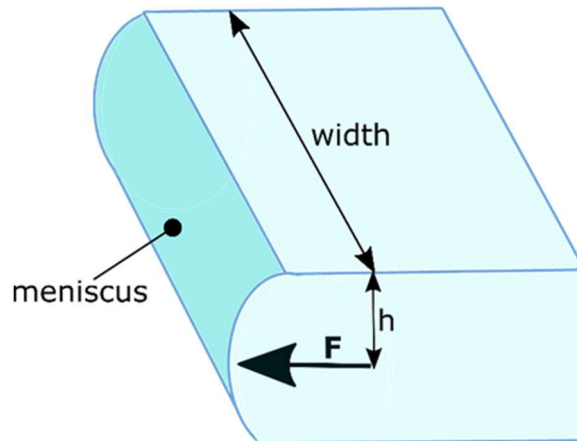


Figure 4.7 Schematic representation of F , the force exerted on the meniscus.

Figure reprinted with permission from [188].

The height of the inlet and waste reservoirs is 5.3 mm with a total volume of 3 ml and 5 ml respectively. The higher volume of the waste reservoir is due to its bigger diameter compared to the one of the inlet. Furthermore, having a waste bigger volume has the advantage of collecting more liquids in case of refilling of medium. The inlet volume of 3 ml was suitable for culturing cells from 1 up to 6 days, depending on the flow rates used without culture medium addition.

At the end of the inlet reservoir, a serpentine channel connects the inlet reservoir, where nutrients are placed, to the cell culture chamber (Figure 4.8). The microchannel has a serpentine shape, which create a tortuous path that can promote a better mixing of reagents, as reported in literature [202]. Moreover, the channel depth is 0.45 mm: this measure was optimized to achieve a flow rate of around few $\mu\text{l}/\text{min}$, necessary for cell culture.

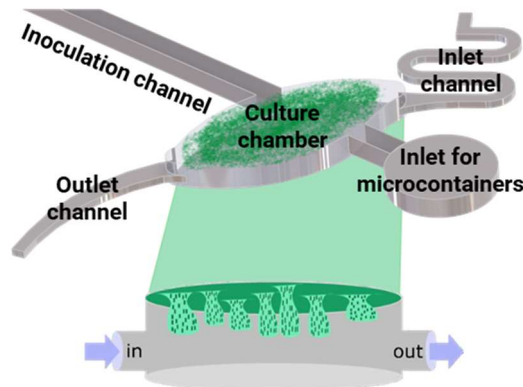


Figure 4.8 CAD model of the cell culture module. Draw of the cell culture chamber showed in detail where the bacterial biofilm growing attached to the top of the chamber is also presented.

An outlet channel connects the cell culture chamber to the waste reservoir. The straight shape facilitates the passage of waste products removed by the flow from the cell chamber.

The inlet and outlet channels were placed at the bottom of the cell chamber (Figure 4.8), both not to disturb bacteria growth on the top of the cell chamber and to avoid possible clogging due to biofilm formation into the channels.

The inoculation channel (Figure 4.8) with a depth of 0.65 mm allows the insertion of a needle for bacteria inoculation and it works also as a bubble trap. The inoculation hole was placed not in close proximity to the cell culture chamber in order to fit the device under the upright objectives of the confocal microscope. To introduce the drug delivery microdevices used as a treatment, a channel was added in close proximity of the cell culture chamber (Figure 4.8).

The cell culture chamber (Figure 4.8) has an inner volume of around 32 μl and a depth of 1 mm. It was designed to promote bacterial biofilm growth and to maximize the surface contact between the microdevices used for treatment and the bacterial biofilm. To prevent bubble formation in the cell culture chamber, this last one was designed with an oval shape without sharp edges.

4.1.1 Mammalian-Cell-culture-on-Disc: design optimization

To culture mammalian cells, the design of the BCoD was optimized for a Mammalian-Cell-culture-on-Disc (CoD) (Figure 4.9). Since mammalian cells grow attached to the bottom of the cell culture chamber, the platform had to be redesigned. For this reason and to minimize the effect of flow velocity over the culture, the inlet and outlet microchannels were placed on the top part of the cell culture chamber. Therefore, in the revised design, the culture medium enters in the cell chamber from the top without damaging the cells which grow at the bottom of the culture chamber. Moreover, the seeding channel is few millimetres longer than the BCoD inoculation channel to allow a better introduction of the syringe for cell seeding due to fabrication changes explained later.

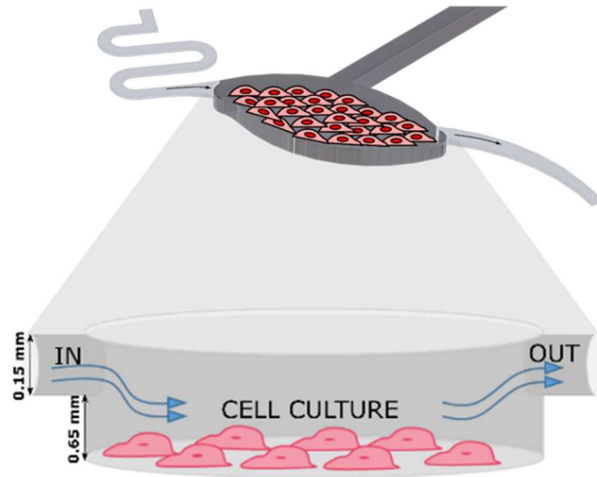


Figure 4.9 Optimized design of the cell culture chamber with microchannels on the top part to allow mammalian cells to grow attached to the bottom of the chamber.

4.2 Bacterial-Culture-on-Disc: fabrication process

Most of the devices used in research and for cell culture need to be disposable to avoid sample contamination [203]. In these kinds of applications it is thus fundamental to consider appropriately the type of material and the fabrication method.

Usually, polymers, such as poly(methyl methacrylate) (PMMA), polycarbonate (PC), polypropylene (PP), poly(dimethyl siloxane) (PDMS) and polystyrene (PS), are used because of their properties, e.g. thermal and chemical stability, biocompatibility [203], [204].

The fabrication processes mainly employed in research are hot embossing, injection molding, laser ablation, micromilling, soft lithography and X-ray lithography [203], [204].

In this project, the materials and the fabrication methods chosen for the development of the two platforms (BCoD and CoD) are compatible with cell cultures, sterilization and treatment reagents used during experiments.

Solidworks 2017 (Dassault Systèmes, Vélizy-Villacoublay, France) was used to design the device. The BCoD has an outer diameter of 100 mm and an inner one of 15.35 mm. It is composed of two layers of 0.60 mm thick PMMA (Axxicon Moulds, Eindhoven, The Netherlands), one layer of 5 mm thick PMMA (Nordisk plast, Randers, Denmark), two layers 0.15 mm thick PSA (ARcare® 90106, Adhesive Research, Limerick, Ireland) and a 0.15 mm cover glass (Gerhard Menzel B.V.&Co.KG, Braunschweig, Germany) to close the cell chamber for enabling confocal scanning laser microscopy detection (design modified from the original one shown and presented in [205]).

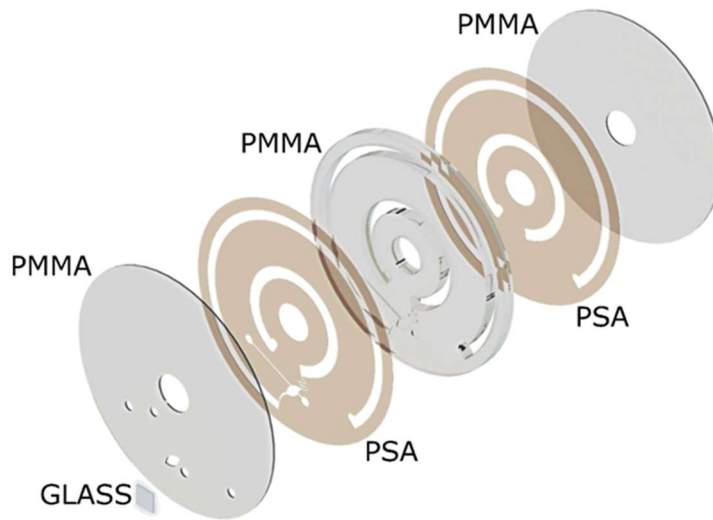


Figure 4.10 Exploded view of the BCoD with 3 layers of PMMA, 2 of PSA and a cover glass. Figure reprinted with permission from [206].

CO₂ laser ablation technique (Epilog Mini 18 30 W system, Epilog, USA) was used to fabricate the three PMMA layers, while micromilling (Mini-Mill/3, Minitech Machinery Corp, GA, US) was employed for the fabrication of microchannels and culture chamber.

A



CO₂ laser

B



Milling machine

C



Graphtec cutting plotter

D



Bonding press

Figure 4.11 Machines used for BCoD fabrication. (A) CO₂ laser, (B) milling machine, (C) Graphtec cutting plotter, (D) bonding press

CO₂ laser ablation is a photothermal process, in which an infrared radiation at a wavelength of 10.6 μm is continuously emitted by the CO₂ laser on the material. In the exact moment the laser beam meets the surface, the temperature rises immediately and the material first melts and then decomposes. In particular, at the boiling temperature, PMMA vaporizes in the form of monomers, leading to the formation of cavities [207]. However, if the process parameters are not optimized, part of the melted polymer can redeposit on the edge of the cut. These melted particles proved to be toxic for cells, which makes this technique unsuitable to fabricate the cell culture chamber using CO₂ laser engraving technique [208].

For this reason, micromilling technique was implemented for the fabrication of inlet and outlet channels and cell culture chamber. Milling is a subtractive manufacturing process, in which cutting tools are used to remove material and create micro-features

from bulk material [209]. A milling set-up is constituted of a worktable, which is able to move in xy plane and where the workpiece is placed, a spindle moving in z plane and a rotating cutting tool fixed on the spindle. First, a CAD design is loaded as a Computer numerical control (CNC) code on the machine software. The CNC code is created using a dedicated software, as for example CimatronE (Giv'at Shmuel, Israel), which was used in this project. Once the CNC code is ready and uploaded on the software of the milling machine, the workpiece is fixed on the worktable with screws or double adhesive tape. Before starting the process, the rotating tool is manually aligned in the z plane, thus introducing an experimental error. During the cutting process, the rotating tool was cooled down with water.

The adhesive part of the PSA is composed by a layer of clear polyester (MA-69 acrylic hybrid medical grade adhesive). The two PSA layers were cut using a cutting plotter, CE-40, Graphtech, U.S.A., whose software uses as an input a .dxf file of the device design.

The different layers of PMMA were cleaned with sonication in ultrapure water and ethanol and then assembled with the PSA layers using a bonding press (PW 10 H, P/O/Weber, Germany), with a force of 10 KN for 1 min to remove possible air bubbles.

Finally, the cover glass was glued using a silicone glue (Super Clear Silicone, Versachem, Hartford, Connecticut, USA) and let dry overnight.

A sterile environment was kept inside the BCoD by using commercial sterile filters with a 3 mm diameter membrane and a pore size of 0.20 μm (Figure 4.4). The filters were secured on the venting holes with the help of luers fabricated in cyclic olefin-copolymer (COC) (TOPAS grade 5013L-10, Advanced Polymers GmbH, Frankfurt-Höchst, Germany), using injection molding (Victory Tech 80/ 45, Engel, Schwertberg, Austria). Injection molding is a fabrication process where a polymer in the form of

pellet is melted and injected under high pressure into a heated mold cavity [210]. Fabrication steps are also described in the paper written by Seriola et al. [205].

4.2.1 Mammalian-Cell-culture-on-Disc: fabrication optimization

The fabrication process of the CoD platform was optimized to be suitable for mammalian cell culture. The first significant difference between the two platforms can be found in the manufacturing technique used for creating the depth of the culture chamber: in fact, micromilling was not used for the CoD. This is due to the tendency of the cutting tool to create a certain roughness which could influence and disturb mammalian cell growth. Moreover, the design of the CoD was inverted compared to the BCoD, as previously showed in Figure 4.9.

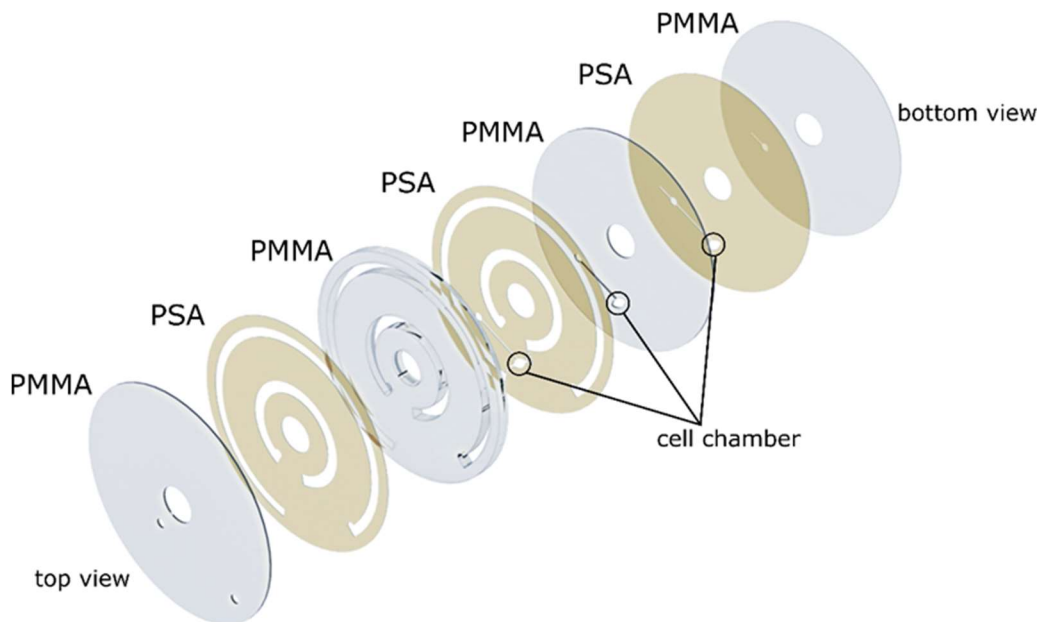


Figure 4.12 Exploded view of the CoD with 4 layers of PMMA and 3 layers of PSA. Figure reprinted with permission from [211].

The CoD consists of 1 layer of 5 mm thick PMMA, 3 layers of 0.5 mm thick PMMA and 3 layers of 0.15 mm thick PSA.

The PMMA and the PSA layers were realized as above described for the BCoD platform. However, since inlet and outlet channels were cut in the PSA, the bonding force was decreased to 1 kN not to clog the channels.

4.3 Flow and shear stress characterization

A stable and constant flow rate over time is essential to culture cells on the platform. To define the relationship between flow rate and the rotational frequency of the spindle motor, calibration curves were constructed both for the BCoD and the CoD. In addition, the stability of the flow rate was tested over days and within platforms.

4.3.1 BCoD and CoD flow characterization

The procedure for the characterization of the flow is the one described by [205].

After the sterilization of the disc, the cell culture medium was inserted in the inlet reservoir until the beginning of the waste reservoir and filters were put in place, sealing the venting holes. Then, the disc was placed on an optical spin stand and the meniscus in the inlet was created using a rotational speed of 2 Hz. Before starting the calibration process, the rotational frequency was set to 0.35 Hz for 2h, to slow down the flow and dissipate energy accumulated during the high rotational speed. Once the process started, the rotational frequencies were gradually increased from 0.60 Hz up to 1 Hz for the BCoD and from 0.70 Hz up to 1 Hz for the CoD. The volume of the liquid was measured at defined times points. The measurement of the liquid volume was extracted from the images taken in the inlet reservoir through a Matlab (MATLAB 9.3, Natick, Massachusetts) code as previously described by [212]. For each frequency, images were taken at three different time points using the camera application software PCO Camware (PCO Camware 64, PCO AG).

The flow rate was calculated in Excel using the formula:

$$\Delta Q = \Delta V / \Delta t \quad \text{Eq. 5}$$

Where:

- ΔQ is the flow rate;
- ΔV is the volume of moved liquid;
- Δt is the interval between every measurement

As shown in Figure 4.13A, for the BCoD a good linear dependency was observed between 0.60 and 0.80 Hz. Variations in flow rate were below 15% RSD (relative standard deviation) when evaluating three discs, while variations in flow stability over 3 days were below 5% RSD (relative standard deviation).

Also for the CoD (Figure 4.13B), a good linear dependency was observed between 0.70 Hz to 1 Hz. Variations in the flow rate were below 15% RSD (relative standard deviation) when evaluating three discs, while variations in stability over 6 days were below 20% RSD (relative standard deviation).

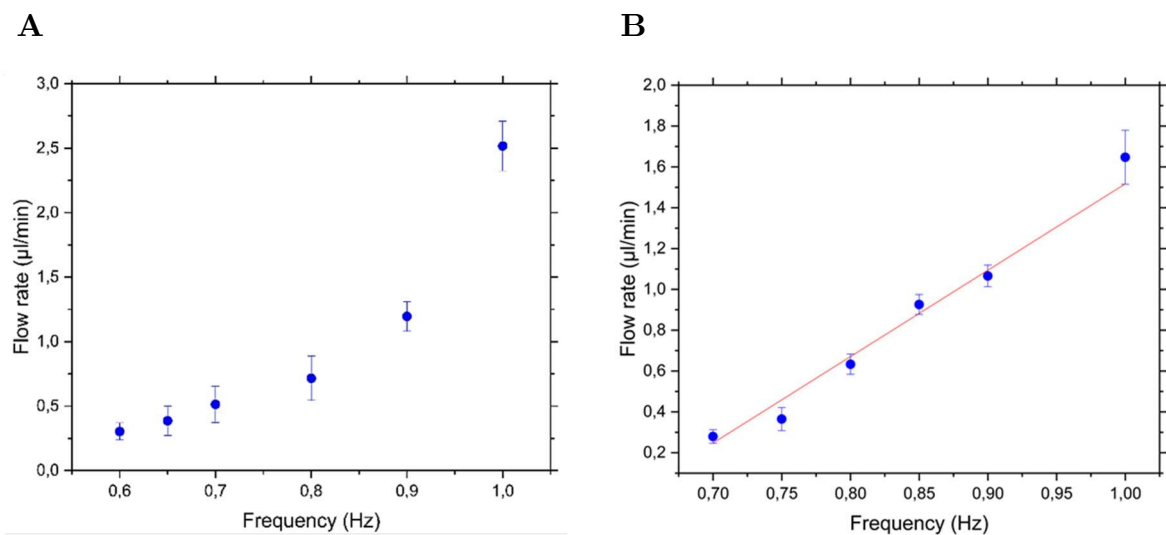


Figure 4.13 Calibration curves of the BCoD and the CoD. **(A)** BCoD calibration curve using 100 times diluted Artificial Sputum Medium (ASM) with 10 times diluted mucin. **(B)** CoD calibration curve using Dulbecco's Modified Eagle Medium (DMEM+). Figure reprinted with permission from [206] and [211].

4.3.2 BCoD and CoD shear stress characterization

In literature, it has been shown that shear stress has an effect on the growth of both bacterial and mammalian cells [213], [214]. For this reason, the shear stress that cells might experience during perfusion culture was evaluated on both platforms.

Computational fluid dynamics (CFD) simulations were performed with COMSOL (COMSOL Multiphysics 5.3a, Stockholm, Sweden) as described in [205]. The flow velocity through the culture chamber and the shear stress effect over cells were quantified.

In the BCoD, the maximum wall shear stress is established at the end of the inlet channel and at the beginning of the outlet channel (Figure 4.14A). The cause of this shear stress value is the sudden expansion and contraction of the geometry, which make the flow velocity locally increase and have higher values in the central part of the cell chamber. The maximum shear stress value in the centre is approximately an order of magnitude higher than the average shear stress in the cell culture chamber. The simulated maximum shear stress at 2 $\mu\text{l}/\text{min}$ (0.8 Hz) is 0.6 mPa. As shown in [215], *P. aeruginosa* growth was unaffected at shear stresses up to 17 mPa. Therefore, since simulations showed that bacteria are exposed to lower shear stresses, we conclude that the flow rate used is appropriate for bacteria growth and biofilm formation.

As expected, in the CoD the shear stress showed the same geometrical dependence (Figure 4.14B). The highest calculated shear stress at a flow rate of 0.6 $\mu\text{l}/\text{min}$ is 0.08 mPa. Mammalian cells are very sensitive to shear stress [214]. However, data shown by Zór et al. [216] demonstrated that a flow rate of 1 $\mu\text{l}/\text{min}$ did not cause any negative effect on a culture of *Saccharomyces cerevisiae*. Moreover, a study by Kim et al. [217] proved that Caco-2 cells did not differentiate when the shear stress is 0.6 mPa. Therefore, we can assume that the lower shear stress present in the CoD cell chamber,

which is 7.5 times lower than the one reported in literature, should not cause any adversary effect.

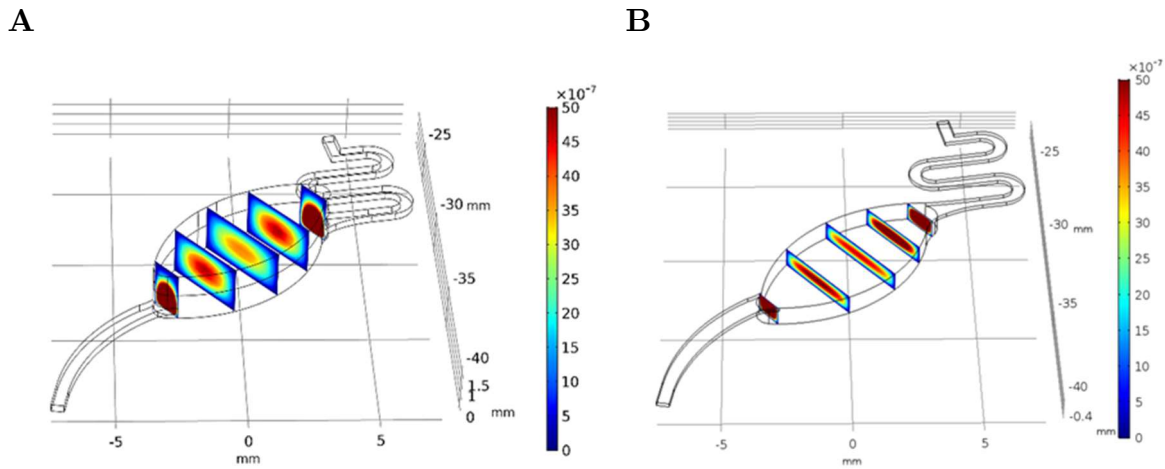


Figure 4.14 Comsol simulations. (A) Flow velocity profile in the BCoD at a flow rate of $1\mu\text{l}/\text{min}$. (B) Flow velocity profile in the CoD at a flow rate of $0.6\mu\text{l}/\text{min}$.

Figure reprinted with permission from [205] and [211].

4.4 BCoD and CoD sterilization process

The process of sterilization of the BCoD and CoD platforms is fundamental to avoid cell culture contamination from other cells of the environment.

Different sterilization methods are usually employed, such as autoclaving, ethylene oxide and radiations (gamma and electron beam radiations) treatments, hydrogen peroxide plasma [218]. However, since these methods were either non compatible with the material and/or fabrication process or not available, in this project the sterilization process was carried out using sodium hydroxide (NaOH). In [216], K. Zór *et al.* demonstrated NaOH efficiency in cleaning *in vitro* systems.

As described in [205], the disc chambers and channels were filled from the inlet reservoir opening with NaOH (0.5 M) using a syringe. The cleaning agent was then left in the BCoD for 20 min and in the CoD for 30 min. Immediately after, NaOH was removed

and the disc was rinsed with sterile water and autoclaved medium three times to remove NaOH completely. At the end, autoclaved filters and luers were mounted on the venting holes.

For both the BCoD and the CoD, the sterilization process was performed manually under a sterile bench.

4.5 Cell inoculation and growth

4.5.1 BCoD cell inoculation and growth

An overnight culture of *P. aeruginosa*, lab strain PAO1, was prepared in Luria Bertani (LB) medium at 37 °C with a final concentration of approximately 4×10^7 cells/ml (OD₆₀₀ of 0.05). LB medium is composed of 10 g/l bacto-tryptone, 5 g/l yeast extract and 5 g/l sodium chloride solubilized in deionized water and sterilized by autoclaving at 121 °C for 15 minutes.

In this project, 10 times diluted mucin and 100 times diluted nutrients ASM was used to culture bacterial cells. To prepare 50 ml of ASM, first, 2 mg of DNA from fish sperm and 25 mg of mucin from porcine stomach (type II) were dissolved in two different bottles filled with 12.5 ml of sterile water and left overnight at 150 rpm in a 30°C room. The two solutions were then mixed together. 50 µl of essential and non (except l-cysteine and l-tyrosine) amino acids stock solution 2.5 mg/ml, 12.5 µl of l-cysteine (dissolved in 0.5 M potassium hydroxide) and 12.5 µl of l-tyrosine (dissolved in sterile water) stock solution 10 mg/ml, 50 µl of ASM salts (diethylenetriaminepentaacetic acid (DTPA) 59 µg/ml, NaCl 50 mg/ml, KCl 22 mg/ml) and 2.5 µl egg yolk were added and mixed with the DNA and the mucin. The final solution was sterilized using a filtration technique with a filter of 0.22 µm pore size.

Once the ASM was ready, 3 ml were introduced into the platform from the inlet reservoir opening until the beginning of the waste reservoir. After placing the BCoD on the spin stand, the platform was spun at a rotational frequency of 2 Hz for a few seconds to create the front of the liquid and then at 0.63 Hz (0.3 $\mu\text{l}/\text{min}$) or 0.70 Hz (1 $\mu\text{l}/\text{min}$) for 2 h to stabilize the flow.

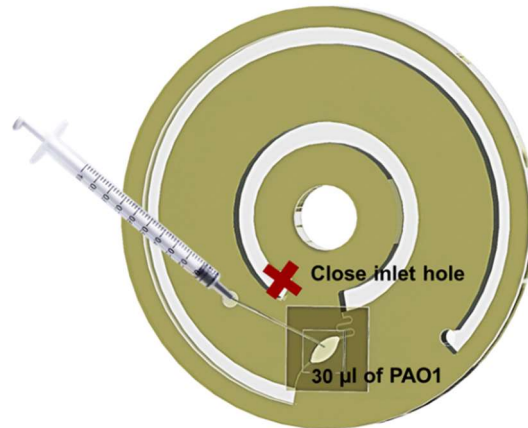


Figure 4.15 Representation of PAO1 inoculation process.

After the flow stabilization, 30 μl of overnight culture of *P. aeruginosa* diluted to $\text{OD}=0.05$ (around 100 times dilution of the overnight culture) were inoculated in the sterilized disc through the inoculation opening (Figure 4.15). While inoculating the bacteria solution, the inlet reservoir opening was kept closed to prevent bacteria from entering the medium reservoir. At the end of the inoculation process, the platform was left in static conditions for 1 h to allow bacteria to adhere to the culture chamber.

The spindle motor set-up was placed in a 37°C incubation room in order to have appropriate culture conditions. A flow rate of 1 $\mu\text{l}/\text{min}$ was used to grow bacterial cells from single cells to biofilm.

4.5.2 CoD cell inoculation and growth

The medium used for mammalian cell culture is Dulbecco's Modified Eagle Medium (DMEM), which contains 4.5 g/L glucose supplemented with 10% (v/v) heat-

inactivated fetal bovine serum (FBS), 1% (v/v) non-essential amino acids (NEAA), 2 mM L-glutamine and 1% (v/v) penicillin-streptomycin (P/S).

The inoculation process of mammalian cells involves a further step compare to the one for bacterial cells. Before introducing the culture medium, 23 μ l of Matrigel (300 μ g/ml) (Corning, United Kingdom) diluted in serum-free DMEM were used to coat the cell chamber in order to provide a good microenvironment for cell attachment. The Matrigel solution was introduced in the cell chamber via the seeding channel. Then, the CoD was left in an incubator at 37°C and with 5% CO₂ levels for 1 h. After the incubation, the platform was filled with cell culture medium from the inlet reservoir opening until the beginning of the waste reservoir.

Before seeding, cells (between passages 8-40) were trypsinized with trypsin/ETDA solution (0.05%) in order to dissociate adherent cells from the flask in which they were being cultured in static conditions. They were then optically evaluated with a bright field microscope (Axiovert 25, Zeiss, Oberkochen, Germany) and counted using an automated cell counting unit (NucleoCounter® NC-200TM, ChemoMetec A/S, Allerød, Denmark).

Different seeding cell density were used:

- 1,5 x 10⁵ cells/cm² for Caco-2 cells;
- 0.75 x 10⁵ for HeLa cells.

The cells were seeded though the cell seeding inlet using a sterile syringe and needle (Figure 4.16). As explained previously, the inlet reservoir opening was kept closed during seeding to avoid cells entering in the serpentine channel and the inlet reservoir.

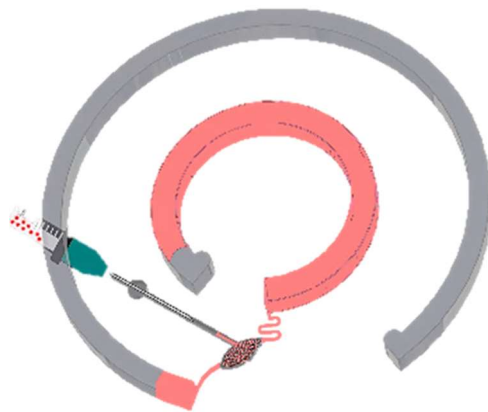


Figure 4.16 Representation of the mammalian cells seeding process.

The CoD was then placed in static conditions in an incubator for 1 h (HeLa cells) or 2 h (Caco-2 cells) to allow cell attachment. The spindle motor was then set at a constant flow rate of 0.6 $\mu\text{l}/\text{min}$.

4.6 BCoD and CoD treatment

4.6.1 BCoD antibiotic treatment

Bacteria were cultured for 48 h at a flow rate of 1 $\mu\text{l}/\text{min}$ before antibiotic treatment. Ciprofloxacin with a final concentration of 4 $\mu\text{g}/\text{ml}$ (10 μM) was chosen as an antibiotic treatment.

As mentioned in Chapter 2.4 “*Bacterial Culture on disc (BCoD) microfluidic platform*”, to test the versatility of the BCoD different antibiotic treatments were administered: bolus injection, microcontainers (MCs) loaded with ciprofloxacin and coated with Chitosan (CHI), and MCs loaded with ciprofloxacin and coated with CHI together with N-acetylcysteine.

To mimic intravenous bolus injection, the antibiotic was added directly into the cell chamber with a syringe.

MCs were introduced using the inoculation channel in close proximity of the cell chamber created for this purpose. In a previous study [132], CHI-coated MCs have already shown promising results in the treatment of biofilm-related infections due to CHI mucoadhesive properties. Instead, CHI/NAC-coated MCs were a new functionalized microdevices, whose coating was tested for the first time during these experiments. As shown in [219], NAC proved to be effective in the treatment of mature biofilms due to its mucolytic properties. In this project, the mucolytic activity of NAC was tested in the presence of CHI.

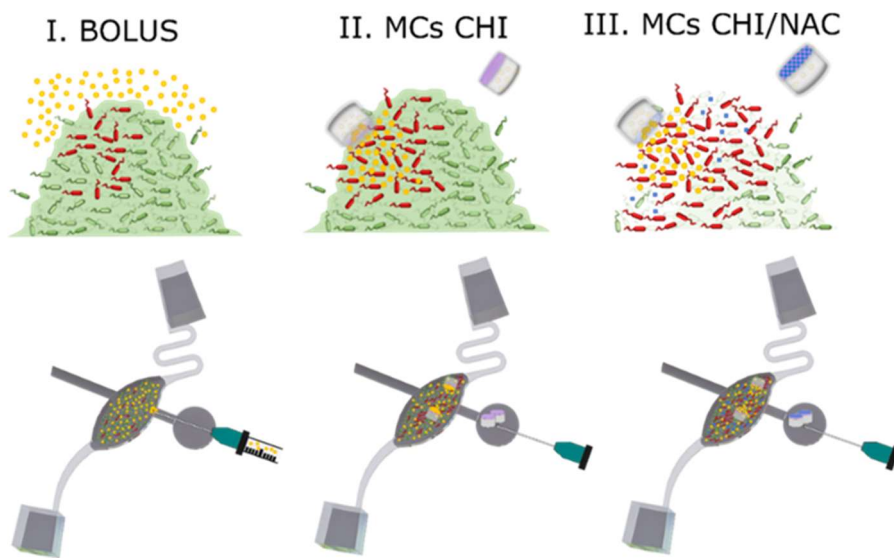


Figure 4.17 Schematic representation of the different antibiotic treatments for biofilm eradication. **(I)** CIP bolus, **(II)** CHI-coated MCs, **(III)** CHI/NAC-coated MCs. Figure reprinted with permission from [206].

4.6.1 CoD doxorubicin treatment

As mentioned in Chapter 3.3 “*Mammalian Cell culture on disc (CoD) microfluidic platform*”, the CoD was used for cytotoxicity studies using doxorubicin as a model anti-cancer drug on HeLa cells.

Before the introduction of the drug, HeLa cells were grown for 24 h at a flow rate of 0.6 $\mu\text{l}/\text{min}$ creating a monolayer of cells. Doxorubicin was then introduced through the

inlet reservoir opening and perfused over time on the culture. Different concentrations were compared: 1 μM , 5 μM , 10 μM , 100 μM .

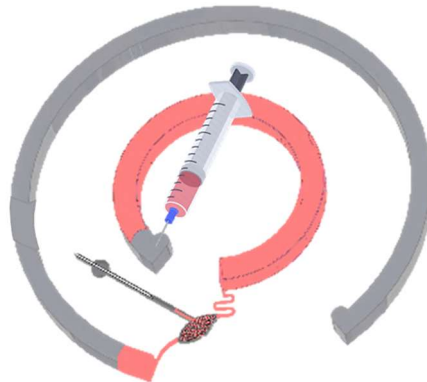


Figure 4.18 Schematic representation of the doxorubicin treatment on HeLa cells.

4.7 Optical monitoring and data analysis

4.7.1 Bacterial biofilm biomass and viability monitoring and data analysis

Bacterial cell monitoring was carried out with confocal laser scanning microscopy (CLSM) technique.

CLSM is an optical technique, in which a laser light is focused on a small spot of a sample. The signal detected from the reflected, transmitted or fluorescent light is then stored to create an image [220]. One of the advantages of CLSM is its ability of scanning through different z planes recording a series of optical sections at different focus positions. At every z plane, images are collected and assembled in order to reconstruct a 3D volume of the sample [221]. Therefore, it gives the possibility of analysing the biofilm growth and its changes [222]. Moreover, confocal microscopy is not an invasive technique and it enables *in situ* detection of living cells over time [223].

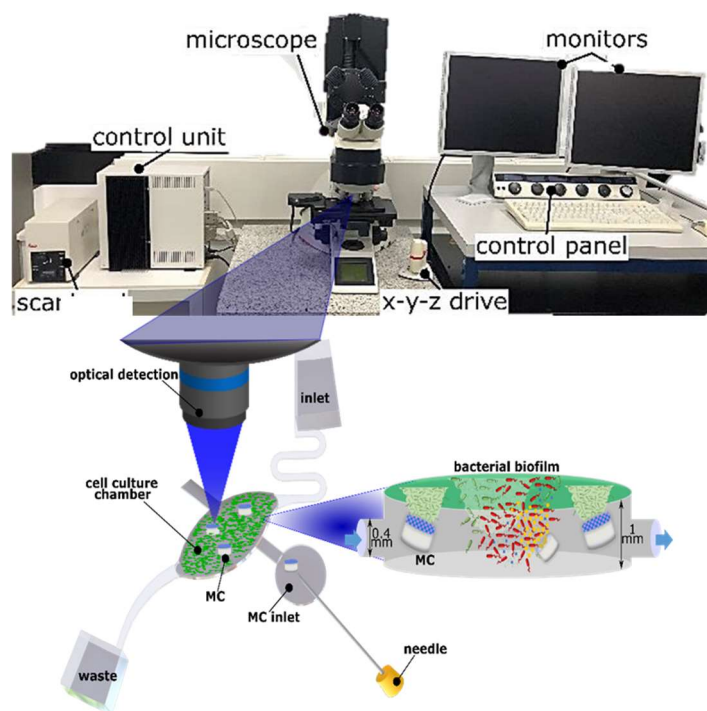


Figure 4.19 Leica SP5 confocal laser scanning microscope with a schematic representation of the cell culture chamber optical detection.

In this project, CLSM was used with a z step of 1 μm to scan the biofilm through the z planes to monitor its growth (Figure 4.19). The choice of the step size is related to the size of *P. aeruginosa* bacterium, which is around 1-3 μm in length [120].

The CLSM used is an upright Leica (Leica SP5 CLSM, Leica Microsystems, Mannheim, Germany) equipped with an argon/krypton laser and detectors and filter sets for simultaneous monitoring of GFP (excitation: 488 nm, emission: 493–558 nm) for live cell imaging (cells fluorescent green) and propidium iodide (excitation: 543 nm, emission: 558–700 nm) for dead cell staining (cells fluorescent red). In fact, as mentioned in Chapter 2.4 “*Bacterial Culture on disc (BCoD) microfluidic platform*”, the PAO1 strain used was genetically modified using a GFP tag to allow the detection of alive bacteria. Instead, 2 μl of 20 mM propidium iodide added in the culture medium were used to detect dead cells. Propidium iodide is a stain capable of entering into the bacterium only when the membrane is damaged, therefore when the bacterium is dead. Images were obtained using a 50x water objective (numerical aperture 0.75). In each

experiment, two biological replicates were used, and eighteen technical replicates were collected from different sections of the culture chamber.

IMARIS software was used to treat the confocal images. Imaris[®] is a software developed by a Swiss company, Bitplane AG (<http://www.bitplane.ch>). This image analysis software enables advanced analysis of images, which represents an indirect tool for biofilm evaluation. From the acquired confocal images, pseudo 3D images with shadow projection, cross-sections, isosurface presentation, and animations can be produced by the software. An example of images treated with Imaris[®] is shown in Figure 4.20.

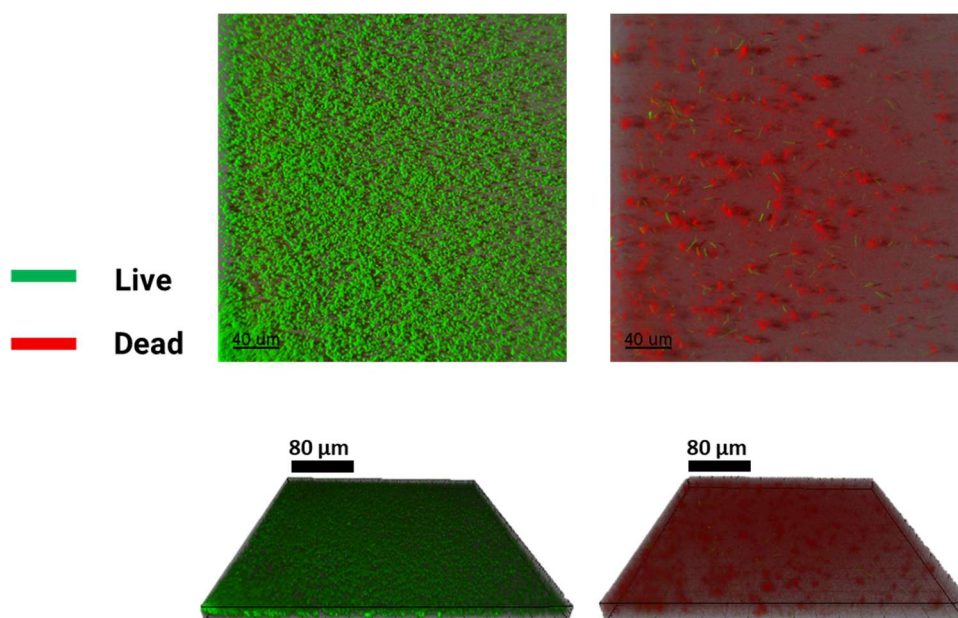


Figure 4.20 Confocal images of a *P. aeruginosa* biofilm after 48 h of growth and 24 h of antibiotic treatment treated using the software Imaris[®].

All the collected images were used as an input to calculate the bacterial biomass. The software used to make biomass quantification and biomass viability was Comstat (Comstat, Technical University of Denmark) (Figure 4.21). Comstat (<http://www.comstat.dk>) is an analysis package often used for quantitative and statistical analysis [224]. It was originally developed as a MATLAB[®] script [224] and later implemented on ImageJ as a plugin [225]. Comstat takes as an input file the

confocal images. The software can provide different output data such as total biomass, thickness distribution, roughness, colonies at substratum and many others. However, the software sometimes showed a limited capacity of discriminating between cells and image noise due to the automatic threshold function. In some cases, it was necessary a manual threshold adjustment, which increased the analysis time and the result variability.

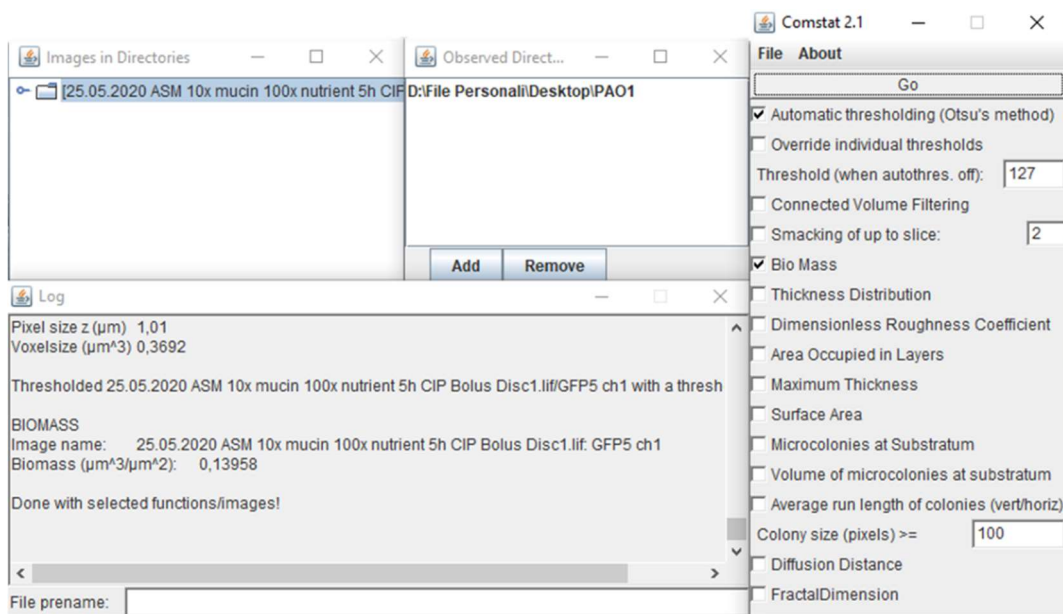


Figure 4.21 Comstat user interface

At the end of the analysis, Origin 2018b (OriginLab Corp, Northampton, USA) was used to display the data. The total biomass and the biomass viability were plotted as a bar chart in relation of the hours of growing and the hours of treatment.

4.7.2 Mammalian cells growth and viability monitoring and data analysis

To monitor mammalian cells growth and treatment a miniaturize integrated optical microscope, also called Microscope-on-Disc (MoD) was developed (Figure 4.21A-B). The optical detection unit was placed on the top of the CoD spindle motor and placed in the incubator. The camera was mounted in close proximity of the cell culture

chamber for the real-time optical monitoring (Figure 4.21C). A 2.4 GHz Wi-Fi receiver/transmitter transfers wirelessly the recorded images to a computer placed outside the incubator. The MoD is thus able of monitoring cells in real-time while the disc is spinning.

As shown in Figure 4.21A, the main components of the optical unit are:

- camera;
- camera controller;
- objective lens;
- focus screw;
- Light Emitting Diode (LED) light.

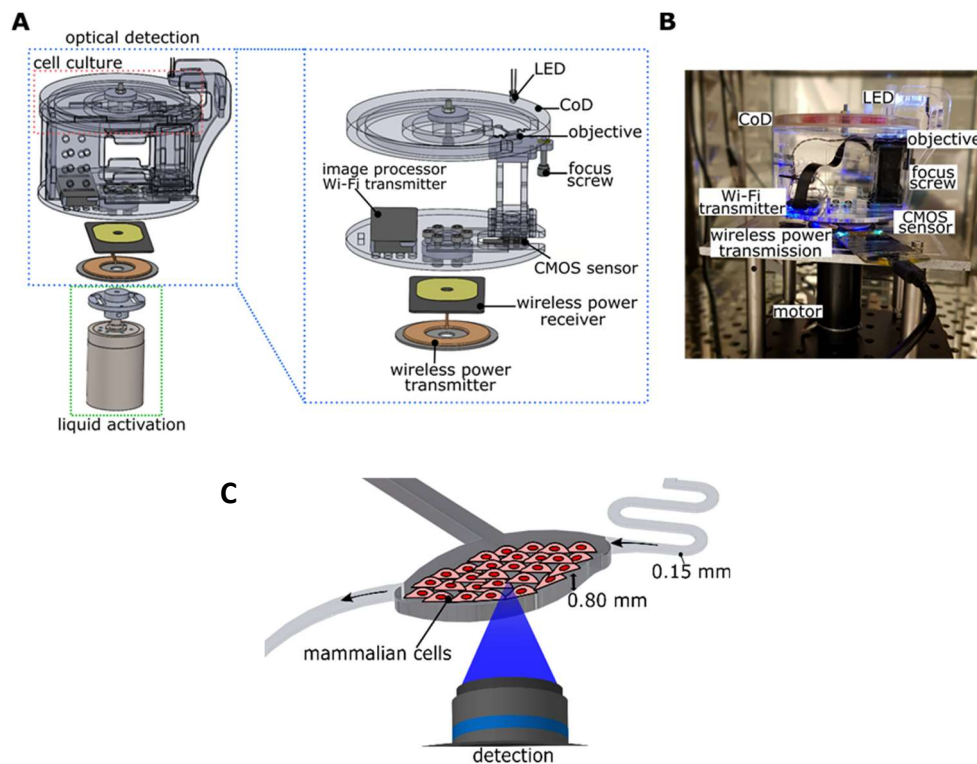


Figure 4.21 Microscope on Disc used for real-time optical detection of mammalian cells. (A) Exploded view of the CMoD with its major components. (B) Photograph of the microfluidic platform in the incubator and its specification. (C) Schematic representation of the cell chamber optical detection

It has a total high of around 85 mm, which, together with the liquid actuation unit, allows a perfect fitting in the cell incubator (Figure 4.21B). The microscope structure is mainly made of PMMA. The structure is also fundamental to separate the CoD from the Complementary Metal-Oxide-Semiconductor (CMOS) sensor, the wireless power transmitter/receiver and the Wi-transmitter, which generate heats capable of damaging cells.

The main optical module is placed inside the PMMA frame and is composed of a CMOS sensor (1280 x 720 pixels with either a 1538 x 865 μm or a 338 x 190 μm field of view), an objective lens and a focus screw. The theoretical resolution is 1.20 x 1.20 μm or 0.26 x 0.26 μm per pixel depending on the field of view. The focus screw is used to bring into focus the cell culture and a movable LED light is used to adjust the light level during optical monitoring.

An iSpy software is able of capturing a maximum of 30 frames per second, cloud storage and real-time video streaming. Moreover, the MoD frame is compatible with different objectives enabling the possibility of having different resolutions. However, a drawback is that this system cannot monitor the whole cell chamber.

As already mentioned in Chapter 3.3 “*Mammalian Cell culture on disc (CoD) microfluidic platform*”, for quantitative analysis of cell proliferation and cell viability, the software Cellari (<https://cellari.io/>) was chosen (Figure 4.22). This software is based on artificial intelligence for image analysis.

At the beginning, MoD images were uploaded on Cellari and annotations regarding alive and dead cells were added manually. This step is fundamental since the software is based on machine learning and a preliminary training is necessary to extract accurate information from the dataset. Once the software was trained, it was able to discriminate between alive and dead cells and to calculate the pixel area of cells in the images taken by the iSpy camera. In fact, Cellari is based on pixel recognition: it is able of recognizing

alive and dead cells depending on their shape. In our case, HeLa cells present an elongated shape when they attach at the bottom of the cell culture chamber during growth, while they have a rounded shape when they detached from the chamber and die after the administration of the drug. In this way, when the software detects a change in cell shape, it highlights the cells and groups them in the two categories of alive and dead. As a result, it gave the total pixel area of the two groups, from which was possible to calculate cell viability.

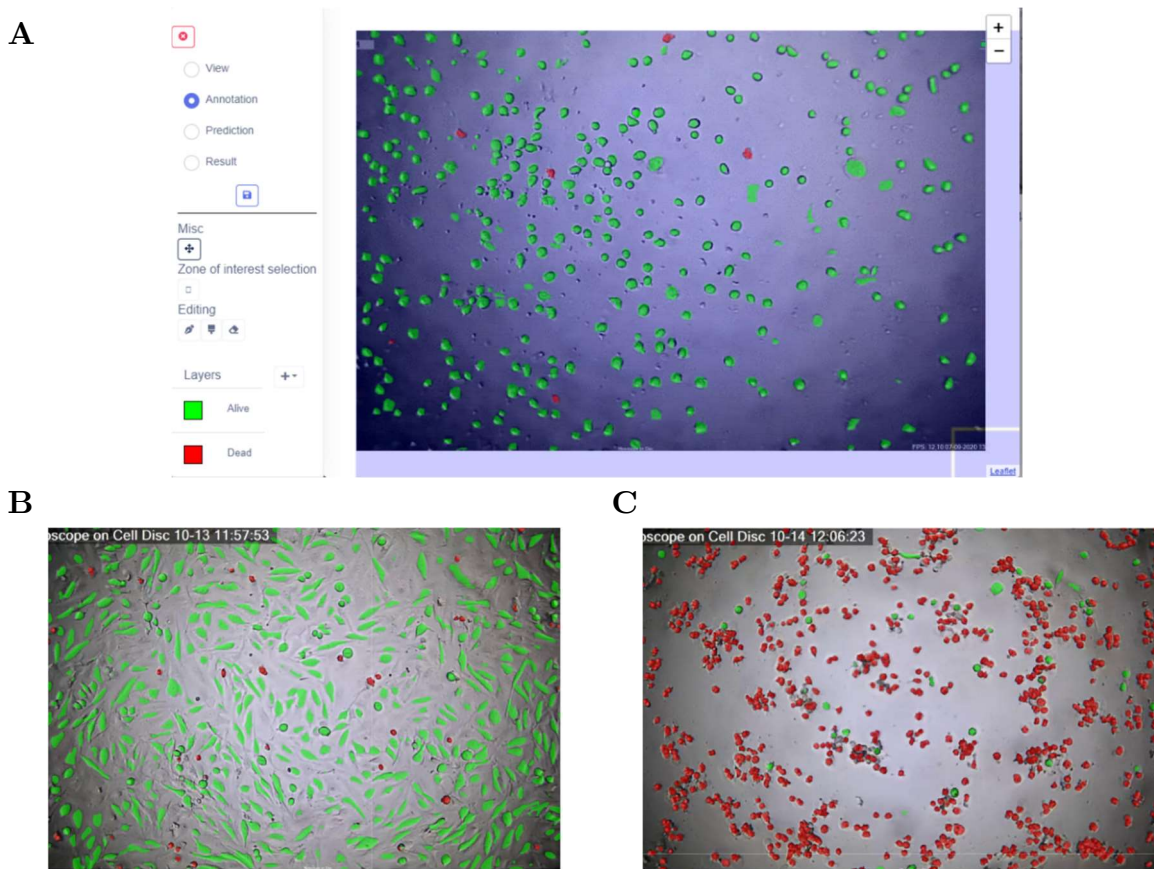


Figure 4.22 Cellari user interface. (A) Manual annotations for training the software. Predictions on alive and dead cells during growth (A) and treatment (B).

To assess MoD reliability, at precise time points images were taken also with a traditional inverted light microscope with a 10x or 20x objective and compared to those taken in real-time with the MoD.

At the end of every experiment, a LIVE/DEAD Cell Imaging Kit (488/570) (Invitrogen, Roskilde, Denmark) was used to determine alive and dead cells to check the numerical results obtained. Green fluorescence for alive cells was measured at ex/em 488 nm/515 nm, while red fluorescence for dead cells at ex/em 570 nm/602 nm. Confocal images were taken with Zeiss LSM 700, Oberkochen, Germany confocal microscope.

5. Results and discussion

5.1 Bacterial Culture on Disc (BCoD) results

BCoD results focus on the formation and growth of *P. aeruginosa* biofilm (lab strain PAO1) and on the efficacy of different antibiotic administration methods on the biofilm. The results about growth and treatment are presented in two different paragraphs.

5.1.1 PAO1 biofilm development and growth

The BCoD platform has proved, as already discussed in a previous work by Seriola et al. [205], to be a useful device to culture PAO1 from single cells to biofilm status in perfusion.

The results obtained using Comstat, the selected software for quantification of biomass are presented in Figure 5.1A. Confocal images treated using Imaris[®] are shown in Figure 5.1B.

The selected flow rate of 1 $\mu\text{l}/\text{min}$ (chosen based on previous studies [205]) guaranteed a proper amount of nutrients and oxygen to make bacteria grow and develop into a multi-layered biofilm in 48 h. The optimized composition of the artificial sputum medium (ASM), 10 times diluted mucin and 100 times diluted nutrients, allowed bacteria to form aggregates already at 6 h (Figure 5.1B), until creating a uniform multi-layered biofilm in the cell chamber, with a biomass of $5.21 \pm 1.49 \mu\text{m}^3/\mu\text{m}^2$ at 24 h. At 48 h the biomass reached a value of $6.35 \pm 2.28 \mu\text{m}^3/\mu\text{m}^2$ (Figure 5.1A).

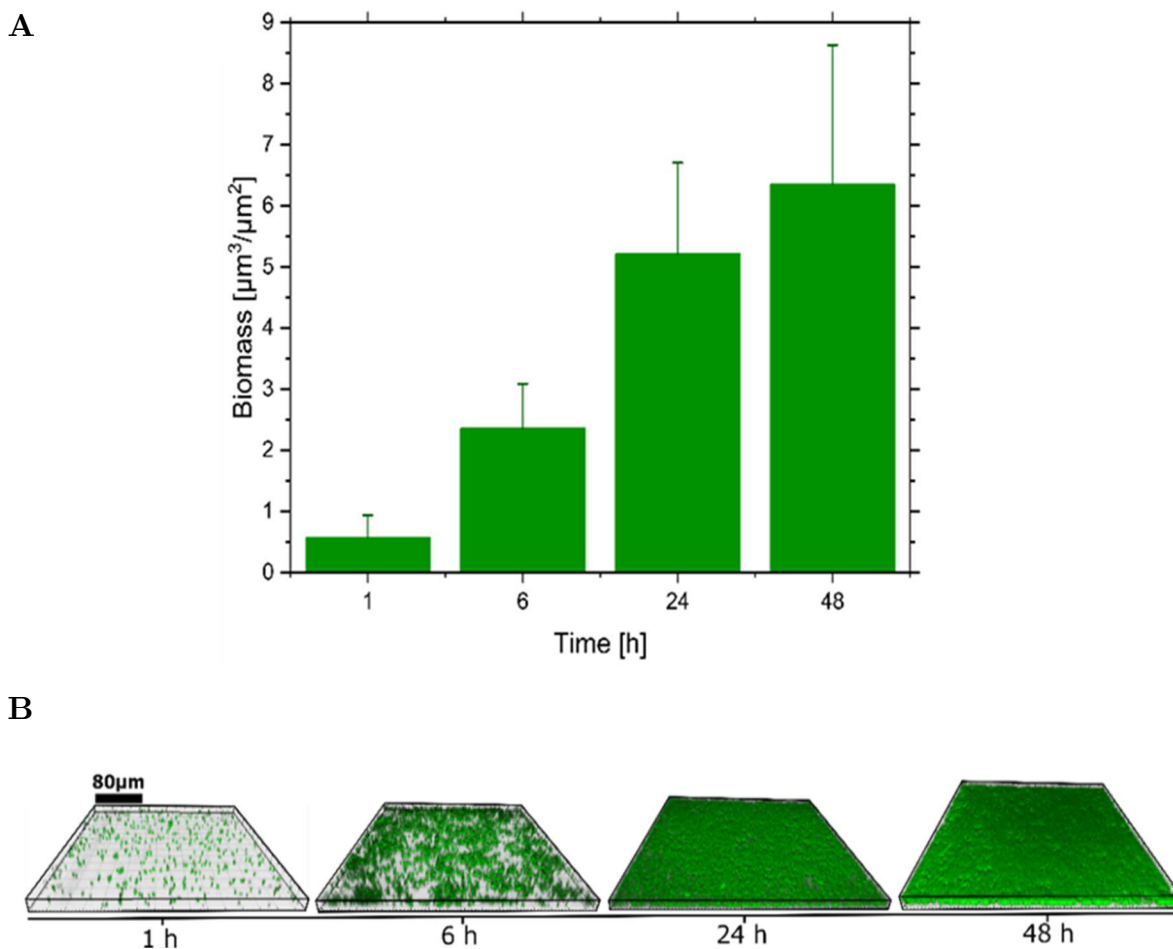


Figure 5.1 Bacterial biofilm growth and biomass quantification in optimized ASM.

(A) Mean and standard deviation (SD) on 6 biological replicates, each with 9 technical replicates resulting in a total of $n=54$ confocal images. (B) Confocal images of PAO1 growth monitored in the same spot at different time points. Figure reprinted with permission from [206].

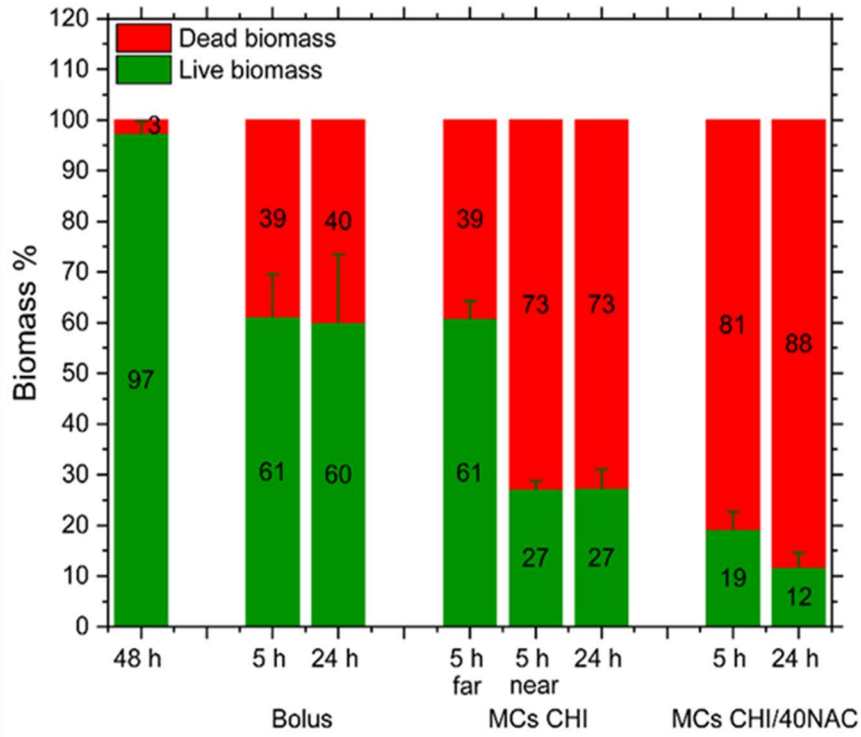
In the cell culture chamber, biofilm developed homogenously (Figure 5.1B) and in all 6 discs the biomass growth was comparable, with only a 15.81% relative standard deviation (RSD) in average of biomass.

5.1.2 PAO1 biofilm treatments

As mentioned in Chapter 2.4 “*Bacterial Culture on disc (BCoD) microfluidic platform*” and explained in details in Chapter 4.6.1 “*BCoD antibiotic treatment*”, different

antibiotic administration methods were selected and compared: I) bolus injection (to mimic intravenous administration on patients), II) microdevices called microcontainers (MCs) coated with Chitosan, or III) Chitosan and N-acetylcysteine (Figure 5.2).

A



B

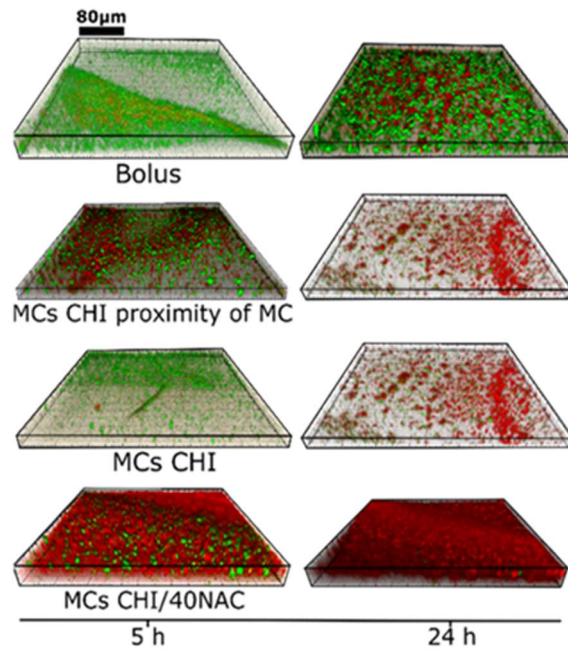


Figure 5.2 Effects of different antibiotic administration methods (bolus injection, MCs coated with Chitosan, MCs coated with Chitosan and N-acetylcysteine) after 5 h and 24 h from treatment introduction on bacterial biofilm. **(A)** Data obtained on a total of n=18 confocal images, **(B)** confocal images of the treatments. Figure reprinted with permission from [206].

In Figure 5.2 the effects of bolus injection and CHI-coated and CHI/NAC-coated MCs treatments are shown at 5 h and 24 h after treatment introduction on the bacterial biofilm. Figure 5.2A shows Comstat quantification of alive and dead biomass, while Figure 5.2B confocal images taken at the two chosen time points and treated with Imaris[®].

The bar chart (Figure 5.2A) shows that almost all biomass was alive before treatment, $97.44 \pm 2.31\%$. It was observed that $61.14 \pm 8.40\%$ of the biomass was still alive after 5 h from the CIP bolus injection and $60.13 \pm 13.28\%$ after 24 h. MC treatment had a better effect of biofilm eradication. CHI-coated MCs killed $72.76 \pm 1.52\%$ of the biomass after 5 h in the area in close proximity of the microdevice, while only $39.12 \pm 3.35\%$ in the rest of the chamber. This could be due to the slow antibiotic released caused by CHI, in fact after 24 h from treatment $27.32 \pm 3.73\%$ of the bacterial biomass was alive in the entire cell culture chamber. The major effect was found with CHI/NAC coated MCs: in fact, after 5 h of treatment only $19.25 \pm 3.50\%$ of the biomass was still alive, reaching a value of $11.78 \pm 2.89\%$ alive biomass after 24 h. This effect is probably due to the synergic effect of Chitosan and N-acetylcysteine which also accelerate the release of antibiotic from the microdevice.

Therefore, the eradication of biomass was enhanced with the use of the coated microdevices, in particular with CHI/NAC-coated MCs. Moreover, it is important to take into consideration the mucoadhesive and mucolytic properties of CHI and NAC respectively.

5.2 Cell Culture on Disc (CoD) results

In this paragraph the results related to the COD are shown. First, the results related to the long-term culture of Caco-2 cells are presented, finishing with the results related to HeLa cell cultures and cytotoxicity assays.

5.2.1 Long-term culture Caco-2 cells

In the first set of experiments, Caco-2 cells were seeded and cultured for 3 days with an initial seeding cell density of $1,5 \times 10^5$ cells/cm². As shown in Figure 5.3, the Microscope on Disc (MOD) was capable of recording high quality images, which proved to be comparable with those taken with a conventional optical microscope.

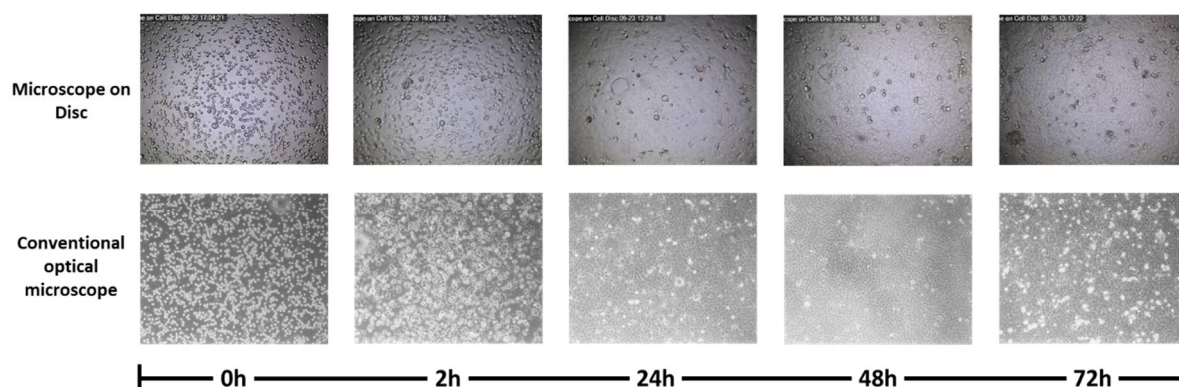


Figure 5.3 Caco-2 cells growth over 72 h. Comparison between MoD images and conventional optical microscope images is also shown.

Caco-2 cells were able to grow on the platform for 3 days at a flow rate of 0.6 μ l/min without the need of adding new medium, which was perfused through the cell culture chamber from the inlet reservoir.

Caco-2 cells viability was established at the end of the experiment using a LIVE/DEAD Cell Imaging Kit and using confocal microscopy. Figure 5.4 shows that the majority of the cells were alive and just a small percentage of cells were dead after 72 h.

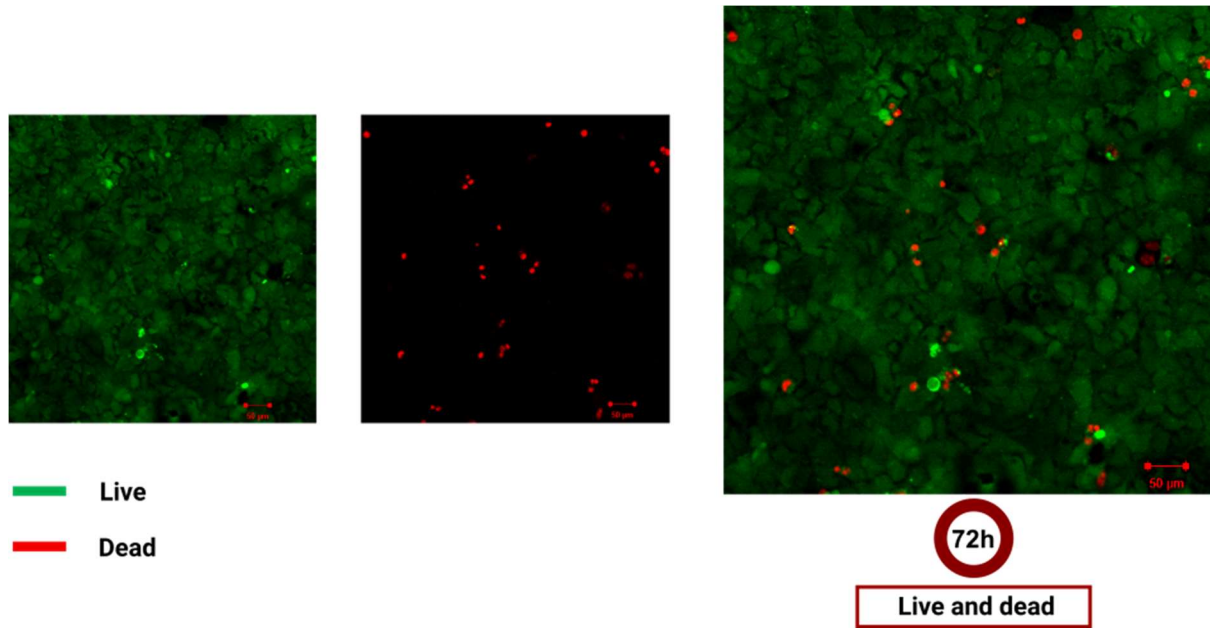


Figure 5.4 Caco-2 cells live and dead staining after 72h using confocal microscopy.

The same experiment was repeated over 6 days. After 72 h with the selected flow rate of $0.6 \mu\text{l}/\text{min}$, it was necessary to add fresh culture medium through the inlet reservoir opening. However, the addition of medium did not compromise neither sterile conditions nor cell growth.

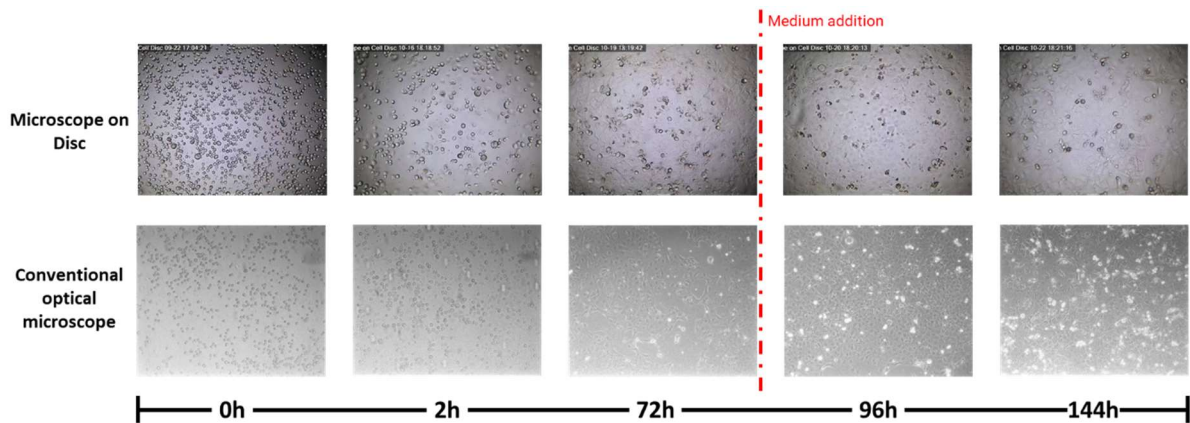


Figure 5.5 Caco-2 cells growth over 6 days. Comparison between MoD images and conventional optical microscope images are shown.

At the end of the experiment, confocal images (Figure 5.6) taken with the LIVE/DEAD Cell Imaging Kit, as explained before, proved that the CoD platform allowed the growth of Caco-2 cells over 6 days.

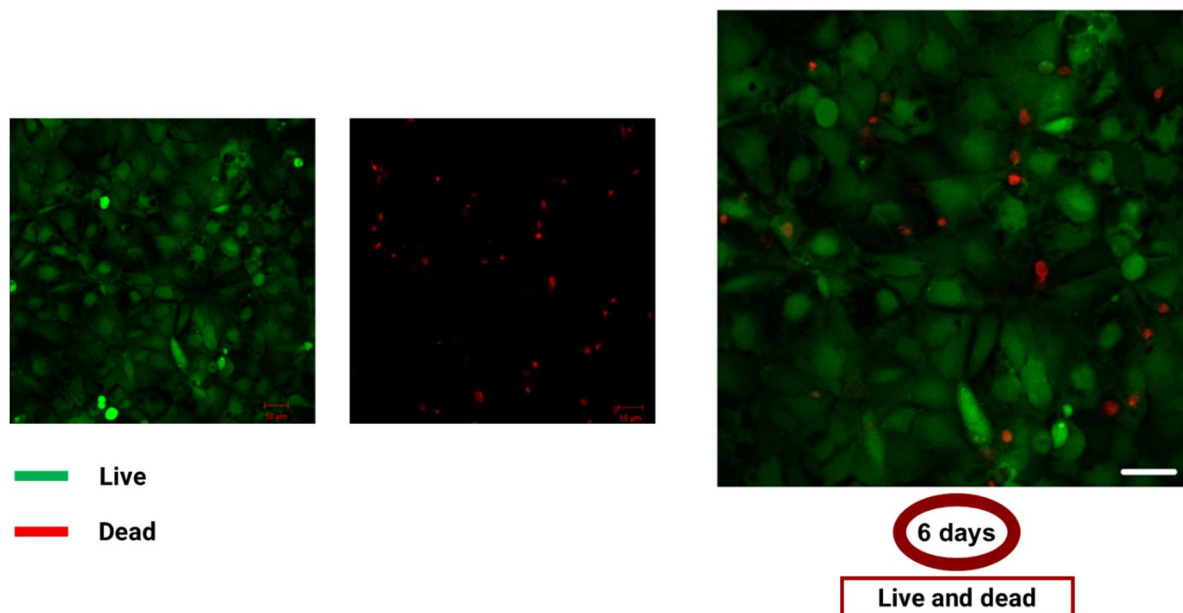


Figure 5.6 Confocal microscope images of Caco-2 cells using live and dead staining after 6 days.

5.2.2 HeLa cell cultures and cytotoxicity assays

As previously discussed in Chapter 4.6.1 “*CoD doxorubicin treatment*”, HeLa cells were cultured on the CoD platform for 24 h with an initial seeding density of $0,75 \times 10^5$ cells/cm² at a flow rate of 0.6 µl/min. The culture was then treated with different concentrations of doxorubicin (DOX): 1 µM, 5 µM, 10 µM, 100 µM.

First, the effects of a concentration of 5 µM DOX were compared to a control culture, where the drug was not added and cells were growth for 48 h on disc. In case of treatment, doxorubicin was added after 24 h of growth. Figure 5.7 shows MoD images of the two cultures, treated and control, at different time points: 0 h, 24 h, 27 h, 29 h and 48 h.

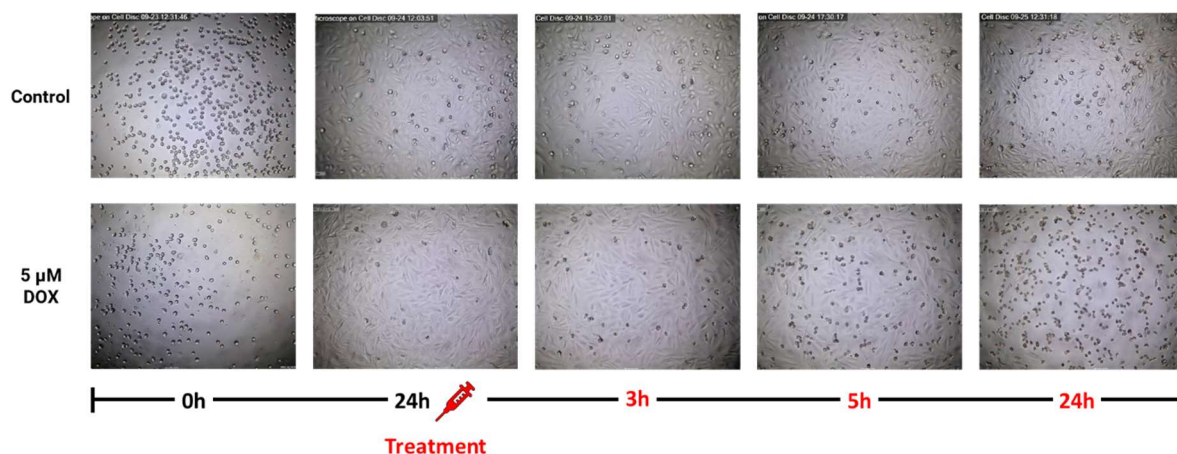


Figure 5.7 HeLa cell cultures: comparison between a control culture (no addition of drug) and a treated culture using 5 μM of DOX.

As shown in Figure 5.7, a significant difference between the two cultures is already visible after 5 h from treatment introduction, when treated cells started to detach from the surface and die.

The quantification of cell viability was carried out using the software Cellari. As explained in Chapter 4.7.2 “*Mammalian cells growth and viability monitoring and data analysis*”, Cellari gave numerical results of cell viability using the MoD pictures as an input. After a first training, the software, which is based on machine learning, was capable of distinguishing between dead and alive cells.

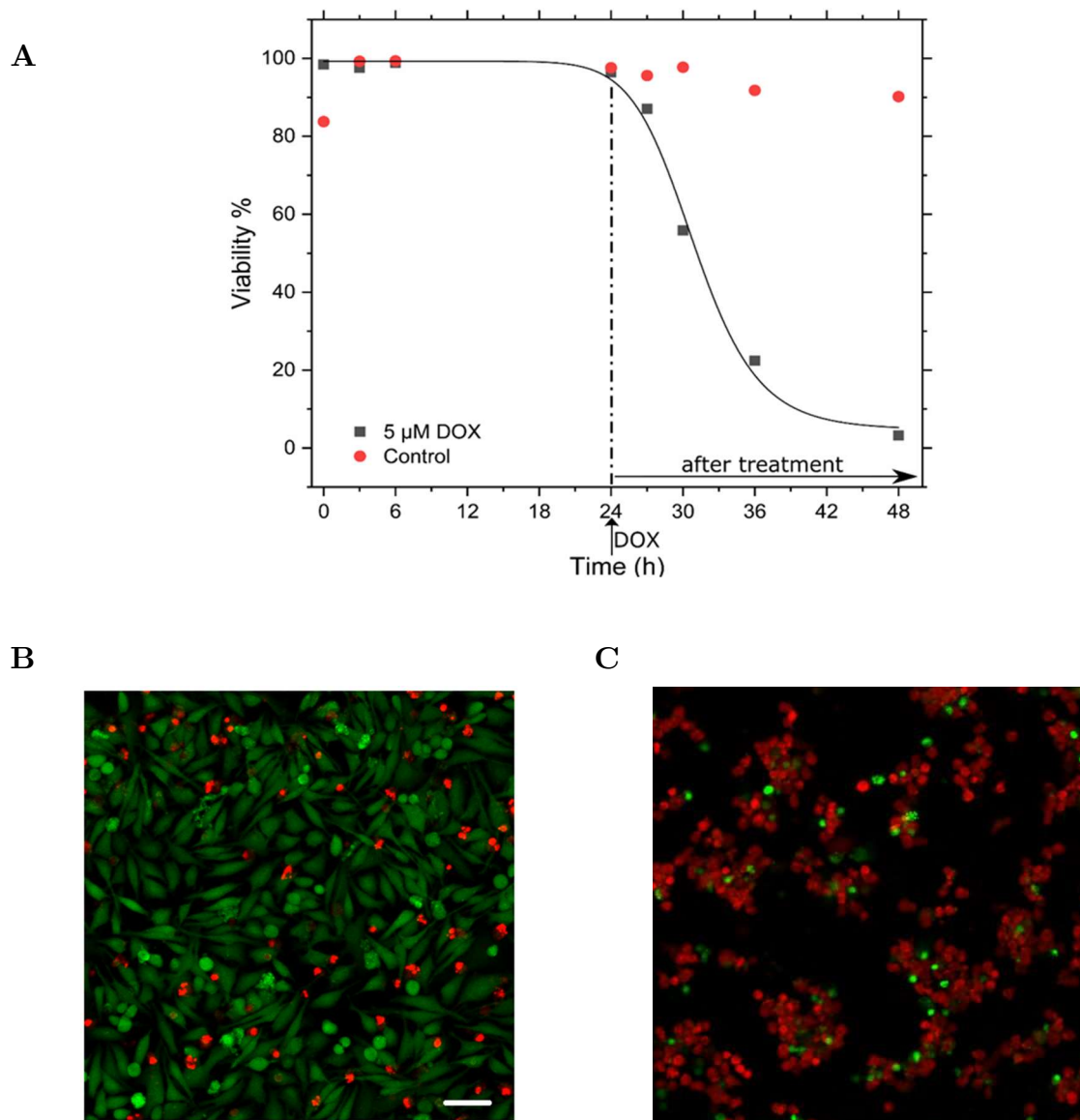


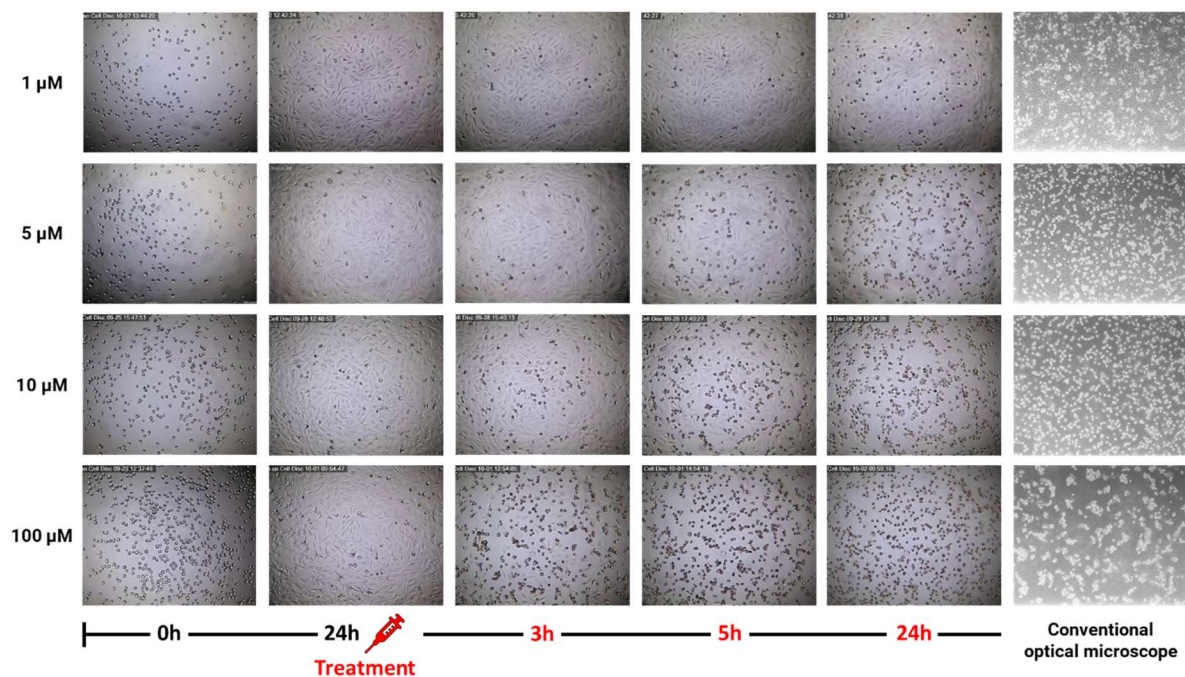
Figure 5.8 Viability comparison between a culture of HeLa cells grown for 48 h at a flow rate of 0.6 μ l/min on the CoD and a treated one using a concentration of 5 μ M of doxorubicin. Treatment was introduced after 24 h of growth (**A**) Cellar quantification of dead and alive cells. (**B**) Live and dead staining of the control culture after 48 h. (**C**) Live and dead staining of the 5 μ M DOX treated culture after 24 h of treatment.

Figure 5.8A shows the numerical quantification of cell viability of both the control culture and the treated one. Cell viability is comparable between the two cultures during the first 24 h, while it decreased significantly in the treated culture already after

5 h from the addition of the drug. In fact, 60% of cells were alive after 5 h from the introduction of DOX. After 24 h of treatment cell viability was decreased at 3.22%. These results were then confirmed by live and dead staining of the two cultures as shown from the confocal images (Figure 5.8B and 5.8C). Confocal images show that a considerable number of cells were still alive after 48 h of growth when considering the control culture, while almost all cells were dead in the case of DOX treatment.

Once the platform proved to provide reliable results, the effects of different concentrations of doxorubicin were tested and compared.

MoD pictures of four different cultures treated with 1 μM , 5 μM , 10 μM and 100 μM DOX are presented in Figure 5.9A. Different time points have been considered: 0 h and 24 h after seeding, and 3 h, 5 h and 24 h after adding the drug. At 24 h of treatment MoD images were also compared to the ones taken with a conventional optical microscope.

A

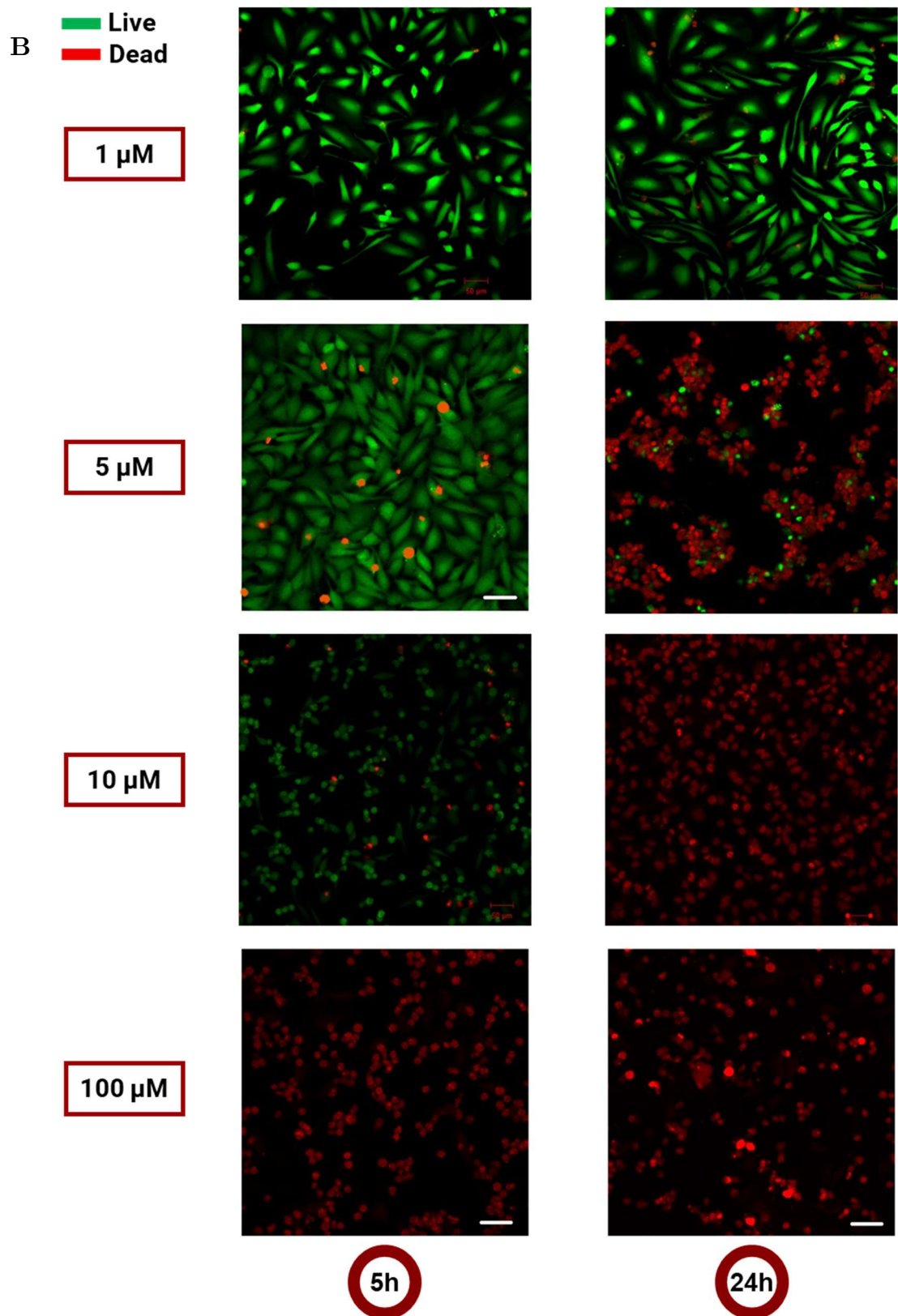
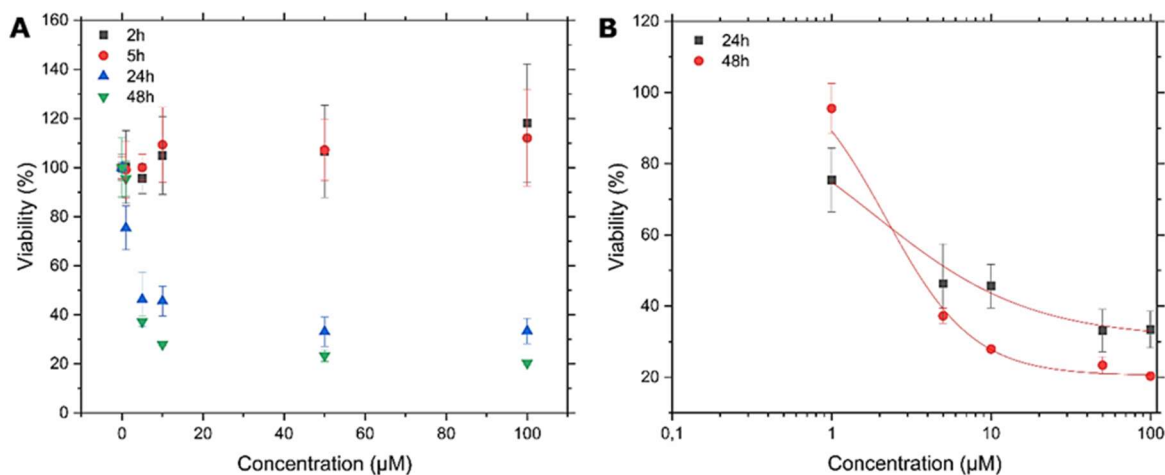


Figure 5.9 Comparison between the effects of 1 μM , 5 μM , 10 μM and 100 μM DOX treatment on HeLa cells grown for 24 h at a flow rate of 0.6 $\mu\text{l}/\text{min}$. (A)

MoD images of HeLa cells at 0 h and 24 h after seeding and at 3 h, 5 h and 24 h after 1 μ M, 5 μ M, 10 μ M and 100 μ M DOX treatment. **(B)** HeLa cell live and dead staining after 5 h and 24 h of treatment with 1 μ M, 5 μ M, 10 μ M and 100 μ M DOX.

As expected, doxorubicin concentration is inversely related to the onset of action. In fact, the higher is the concentration, the faster is the effect. Therefore, a concentration of 100 μ M doxorubicin had a major impact on the culture just after 5 h of treatment, as shown in the confocal images in Figure 5.9B. After 24 h of treatment, almost all cells were dead also with lower concentrations (not considering the 1 μ M concentration where cells were still alive after 24 h from treatment addition) (Figure 5.9B).

These results have been compared with cytotoxicity assay in static. In fact, an MTS assay was carried out for comparison where 5 different concentrations of doxorubicin were tested at different time points (2 h, 5 h, 24 h, 48 h). The concentrations chosen were: 1 μ M, 5 μ M, 10 μ M, 50 μ M, 100 μ M.



C

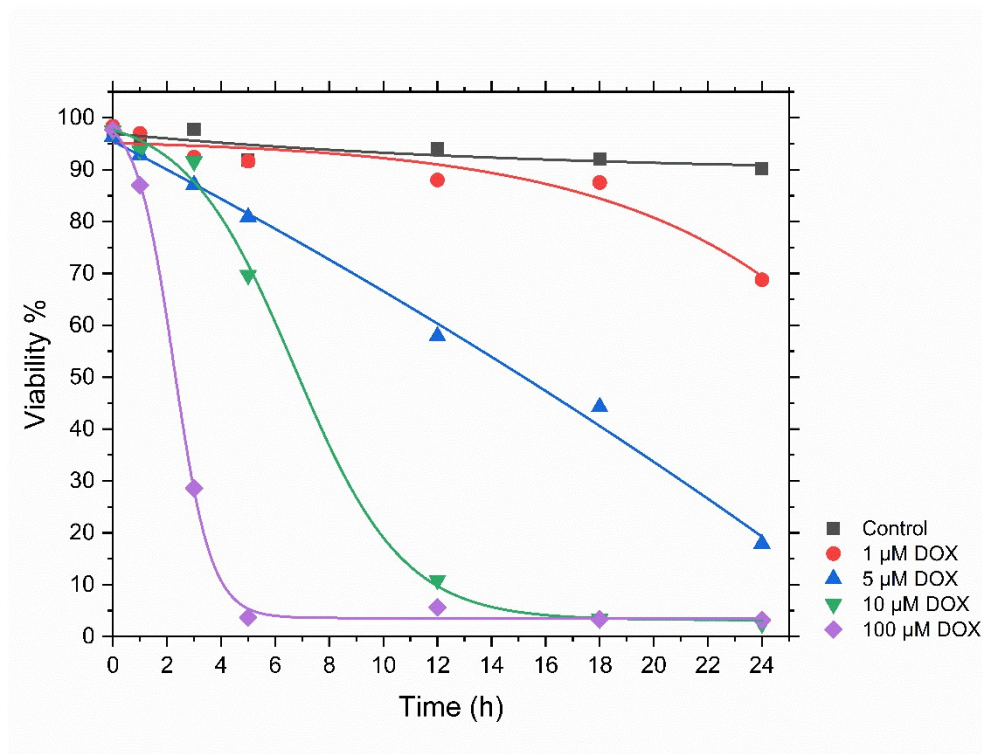


Figure 5.10 Comparison between cytotoxicity assay in static on a conventional 96 well-plate and in flow on the CoD. (A), (B) MTS assay shows the effects of different concentrations of doxorubicin on HeLa cells cultured in static conditions on a 96 well-plate. (C) Cellari quantification of the effects of different concentrations of doxorubicin on HeLa cells cultured in perfusion on the CoD.

The comparison in Figure 5.10 shows a substantial difference in cells viability: after 5 h in static conditions cell viability was above 90% with a concentration of 100 μ M DOX, while in perfusion, at the same time point and with the same drug concentration, it dropped to 4%.

Therefore, these results demonstrate that perfusion had a significant impact on the cell culture during treatment. In fact, it proved to give a faster and a better effect of doxorubicin treatment on HeLa cells.

6. Conclusions and future perspectives

The goal of this thesis was to demonstrate the relevance of a novel centrifugal microfluidic platform for long-term cell culture in flow and drug screening.

The Lab-on-a-Disc (LoD) platform presented was successfully used for long-term cell culture in perfusion of both bacterial and mammalian cells and drug testing using different antibiotic administration methods when growing bacterial biofilm and an anti-cancer drug when treating mammalian cancer cells.

In the first application, *Pseudomonas Aeruginosa* was cultured from single cells to mature biofilm and was treated with antibiotic ciprofloxacin administered using different methods, such as bolus injection or microdevices, also called microcontainers, coated with different polymeric lids. The Bacterial-Culture-on-Disc (BCoD) was designed and efficiently optimized and tested to enable the growth of the biofilm and to evaluate the efficacy of the treatments.

In the second application, Caco-2 cells were used to assess the possibility of culturing mammalian cells for long-term culture on the platform, while HeLa cells were used to perform cytotoxicity assays. The Cell-on-Disc (CoD) design was particularly optimized for mammalian cell culture and real-time optical monitoring.

In both applications, the LoD platform proved to be a robust tool for cell culture in dynamic conditions. In fact, flow velocity and shear stress for both bacterial and mammalian cells on disc did not have any adversary effect on cells. Moreover, it gave similar or even better results than the ones obtained with conventional *in vitro* systems.

The disc-shaped *in vitro* system presented in this thesis demonstrated to be a versatile, user friendly and reliable device that can represent a possible alternative to traditional *in vitro* cell culture systems and can become an indispensable tool for researchers.

Furthermore, its simple design, the low amount of reagent required, and the cost-effective set-up can be fundamental advantages in the initial phase of drug screening and diagnostics.

However, some improvements can be done. In fact, the fabrication process could be adapted for large scale production implementing injection molding, or it can be optimized to be compatible with other sterilization processes, such as autoclaving. In addition, more cell chambers could be added to the original design to increase the platform throughput.

The LoD platforms could be also used for further applications, such as a co-culture of bacterial and mammalian cells to try to mimic even better certain *in vivo* conditions and to investigate drug effects in different conditions.

References

- [1] S. Duttagupta, “Outcomes research and drug development.,” *Perspect. Clin. Res.*, vol. 1, no. 3, pp. 104–5, Jul. 2010, Accessed: Nov. 09, 2020. [Online]. Available: <http://www.ncbi.nlm.nih.gov/pubmed/21814630>.
- [2] P. Preziosi, “Drug Development,” in *Comprehensive Medicinal Chemistry II*, Elsevier, 2007, pp. 173–202.
- [3] P. R. Robuck and J. I. Wurzelmann, “Understanding the Drug Development Process,” *Inflamm. Bowel Dis.*, vol. 11, no. SUPPL. 1, pp. S13–S16, Nov. 2005, doi: 10.1097/01.MIB.0000184851.46440.a3.
- [4] N. E. McKenzie, “The drug development process,” in *Fundamentals of Cancer Prevention*, Springer Berlin Heidelberg, 2005, pp. 205–213.
- [5] C. Horien and P. Yuan, “Focus: Drug Development,” *Yale J. Biol. Med.*, vol. 90, no. 1, p. 1, 2017, Accessed: Oct. 10, 2020. [Online]. Available: <https://www.ncbi.nlm.nih.gov/pmc/articles/PMC5369027/>.
- [6] S. Doggrell, “Drug development,” Sheila Doggrell, 2012.
- [7] K. L. Steinmetz and E. G. Spack, “The basics of preclinical drug development for neurodegenerative disease indications,” *BMC Neurol.*, vol. 9, no. SUPPL. 1, p. S2, Jun. 2009, doi: 10.1186/1471-2377-9-S1-S2.
- [8] “The Drug Development Process | FDA.” <https://www.fda.gov/patients/learn-about-drug-and-device-approvals/drug-development-process> (accessed Oct. 10, 2020).
- [9] G. A. Van Norman, “Drugs and Devices: Comparison of European and U.S.

- Approval Processes,” *JACC Basic to Transl. Sci.*, vol. 1, no. 5, pp. 399–412, Aug. 2016, doi: 10.1016/j.jacbts.2016.06.003.
- [10] R. C. Dart, “Monitoring risk: Post marketing surveillance and signal detection,” *Drug Alcohol Depend.*, vol. 105, pp. 26–32, 2009, doi: 10.1016/j.drugalcdep.2009.08.011.
- [11] “Drug development: the journey of a medicine from lab to shelf | Career Feature | Pharmaceutical Journal.” <https://www.pharmaceutical-journal.com/test-tomorrows-pharmacist/tomorrows-pharmacist/drug-development-the-journey-of-a-medicine-from-lab-to-shelf/20068196.article?firstPass=false> (accessed Oct. 11, 2020).
- [12] “Biopharmaceutical Research & Development: The Process Behind New Medicines.” http://pharma-docs.phrma.org/sites/default/files/pdf/rd_brochure_022307.pdf (accessed Oct. 11, 2020).
- [13] J. Saji Joseph, S. Tebogo Malindisa, and M. Ntwasa, “Two-Dimensional (2D) and Three-Dimensional (3D) Cell Culturing in Drug Discovery,” in *Cell Culture*, IntechOpen, 2019.
- [14] M. Nikolic, T. Sustersic, and N. Filipovic, “In vitro models and on-chip systems: Biomaterial interaction studies with tissues generated using lung epithelial and liver metabolic cell lines,” *Frontiers in Bioengineering and Biotechnology*, vol. 6, no. SEP. Frontiers Media S.A., p. 120, Sep. 03, 2018, doi: 10.3389/fbioe.2018.00120.
- [15] D. D. Allen, R. Caviedes, A. M. Cárdenas, T. Shimahara, J. Segura-Aguilar, and P. A. Caviedes, “Cell lines as in vitro models for drug screening and toxicity studies,” *Drug Dev. Ind. Pharm.*, vol. 31, no. 8, pp. 757–768, 2005, doi:

10.1080/03639040500216246.

- [16] M. A. Cabrera-Pérez, M. Bermejo Sanz, V. M. Sanjuan, M. Gonz Alez-Alvarez, and I. Gonz Alez Alvarez, “2 - Importance and applications of cell- and tissue-based in vitro models for drug permeability screening in early stages of drug development,” *Concepts Model. Drug Permeability Stud.*, pp. 3–29, 2016, doi: 10.1016/B978-0-08-100094-6.00002-X.
- [17] K. Duval, H. Grover, L.-H. Han, Y. Mou, A. F. Pegoraro, J. Fredberg, Z. Chen, * K Duval, H. Grover, and L.-H. Han, “Modeling Physiological Events in 2D vs. 3D Cell Culture,” 2017, doi: 10.1152/physiol.00036.2016.
- [18] “In Vitro | Definition of In Vitro by Oxford Dictionary .” https://www.lexico.com/definition/in_vitro (accessed Oct. 13, 2020).
- [19] C. Carvalho, S. A. M. Varela, L. Ferreira Bastos, I. Orfão, V. Beja, M. Sapage, T. A. Marques, A. Knight, and L. Vicente, “The Relevance of In Silico, In Vitro and Non-human Primate Based Approaches to Clinical Research on Major Depressive Disorder,” doi: 10.1177/0261192919885578.
- [20] S. W. at the O. T. Candice Tang, “In vitro vs. In vivo: Is One Better? | UHN Research.” <https://www.uhnresearch.ca/news/vitro-vs-vivo-one-better> (accessed Oct. 13, 2020).
- [21] R. Rezaee and M. Abdollahi, “The importance of translatability in drug discovery,” *Expert Opin. Drug Discov.*, vol. 12, no. 3, pp. 237–239, 2017, doi: 10.1080/17460441.2017.1281245.
- [22] C. Cates and M. Couto, “In vivo physiological research in the US: regulatory and ethical issues,” *Open Access Anim. Physiol.*, vol. 7, p. 1, Dec. 2014, doi: 10.2147/oaap.s51714.

- [23] M. Kapałczyńska, T. Kolenda, W. Przybyła, M. Zajączkowska, A. Teresiak, V. Filas, M. Ibbs, R. Bliźniak, Ł. Łuczewski, and K. Lamperska, “2D and 3D cell cultures – a comparison of different types of cancer cell cultures,” *Arch. Med. Sci.*, vol. 14, no. 4, pp. 910–919, 2018, doi: 10.5114/aoms.2016.63743.
- [24] I. Meyvantsson and D. J. Beebe, “Cell Culture Models in Microfluidic Systems,” *Annu. Rev. Annu. Rev. Anal. Chem.*, vol. 1, pp. 423–449, 2008, doi: 10.1146/annurev.anchem.1.031207.113042.
- [25] V. Charwat and D. Egger, “The Third Dimension in Cell Culture: From 2D to 3D Culture Formats,” *Cell Cult. Technol. Learn. Mater. Biosci.*, 2018, doi: 10.1007/978-3-319-74854-2_5.
- [26] J. A. Burdick and G. Vunjak-Novakovic, “Engineered microenvironments for controlled stem cell differentiation,” *Tissue Engineering - Part A*, vol. 15, no. 2. Mary Ann Liebert Inc., pp. 205–219, Feb. 01, 2009, doi: 10.1089/ten.tea.2008.0131.
- [27] P. Pinton, R. Tikkanen, W. Berger, C. R. A Regenbrecht, M. Gaebler, A. Silvestri, J. Haybaeck, P. Reichardt, C. D. Lowery, L. F. Stancato, and G. Zybarth, “Three-Dimensional Patient-Derived In Vitro Sarcoma Models: Promising Tools for improving Clinical Tumor Management,” vol. 7, p. 1, 2017, doi: 10.3389/fonc.2017.00203.
- [28] E. Campodoni, E. B. Heggset, A. Rashad, G. B. Ramírez-Rodríguez, K. Mustafa, K. Syverud, A. Tampieri, and M. Sandri, “Polymeric 3D scaffolds for tissue regeneration: Evaluation of biopolymer nanocomposite reinforced with cellulose nanofibrils,” *Mater. Sci. Eng. C*, vol. 94, pp. 867–878, Jan. , doi: 10.1016/j.msec.2018.10.026.
- [29] Y. H. Tsou, J. Khoneisser, P. C. Huang, and X. Xu, “Hydrogel as a bioactive

- material to regulate stem cell fate,” *Bioactive Materials*, vol. 1, no. 1. KeAi Communications Co., pp. 39–55, Sep. 01, 2016, doi: 10.1016/j.bioactmat.2016.05.001.
- [30] E. Fennema, N. Rivron, J. Rouwkema, C. Van Blitterswijk, and J. De Boer, “Spheroid culture as a tool for creating 3D complex tissues,” *Trends Biotechnol.*, vol. 31, pp. 108–115, 2013, doi: 10.1016/j.tibtech.2012.12.003.
- [31] X. Liu and P. Raju, “In Vitro Cancer Model for Drug Testing,” in *Comprehensive Biotechnology, Second Edition*, vol. 5, Elsevier Inc., 2011, pp. 543–549.
- [32] K. Subramanian, D. J. Owens, R. Raju, M. Firpo, T. D. O’Brien, C. M. Verfaillie, and W.-S. Hu, “Spheroid Culture for Enhanced Differentiation of Human Embryonic Stem Cells to Hepatocyte-Like Cells,” *Stem Cells Dev.*, vol. 23, no. 2, pp. 124–131, Jan. 2014, doi: 10.1089/scd.2013.0097.
- [33] A. Ahluwalia, G. Mattei, S. Sartori, S. Caddeo, and M. Boffito, “Tissue Engineering Approaches in the Design of Healthy and Pathological In Vitro Tissue Models,” vol. 5, 2017, doi: 10.3389/fbioe.2017.00040.
- [34] Y. Luo, G. Engelmayr, D. T. Auguste, L. da Silva Ferreira, J. M. Karp, R. Saigal, and R. Langer, “3D Scaffolds,” in *Principles of Tissue Engineering: Fourth Edition*, Elsevier Inc., 2013, pp. 475–494.
- [35] F. C. Fierz, F. Beckmann, M. Huser, S. H. Irsen, B. Leukers, F. Witte, Ö. Degistirici, A. Andronache, M. Thie, and B. Müller, “The morphology of anisotropic 3D-printed hydroxyapatite scaffolds,” *Biomaterials*, vol. 29, no. 28, pp. 3799–3806, Oct. 2008, doi: 10.1016/j.biomaterials.2008.06.012.
- [36] D. Y. Fozdar, P. Soman, J. W. Lee, L. H. Han, and S. Chen, “Three-dimensional polymer constructs exhibiting a tunable negative poisson’s ratio,” *Adv. Funct. Mater.*, vol. 21, no. 14, pp. 2712–2720, Jul. 2011, doi: 10.1002/adfm.201002022.

- [37] N. Kasoju, D. Kubies, T. Sedlačák, O. Janoušková, J. Koubková, M. M. Kumorek, and F. Rypáček, “Polymer scaffolds with no skin-effect for tissue engineering applications fabricated by thermally induced phase separation,” *Biomed. Mater.*, vol. 11, no. 1, p. 015002, Jan. 2016, doi: 10.1088/1748-6041/11/1/015002.
- [38] J. Xiao, H. Duan, Z. Liu, Z. Wu *et al.*, “Construction of the recellularized corneal stroma using porous acellular corneal scaffold,” *Biomaterials*, vol. 32, no. 29, pp. 6962–6971, Oct. 2011, doi: 10.1016/j.biomaterials.2011.05.084.
- [39] A. Salerno, D. Guarnieri, M. Iannone, S. Zeppetelli, and P. A. Netti, “Effect of micro-and macroporosity of bone tissue three-dimensional- poly(ϵ -caprolactone) scaffold on human mesenchymal stem cells invasion, proliferation, and differentiation in vitro,” *Tissue Eng. - Part A*, vol. 16, no. 8, pp. 2661–2673, Aug. 2010, doi: 10.1089/ten.tea.2009.0494.
- [40] N. Annabi, A. Tamayol, J. A. Uquillas, M. Akbari, L. E. Bertassoni, C. Cha, G. Camci-Unal, M. R. Dokmeci, N. A. Peppas, and A. Khademhosseini, “25th anniversary article: Rational design and applications of hydrogels in regenerative medicine,” *Advanced Materials*, vol. 26, no. 1. John Wiley & Sons, Ltd, pp. 85–124, Jan. 08, 2014, doi: 10.1002/adma.201303233.
- [41] K. Hattori, S. Sugiura, and T. Kanamori, “Microfluidic perfusion culture,” *Methods Mol. Biol.*, vol. 1104, pp. 251–263, 2014, doi: 10.1007/978-1-62703-733-4_17.
- [42] C. A. Freeman, P. S. D. Samuel, and D. S. Kompala, “Compact Cell Settlers for Perfusion Cultures of Microbial (and Mammalian) Cells,” *Biotechnol. Prog.*, vol. 33, no. 4, pp. 913–922, Jul. 2017, doi: 10.1002/btpr.2533.
- [43] V. van Duinen, S. J. Trietsch, J. Joore, P. Vulto, and T. Hankemeier, “Microfluidic 3D cell culture: From tools to tissue models,” *Current Opinion in*

- Biotechnology*, vol. 35. Elsevier Ltd, pp. 118–126, Dec. 01, 2015, doi: 10.1016/j.copbio.2015.05.002.
- [44] A. Heiskanen, J. Emnéus, and M. Dufva, “Perfusion Based Cell Culture Chips,” Springer, Dordrecht, 2010, pp. 427–452.
- [45] I. Martin, D. Wendt, and M. Heberer, “The role of bioreactors in tissue engineering,” doi: 10.1016/j.tibtech.2003.12.001.
- [46] M. C. Annesini, L. Marrelli, V. Piemonte, L. Turchetti, M. C. Annesini, L. Marrelli, V. Piemonte, and L. Turchetti, “Bioreactors,” in *Artificial Organ Engineering*, Springer London, 2017, pp. 83–114.
- [47] R. Obregón, J. Ramón-Azcón, and S. Ahadian, “Bioreactors in Tissue Engineering,” in *Tissue Engineering for Artificial Organs: Regenerative Medicine, Smart Diagnostics and Personalized Medicine*, vol. 1–2, Wiley-VCH Verlag, 2016, pp. 169–213.
- [48] M. J. Powers, K. Domansky, M. R. Kaazempur-Mofrad, A. Kalezi, A. Capitano, A. Upadhyaya, P. Kurzawski, K. E. Wack, D. B. Stolz, R. Kamm, and L. G. Grif®th, “A Microfabricated Array Bioreactor for Perfused 3D Liver Culture,” doi: 10.1002/bit.10143.
- [49] J. Filant, P. Nejad, A. Paul, B. Simonson, S. Srinivasan, X. Zhang, L. Balaj, S. Das, R. Gandhi, L. C. Laurent, and A. K. Sood, “Isolation of extracellular RNA from serum/plasma,” in *Methods in Molecular Biology*, vol. 1740, Humana Press Inc., 2018, pp. 43–57.
- [50] R. Faschian, S. De, and R. Pörtner, “Multi-Fixed-Bed Bioreactor System Applied for Bioprocess Development of Immobilized Lactic Acid Bacteria,” *Open Biotechnol. J.*, vol. 10, no. 1, pp. 1–9, Feb. 2016, doi: 10.2174/1874070701610010001.

- [51] J. Hansmann, F. Groeber, A. Kahlig, C. Kleinhans, and H. Walles, “Bioreactors in tissue engineering-principles, applications and commercial constraints,” *Biotechnol. J.*, vol. 8, no. 3, pp. 298–307, Mar. 2013, doi: 10.1002/biot.201200162.
- [52] R. Krull, S. Llad O-Maldonado, T. Lorenz, S. Demming, S. Büttgenbach, and • S Büttgenbach, “Chapter 4 Microbioreactors,” 2016, doi: 10.1007/978-3-319-26920-7_4.
- [53] E. Cimetta, E. Figallo, C. Cannizzaro, N. Elvassore, and G. Vunjak-Novakovic, “Micro-bioreactor arrays for controlling cellular environments: Design principles for human embryonic stem cell applications,” *Methods*, vol. 47, no. 2, pp. 81–89, Feb. 2009, doi: 10.1016/j.ymeth.2008.10.015.
- [54] V. Y. Soldatow, E. L. Lecluyse, L. G. Griffith, and I. Rusyn, “In vitro models for liver toxicity testing,” *Toxicology Research*, vol. 2, no. 1. Royal Society of Chemistry, pp. 23–39, Jan. 01, 2013, doi: 10.1039/c2tx20051a.
- [55] D. Mijatovic, J. C. T. Eijkel, and A. Van Den Berg, “Technologies for nanofluidic systems: top-down vs. bottom-up-a review,” 2005, doi: 10.1039/b416951d.
- [56] G. M. Whitesides, “The origins and the future of microfluidics,” *Nature*, vol. 442, no. 7101. Nature Publishing Group, pp. 368–373, Jul. 27, 2006, doi: 10.1038/nature05058.
- [57] F. Bragheri, R. Martinez Vazquez, and R. Osellame, “Microfluidics,” in *Three-Dimensional Microfabrication Using Two-Photon Polymerization: Fundamentals, Technology, and Applications*, Elsevier Inc., 2016, pp. 310–334.
- [58] J. A. Thompson, J. A. Thompson, and J. A. Thompson, “MICROFLUIDIC DEVICES,” 2011, Accessed: Oct. 31, 2020. [Online]. Available: <http://citeseerx.ist.psu.edu/viewdoc/summary?doi=10.1.1.343.232>.

- [59] D. Devadas and E. W. K. Young, “Microfluidics for Cell Culture,” 2016, doi: 10.1007/978-3-319-30019-1_15.
- [60] A. J. DeMello, “Control and detection of chemical reactions in microfluidic systems,” *Nature*, vol. 442, no. 7101. Nature Publishing Group, pp. 394–402, Jul. 27, 2006, doi: 10.1038/nature05062.
- [61] P. J. Hung, P. J. Lee, P. Sabounchi, R. Lin, and L. P. Lee, “Continuous perfusion microfluidic cell culture array for high-throughput cell-based assays,” *Biotechnol. Bioeng.*, vol. 89, no. 1, pp. 1–8, Jan. 2005, doi: 10.1002/bit.20289.
- [62] P. Yager, T. Edwards, E. Fu, K. Helton, K. Nelson, M. R. Tam, and B. H. Weigl, “Microfluidic diagnostic technologies for global public health,” *Nature*, vol. 442, no. 7101. Nature Publishing Group, pp. 412–418, Jul. 27, 2006, doi: 10.1038/nature05064.
- [63] T. M. Squires and S. R. Quake, “Microfluidics: Fluid physics at the nanoliter scale,” *Rev. Mod. Phys.*, vol. 77, no. 3, pp. 977–1026, Jul. 2005, doi: 10.1103/RevModPhys.77.977.
- [64] M. Sharafeldin, T. Chen, G. U. Ozkaya, D. Choudhary, A. A. Molinolo, J. S. Gutkind, and J. F. Rusling, “Detecting cancer metastasis and accompanying protein biomarkers at single cell levels using a 3D-printed microfluidic immunoarray,” *Biosens. Bioelectron.*, vol. 171, p. 112681, Jan. 2021, doi: 10.1016/j.bios.2020.112681.
- [65] H. J. Kim, B. H. Kim, and Y. H. Seo, “Immunoreaction-based Microfluidic Diagnostic Device for the Detection of Prostate-Specific Antigen,” *Biochip J.*, vol. 12, no. 2, pp. 154–162, Jun. 2018, doi: 10.1007/s13206-017-2208-6.
- [66] L. Gerardo Villa-Diaz, Y. Torisawa, T. Uchida, J. Ding, N. Correa Nogueira-de-Souza, K. O. Sue, S. Takayama, and G. Daniel Smith, “Microfluidic culture of

- single human embryonic stem cell colonies,” doi: 10.1039/b820380f.
- [67] S. H. Au, M. Dean Chamberlain, S. Mahesh, M. V Sefton, and A. R. Wheeler, “Lab on a Chip Hepatic organoids for microfluidic drug screening †,” vol. 14, p. 3290, 2014, doi: 10.1039/c4lc00531g.
- [68] K. Shik Mun, K. Arora, Y. Huang, F. Yang, S. Yarlagadda, Y. Ramananda, M. Abu-El-Haija, J. J. Palermo, B. N. Appakalai, J. D. Nathan, and A. P. Naren, “Patient-derived pancreas-on-a-chip to model cystic fibrosis-related disorders,” *Nat. Commun.*, vol. 10, no. 1, Dec. 2019, doi: 10.1038/s41467-019-11178-w.
- [69] N. Beißner, T. Lorenz, S. Reichl, and • S Reichl, “Organ on Chip,” 2016, doi: 10.1007/978-3-319-26920-7_11.
- [70] K. W. Oh, “6 Lab-on-chip (LOC) devices and microfluidics for biomedical applications,” 2013. doi: 10.1533/9780857096272.2.150.
- [71] J. H. Sung and M. L. Shuler, “Prevention of air bubble formation in a microfluidic perfusion cell culture system using a microscale bubble trap,” *Biomed. Microdevices*, vol. 11, no. 4, pp. 731–738, Feb. 2009, doi: 10.1007/s10544-009-9286-8.
- [72] Z. Cai, “Physics and Applications of a PDMS Based Centrifugal Microfluidic System,” *LSU Dr. Diss.*, 2015.
- [73] N. Convery and N. Gadegaard, “30 years of microfluidics,” *Micro and Nano Engineering*, vol. 2. Elsevier B.V., pp. 76–91, Mar. 01, 2019, doi: 10.1016/j.mne.2019.01.003.
- [74] R. Gorkin, J. Park, J. Siegrist, M. Amasia, B. S. Lee, J.-M. Park, J. Kim, H. Kim, M. Madou, and Y.-K. Cho, “Centrifugal microfluidics for biomedical applications,” doi: 10.1039/b924109d.

- [75] M. Tang, G. Wang, S. K. Kong, and H. P. Ho, “A review of biomedical centrifugal microfluidic platforms,” *Micromachines*, vol. 7, no. 2. MDPI AG, 2016, doi: 10.3390/mi7020026.
- [76] J. Kim, S. H. Jang, G. Jia, J. V. Zoval, N. A. Da Silva, and M. J. Madou, “Cell lysis on a microfluidic CD (compact disc),” *Lab Chip*, vol. 4, no. 5, pp. 516–522, Oct. 2004, doi: 10.1039/b401106f.
- [77] J. Steigert, M. Grumann, T. Brenner, K. Mittenbühler *et al.*, “Integrated Sample Preparation, Reaction, and Detection on a High-Frequency Centrifugal Microfluidic Platform,” *JALA J. Assoc. Lab. Autom.*, vol. 10, no. 5, pp. 331–341, Oct. 2005, doi: 10.1016/j.jala.2005.07.002.
- [78] S. Haeberle and R. Zengerle, “Microfluidic platforms for lab-on-a-chip applications,” *Lab on a Chip*, vol. 7, no. 9. Royal Society of Chemistry, pp. 1094–1110, 2007, doi: 10.1039/b706364b.
- [79] N. Thomas, A. Ocklind, I. Blikstad, S. Griffiths, M. Kenrick, H. Derand, G. Ekstrand, C. Ellström, A. Larsson, and P. Andersson, “Integrated Cell Based Assays in Microfabricated Disposable CD Devices,” in *Micro Total Analysis Systems 2000*, Springer Netherlands, 2000, pp. 249–252.
- [80] L. F. Westblade, J. Errington, and T. Dörr, “Antibiotic tolerance,” *PLOS Pathog.*, vol. 16, no. 10, p. e1008892, Oct. 2020, doi: 10.1371/journal.ppat.1008892.
- [81] A. Macgowan and E. Macnaughton, “Antibiotic resistance,” 2013. doi: 10.1016/j.mpmed.2013.08.002.
- [82] K. Lewis, “Leading Edge The Science of Antibiotic Discovery,” 2020, doi: 10.1016/j.cell.2020.02.056.

- [83] J. Davies, “Antibiotic Resistance,” 2013, doi: 10.1016/B978-0-12-374984-0.00068-1.
- [84] D. Davies, “Understanding biofilm resistance to antibacterial agents,” *Nature Reviews Drug Discovery*, vol. 2, no. 2. Nature Publishing Group, pp. 114–122, Feb. 2003, doi: 10.1038/nrd1008.
- [85] Rodney M. Donlan, “Biofilms and Device-Associated Infections ,” *Emerg. Infect. Dis.*, vol. 7, no. 2, pp. 277–281, 2001.
- [86] T. R. Bott, *Industrial biofouling*. Elsevier B.V., 2011.
- [87] M. Batté, B. M. R. Appenzeller, D. Grandjean, S. Fass, V. Gauthier, F. Jorand, L. Mathieu, M. Boualam, S. Saby, and J. C. Block, “Biofilms in drinking water distribution systems,” *Rev. Environ. Sci. Biotechnol.*, vol. 2, no. 2–4, pp. 147–168, 2003, doi: 10.1023/B:RESB.0000040456.71537.29.
- [88] S. Galié, C. García-Gutiérrez, E. M. Miguélez, C. J. Villar, and F. Lombó, “Biofilms in the food industry: Health aspects and control methods,” *Frontiers in Microbiology*, vol. 9, no. MAY. Frontiers Media S.A., May 07, 2018, doi: 10.3389/fmicb.2018.00898.
- [89] L. Passerini, K. Lam, J. W. Costerton, and E. G. King, “Biofilms on indwelling vascular catheters,” *Crit. Care Med.*, vol. 20, no. 5, pp. 665–673, May 1992, doi: 10.1097/00003246-199205000-00020.
- [90] S. J. Mcconoughey, R. Howlin, J. F. Granger, M. M. Manring, J. H. Calhoun, M. Shirlif, S. Kathju, and P. Stoodley, “Biofilms in periprosthetic orthopedic infections HHS Public Access,” *Futur. Microbiol*, vol. 9, no. 8, pp. 987–1007, 2014, doi: 10.2217/fmb.14.64.
- [91] V. Nandakumar, S. Chittaranjan, V. M. Kurian, and M. Doble, “Characteristics

- of bacterial biofilm associated with implant material in clinical practice,” *Polymer Journal*, vol. 45, no. 2. Nature Publishing Group, pp. 137–152, Feb. 11, 2013, doi: 10.1038/pj.2012.130.
- [92] S. Satpathy, S. Kumar Sen, S. Pattanaik, and S. Raut, “Review on bacterial biofilm: An universal cause of contamination,” 2016, doi: 10.1016/j.bcab.2016.05.002.
- [93] M. Jamal, W. Ahmad, S. Andleeb, F. Jalil, M. Imran, M. A. Nawaz, T. Hussain, M. Ali, M. Rafiq, and M. A. Kamil, “Bacterial biofilm and associated infections,” *Journal of the Chinese Medical Association*, vol. 81, no. 1. Elsevier Ltd, pp. 7–11, Jan. 01, 2018, doi: 10.1016/j.jcma.2017.07.012.
- [94] H. C. Flemming, T. R. Neu, and D. J. Wozniak, “The EPS matrix: The ‘House of Biofilm Cells,’” *Journal of Bacteriology*, vol. 189, no. 22. American Society for Microbiology (ASM), pp. 7945–7947, Nov. 2007, doi: 10.1128/JB.00858-07.
- [95] A. D. Verderosa, M. Totsika, and K. E. Fairfull-Smith, “Bacterial Biofilm Eradication Agents: A Current Review,” *Frontiers in Chemistry*, vol. 7. Frontiers Media S.A., p. 824, Nov. 28, 2019, doi: 10.3389/fchem.2019.00824.
- [96] R. Vasudevan, “Biofilms: Microbial Cities of Scientific Significance,” *J. Microbiol. Exp.*, vol. 1, no. 3, Jun. 2014, doi: 10.15406/jmen.2014.01.00014.
- [97] J. Kim, H. D. Park, and S. Chung, “Microfluidic approaches to bacterial biofilm formation,” *Molecules*, vol. 17, no. 8. Multidisciplinary Digital Publishing Institute (MDPI), pp. 9818–9834, Aug. 2012, doi: 10.3390/molecules17089818.
- [98] R. M. Donlan, “Biofilms: Microbial life on surfaces,” *Emerging Infectious Diseases*, vol. 8, no. 9. Centers for Disease Control and Prevention (CDC), pp. 881–890, 2002, doi: 10.3201/eid0809.020063.

- [99] H.-C. Flemming and J. Wingender, “Relevance of microbial extracellular polymeric substances (EPSs)-Part I: Structural and ecological aspects,” 2001. Accessed: Nov. 11, 2020. [Online]. Available: <https://iwaponline.com/wst/article-pdf/43/6/1/429621/1.pdf>.
- [100] T. J. Kinnari, J. Esteban, N. Z. Martin-de-Hijas, O. Sánchez-Muñoz, S. Sánchez-Salcedo, M. Colilla, M. Vallet-Regí, and E. Gomez-Barrena, “Influence of surface porosity and pH on bacterial adherence to hydroxyapatite and biphasic calcium phosphate bioceramics,” *J. Med. Microbiol.*, vol. 58, no. 1, pp. 132–137, Jan. 2009, doi: 10.1099/jmm.0.002758-0.
- [101] M. M. Salek, S. M. Jones, and R. J. Martinuzzi, “The influence of flow cell geometry related shear stresses on the distribution, structure and susceptibility of *Pseudomonas aeruginosa* 01 biofilms,” *Biofouling*, vol. 25, no. 8, pp. 711–725, Nov. 2009, doi: 10.1080/08927010903114603.
- [102] L. Hall-Stoodley, J. W. Costerton, and P. Stoodley, “Bacterial biofilms: From the natural environment to infectious diseases,” *Nature Reviews Microbiology*, vol. 2, no. 2. Nature Publishing Group, pp. 95–108, Feb. 2004, doi: 10.1038/nrmicro821.
- [103] M. B. Miller and B. L. Bassler, “QUORUM SENSING IN BACTERIA,” 2001. Accessed: Nov. 12, 2020. [Online]. Available: www.annualreviews.org.
- [104] C. D. Nadell, J. B. Xavier, S. A. Levin, and K. R. Foster, “The evolution of quorum sensing in bacterial biofilms,” *PLoS Biol.*, vol. 6, no. 1, pp. 0171–0179, Jan. 2008, doi: 10.1371/journal.pbio.0060014.
- [105] P. S. Stewart and J. W. Costerton, “Antibiotic resistance of bacteria in biofilms,” *Lancet*, vol. 358, no. 9276. Elsevier Limited, pp. 135–138, Jul. 14, 2001, doi: 10.1016/S0140-6736(01)05321-1.
- [106] I. Levin-Reisman, A. Brauner, I. Ronin, and N. Q. Balaban, “Epistasis between

- antibiotic tolerance, persistence, and resistance mutations,” doi: 10.1038/s41579-019-0196-3.
- [107] I. Olsen, “Biofilm-specific antibiotic tolerance and resistance,” doi: 10.1007/s10096-015-2323-z.
- [108] J. M. Andrews, “Determination of minimum inhibitory concentrations,” *J. Antimicrob. Chemother.*, vol. 48, no. SUPPL. 1, pp. 5–16, Jul. 2001, doi: 10.1093/jac/48.suppl_1.5.
- [109] G. Kapoor, S. Saigal, and A. Elongavan, “Action and resistance mechanisms of antibiotics: A guide for clinicians,” 2017, doi: 10.4103/joacp.JOACP_349_15.
- [110] H. Ullah and S. Ali, “Classification of Anti-Bacterial Agents and Their Functions,” 2017, doi: 10.5772/intechopen.68695.
- [111] O. Ciofu and T. Tolker-Nielsen, “Antibiotic tolerance and resistance in biofilms,” in *Biofilm Infections*, Springer New York, 2011, pp. 215–229.
- [112] M. R. W. Brown, D. G. Allison, and P. Gilbert, “Resistance of bacterial biofilms to antibiotics a growth-rate related effect?,” *J. Antimicrob. Chemother.*, vol. 22, no. 6, pp. 777–780, Dec. 1988, doi: 10.1093/jac/22.6.777.
- [113] A. L. Spoering and K. Lewis, “Biofilms and planktonic cells of *Pseudomonas aeruginosa* have similar resistance to killing by antimicrobials,” *J. Bacteriol.*, vol. 183, no. 23, pp. 6746–6751, Dec. 2001, doi: 10.1128/JB.183.23.6746-6751.2001.
- [114] J. J. Harrison, H. Ceri, N. J. Roper, E. A. Badry, K. M. Sproule, and R. J. Turner, “Persister cells mediate tolerance to metal oxyanions in *Escherichia coli*,” doi: 10.1099/mic.0.27794-0.
- [115] K. Lewis, “Riddle of biofilm resistance,” *Antimicrobial Agents and Chemotherapy*, vol. 45, no. 4. American Society for Microbiology Journals, pp. 999–1007, Apr.

- 01, 2001, doi: 10.1128/AAC.45.4.999-1007.2001.
- [116] E. Tacconelli, E. Carrara, A. Savoldi, S. Harbarth *et al.*, “Discovery, research, and development of new antibiotics: the WHO priority list of antibiotic-resistant bacteria and tuberculosis,” *www.thelancet.com/infection*, vol. 18, 2018, doi: 10.1016/S1473-3099(17)30753-3.
- [117] K. Lewis, “The Science of Antibiotic Discovery,” *Cell*, vol. 181, no. 1. Cell Press, pp. 29–45, Apr. 02, 2020, doi: 10.1016/j.cell.2020.02.056.
- [118] K. Abdelraouf and V. H. Tam, “Pseudomonas,” 2017, doi: 10.1007/978-3-319-47266-9_9.
- [119] B. A. Woodworth, E. Tamashiro, G. Bhargave, N. A. Cohen, and J. N. Palmer, “An in vitro model of Pseudomonas aeruginosa biofilms on viable airway epithelial cell monolayers,” *Am. J. Rhinol.*, vol. 22, no. 3, pp. 235–238, May 2008, doi: 10.2500/ajr.2008.22.3178.
- [120] D. L. Paterson and B.-N. Kim, “Pseudomonas aeruginosa,” in *Antimicrobial Drug Resistance*, Totowa, NJ: Humana Press, 2009, pp. 811–817.
- [121] C. K. Stover, X. Q. Pham, A. L. Erwin, S. D. Mizoguchi *et al.*, “Complete genome sequence of Pseudomonas aeruginosa PAO1, an opportunistic pathogen,” *Nature*, vol. 406, no. 6799, pp. 959–964, Aug. 2000, doi: 10.1038/35023079.
- [122] W. Wu, Y. Jin, and S. Jin, “Pseudomonas aeruginosa,” 2015, doi: 10.1016/B978-0-12-397169-2.00041-X.
- [123] Y. F. Berrouane, L. A. McNutt, B. J. Buschelman, P. R. Rhomberg, M. D. Sanford, R. J. Hollis, M. A. Pfaller, and L. A. Herwaldt, “Outbreak of severe Pseudomonas aeruginosa infections caused by a contaminated drain in a Whirlpool Bathtub,” *Clin. Infect. Dis.*, vol. 31, no. 6, pp. 1331–1337, Dec. 2000,

doi: 10.1086/317501.

- [124] L. B. Rice, “Challenges in Identifying New Antimicrobial Agents Effective for Treating Infections with *Acinetobacter baumannii* and *Pseudomonas aeruginosa*,” *Clin. Infect. Dis.*, vol. 43, no. Supplement_2, pp. S100–S105, Sep. 2006, doi: 10.1086/504487.
- [125] E. B. M. Breidenstein, C. de la Fuente-Núñez, and R. E. W. Hancock, “*Pseudomonas aeruginosa*: All roads lead to resistance,” *Trends in Microbiology*, vol. 19, no. 8. Elsevier Current Trends, pp. 419–426, Aug. 01, 2011, doi: 10.1016/j.tim.2011.04.005.
- [126] T. I. Nicas and R. E. W. Hancock, “*Pseudomonas aeruginosa* Outer Membrane Permeability: Isolation of a Porin Protein F-Deficient Mutant,” 1983.
- [127] E. J. Joo, C. I. Kang, Y. E. Ha, S. J. Kang, S. Y. Park, D. R. Chung, K. R. Peck, N. Y. Lee, and J. H. Song, “Risk factors for mortality in patients with *Pseudomonas aeruginosa* bacteremia: Clinical impact of antimicrobial resistance on outcome,” *Microb. Drug Resist.*, vol. 17, no. 2, pp. 305–312, Jun. 2011, doi: 10.1089/mdr.2010.0170.
- [128] L. Lambertsen, C. Sternberg, and S. Molin, “Mini-Tn7 transposons for site-specific tagging of bacteria with fluorescent proteins,” *Environ. Microbiol.*, vol. 6, no. 7, pp. 726–732, Jul. 2004, doi: 10.1111/j.1462-2920.2004.00605.x.
- [129] P. C. Sharma, A. Jain, S. Jain, R. Pahwa, and M. S. Yar, “Ciprofloxacin: review on developments in synthetic, analytical, and medicinal aspects,” *J. Enzyme Inhib. Med. Chem.*, vol. 25, no. 4, pp. 577–589, Aug. 2010, doi: 10.3109/14756360903373350.
- [130] F. Follath, M. Bindschedler, M. Wenk, R. Frei, H. Stalder, and H. Reber, “Use of ciprofloxacin in the treatment of *Pseudomonas aeruginosa* infections,” *Eur. J.*

- Clin. Microbiol.*, vol. 5, no. 2, pp. 236–240, Apr. 1986, doi: 10.1007/BF02013997.
- [131] L. H. Nielsen, S. S. Keller, K. C. Gordon, A. Boisen, T. Rades, and A. Müllertz, “Spatial confinement can lead to increased stability of amorphous indomethacin,” *Eur. J. Pharm. Biopharm.*, vol. 81, no. 2, pp. 418–425, Jun. 2012, doi: 10.1016/j.ejpb.2012.03.017.
- [132] S. E. Birk, J. A. J. Haagensen, H. K. Johansen, S. Molin, L. H. Nielsen, and A. Boisen, “Microcontainer Delivery of Antibiotic Improves Treatment of *Pseudomonas aeruginosa* Biofilms,” *Adv. Healthc. Mater.*, vol. 9, no. 10, May 2020, doi: 10.1002/adhm.201901779.
- [133] O. Osakwe, “Preclinical In Vitro Studies: Development and Applicability,” in *Social Aspects of Drug Discovery, Development and Commercialization*, Elsevier, 2016, pp. 129–148.
- [134] R. M. Mader, “Editorial DDT: Cancer models in drug development,” *Drug Discovery Today: Disease Models*, vol. 21. Elsevier Ltd, pp. 1–2, Feb. 03, 2016, doi: 10.1016/j.ddmod.2017.10.001.
- [135] E. Kaemmerer, T. E. Rodriguez Garzon, A. M. Lock, C. J. Lovitt, and V. M. Avery, “Innovative in vitro models for breast cancer drug discovery,” *Drug Discovery Today: Disease Models*, vol. 21. Elsevier Ltd, pp. 11–16, Feb. 03, 2016, doi: 10.1016/j.ddmod.2017.02.002.
- [136] P. Mirabelli, L. Coppola, and M. Salvatore, “Cancer cell lines are useful model systems for medical research,” *Cancers*, vol. 11, no. 8. MDPI AG, Aug. 01, 2019, doi: 10.3390/cancers11081098.
- [137] H. Sun, E. C. Chow, S. Liu, Y. Du, and K. S. Pang, “The Caco-2 cell monolayer: usefulness and limitations,” *Expert Opin. Drug Metab. Toxicol.*, vol. 4, no. 4, pp. 395–411, Apr. 2008, doi: 10.1517/17425255.4.4.395.

- [138] Y. Sambuy, I. De Angelis, G. Ranaldi, M. L. Scarino, A. Stammati, and F. Zucco, “The Caco-2 cell line as a model of the intestinal barrier: Influence of cell and culture-related factors on Caco-2 cell functional characteristics,” *Cell Biology and Toxicology*, vol. 21, no. 1. Cell Biol Toxicol, pp. 1–26, Jan. 2005, doi: 10.1007/s10565-005-0085-6.
- [139] A. L. Rao and G. G. Sankar, “CACO-2 CELLS: AN OVERVIEW,” 2009. Accessed: Nov. 16, 2020. [Online]. Available: www.jprhc.com.
- [140] “ATCC - Growth rate of ATCC HTB-37-493.” https://www.lgcstandards-atcc.org/Global/FAQs/1/A/Growth_rate_of_ATCC_HTB-37-493.aspx?geo_country=dk# (accessed Nov. 16, 2020).
- [141] yreid, “SOP: Thawing, Propagating and Cryopreserving of NCI-PBCF-HTB37 (Caco-2),” 2010. Accessed: Nov. 16, 2020. [Online]. Available: <http://www.atcc.org/ATCCAdvancedCatalogSearch/ProductDetails/tabid/452/Default.aspx?ATC>.
- [142] É. Hellinger, L. Bakk, P. Pócza, K. Tihanyi, and M. Vastag, “Drug penetration model of vinblastine-treated Caco-2 cultures,” *Eur. J. Pharm. Sci.*, vol. 41, pp. 96–106, 2010, doi: 10.1016/j.ejps.2010.05.015.
- [143] T. Lea, “Caco-2 cell line,” in *The Impact of Food Bioactives on Health: In Vitro and Ex Vivo Models*, Springer International Publishing, 2015, pp. 103–111.
- [144] M. Shimizu, “Interaction between Food Substances and the Intestinal Epithelium,” 2010, doi: 10.1271/bbb.90730.
- [145] G. T. Knipp, N. F. H. Ho, C. L. Barsuhn, and R. T. Borchardt, “Paracellular Diffusion in Caco-2 Cell Monolayers: Effect of Perturbation on the Transport of Hydrophilic Compounds That Vary in Charge and Size,” *J. Pharm. Sci.*, vol. 86, no. 10, pp. 1105–1110, Oct. 1997, doi: 10.1021/js9700309.

- [146] A. S. Tang, P. J. Chikhale, P. K. Shah, and R. T. Borchardt, "Utilization of a Human Intestinal Epithelial Cell Culture System (Caco-2) for Evaluating Cytoprotective Agents," *Pharm. Res. An Off. J. Am. Assoc. Pharm. Sci.*, vol. 10, no. 11, pp. 1620–1626, 1993, doi: 10.1023/A:1018976804403.
- [147] I. N. Lyapun, B. G. Andryukov, and M. P. Bynina, "HeLa Cell Culture: Immortal Heritage of Henrietta Lacks," *Molecular Genetics, Microbiology and Virology*, vol. 34, no. 4. Pleiades Publishing, pp. 195–200, Oct. 01, 2019, doi: 10.3103/S0891416819040050.
- [148] H. H. Heng, "HeLa genome versus donor's genome," *Nature*, vol. 501, no. 7466. Nature Publishing Group, p. 167, Sep. 11, 2013, doi: 10.1038/501167d.
- [149] L. Hayflick and P. S. Moorhead, "THE SERIAL CULTIVATION OF HUMAN DIPLOID CELL STRAINS'," 1961.
- [150] L. Wu and X. Qu, "Cancer biomarker detection: Recent achievements and challenges," *Chem. Soc. Rev.*, vol. 44, no. 10, pp. 2963–2997, May 2015, doi: 10.1039/c4cs00370e.
- [151] A. Sfeir and T. De Lange, "Removal of shelterin reveals the telomere end-protection problem," *Science (80-.)*, vol. 336, no. 6081, pp. 593–597, May 2012, doi: 10.1126/science.1218498.
- [152] J. J. M. Landry, P. T. Pyl, T. Rausch, T. Zichner *et al.*, "The genomic and transcriptomic landscape of a hela cell line," *G3 Genes, Genomes, Genet.*, vol. 3, no. 8, pp. 1213–1224, Aug. 2013, doi: 10.1534/g3.113.005777.
- [153] J. M. J. Van Den Bergh, K. Guerti, Y. Willemen, E. Lion, N. Cools, H. Goossens, A. Vorsters, V. F. I. Van Tendeloo, S. Anguille, P. Van Damme, and E. L. J. M. Smits, "HPV vaccine stimulates cytotoxic activity of killer dendritic cells and natural killer cells against HPV-positive tumour cells," *J. Cell. Mol. Med.*, vol.

- 18, no. 7, pp. 1372–1380, 2014, doi: 10.1111/jcmm.12284.
- [154] W. F. Scherer, J. T. Syverton, and G. O. Gey, “Studies on the propagation in vitro of Poliomyelitis viruses,” 1953, Accessed: Nov. 17, 2020. [Online]. Available: <http://rupress.org/jem/article-pdf/97/5/695/1185141/695.pdf>.
- [155] K. K. Takemoto and K. Habel, “Virus-cell relationship in a carrier culture of HeLa cells and Coxsackie A9 virus,” *Virology*, vol. 7, no. 1, pp. 28–44, Jan. 1959, doi: 10.1016/0042-6822(59)90175-8.
- [156] P. Nobis, R. Zibirre, G. Meyer, J. Kühne, G. Warnecke, and G. Koch, “Production of a monoclonal antibody against an epitope on HeLa cells that is the functional poliovirus binding site,” *J. Gen. Virol.*, vol. 66, no. 12, pp. 2563–2569, 1985, doi: 10.1099/0022-1317-66-12-2563.
- [157] K. Takara, T. Sakaeda, T. Yagami, H. Kobayashi, N. Ohmoto, M. Horinouchi, K. Nishiguchi, and K. Okumura, “Cytotoxic effects of 27 anticancer drugs in HeLa and MDR1-overexpressing derivative cell lines,” *Biol. Pharm. Bull.*, vol. 25, no. 6, pp. 771–778, Jun. 2002, doi: 10.1248/bpb.25.771.
- [158] A. L. Svalastog and Lucia Martinelli, “Representing life as opposed to being: The bio-objectification process of the hela cells and its relation to personalized medicine,” *Croat. Med. J.*, vol. 54, no. 4, pp. 397–402, 2013, doi: 10.3325/cmj.2013.54.397.
- [159] J. R. Masters, “HeLa cells 50 years on: The good, the bad and the ugly,” *Nature Reviews Cancer*, vol. 2, no. 4. European Association for Cardio-Thoracic Surgery, pp. 315–319, 2002, doi: 10.1038/nrc775.
- [160] “Overview of Cell Viability and Survival | Cell Signaling Technology.” https://www.cellsignal.com/contents/_/synopsis-of-cell-proliferation-metabolic-status-and-cell-death/cell-viability-and-survival (accessed Nov. 17, 2020).

- [161] A. Adan, Y. Kiraz, and Y. Baran, “Cell Proliferation and Cytotoxicity Assays,” *Curr. Pharm. Biotechnol.*, vol. 17, no. 14, pp. 1213–1221, Aug. 2016, doi: 10.2174/1389201017666160808160513.
- [162] T. L. Riss, R. A. Moravec, A. L. Niles, S. Duellman, H. A. Benink, T. J. Worzella, and L. Minor, *Cell Viability Assays*. Eli Lilly & Company and the National Center for Advancing Translational Sciences, 2004.
- [163] T. Riss, A. Niles, R. Moravec, N. Karassina, and J. Vidugiriene, *Cytotoxicity Assays: In Vitro Methods to Measure Dead Cells*. Eli Lilly & Company and the National Center for Advancing Translational Sciences, 2004.
- [164] J. W. Harbell, S. W. Koontz, R. W. Lewis, D. Lovell, and D. Acosta, “Cell cytotoxicity assays,” in *Food and Chemical Toxicology*, 1997, vol. 35, no. 1, pp. 79–126, doi: 10.1016/S0278-6915(96)00101-9.
- [165] L. Cai, X. Qin, Z. Xu, Y. Song, H. Jiang, Y. Wu, H. Ruan, and J. Chen, “Comparison of Cytotoxicity Evaluation of Anticancer Drugs between Real-Time Cell Analysis and CCK-8 Method,” *ACS Omega*, vol. 4, no. 7, pp. 12036–12042, Jul. 2019, doi: 10.1021/acsomega.9b01142.
- [166] W. Strober, “Trypan Blue Exclusion Test of Cell Viability,” *Curr. Protoc. Immunol.*, vol. 111, no. 1, p. A3.B.1-A3.B.3, Nov. 2015, doi: 10.1002/0471142735.ima03bs111.
- [167] J. A. Plumb, “Cell sensitivity assays: the MTT assay.,” *Methods Mol. Med.*, vol. 88, pp. 165–169, 2004, doi: 10.1007/978-1-61779-080-5_20.
- [168] S. P. M. Crouch, R. Kozlowski, K. J. Slater, and J. Fletcher, “The use of ATP bioluminescence as a measure of cell proliferation and cytotoxicity,” *J. Immunol. Methods*, vol. 160, no. 1, pp. 81–88, Jan. 1993, doi: 10.1016/0022-1759(93)90011-U.

- [169] W. Voigt, "Sulforhodamine B assay and chemosensitivity.," *Methods Mol. Med.*, vol. 110, pp. 39–48, 2005, doi: 10.1385/1-59259-869-2:039.
- [170] A. L. Niles, R. A. Moravec, P. Eric Hesselberth, M. A. Scurria, W. J. Daily, and T. L. Riss, "A homogeneous assay to measure live and dead cells in the same sample by detecting different protease markers," *Anal. Biochem.*, vol. 366, no. 2, pp. 197–206, Jul. 2007, doi: 10.1016/j.ab.2007.04.007.
- [171] N. A. P. Franken, H. M. Rodermond, J. Stap, J. Haveman, and C. van Bree, "Clonogenic assay of cells in vitro," *Nat. Protoc.*, vol. 1, no. 5, pp. 2315–2319, Dec. 2006, doi: 10.1038/nprot.2006.339.
- [172] Y. Ozaki, "INTRODUCTION TO RAMAN SPECTROSCOPY."
- [173] G. Fridman, A. Shereshevsky, M. M. Jost, A. D. Brooks, A. Fridman, A. Gutsol, V. Vasilets, and G. Friedman, "Floating electrode dielectric barrier discharge plasma in air promoting apoptotic behavior in Melanoma skin cancer cell lines," *Plasma Chem. Plasma Process.*, vol. 27, no. 2, pp. 163–176, Apr. 2007, doi: 10.1007/s11090-007-9048-4.
- [174] X. Chen, X. Zhao, Y. Gao, J. Yin, M. Bai, and F. Wang, "Green synthesis of gold nanoparticles using carrageenan oligosaccharide and their in vitro antitumor activity," *Mar. Drugs*, vol. 16, no. 8, Aug. 2018, doi: 10.3390/md16080277.
- [175] C. Carvalho, R. Santos, S. Cardoso, S. Correia, P. Oliveira, M. Santos, and P. Moreira, "Doxorubicin: The Good, the Bad and the Ugly Effect," *Curr. Med. Chem.*, vol. 16, no. 25, pp. 3267–3285, Jul. 2009, doi: 10.2174/092986709788803312.
- [176] J. O'Shaughnessy, "Liposomal Anthracyclines for Breast Cancer: Overview," *Oncologist*, vol. 8, no. S2, pp. 1–2, Aug. 2003, doi: 10.1634/theoncologist.8-suppl_2-1.

- [177] R. Petrioli, A. I. Fiaschi, E. Francini, A. Pascucci, and G. Francini, “The role of doxorubicin and epirubicin in the treatment of patients with metastatic hormone-refractory prostate cancer,” *Cancer Treatment Reviews*, vol. 34, no. 8, pp. 710–718, Dec. 2008, doi: 10.1016/j.ctrv.2008.05.004.
- [178] D. M. Gershenson, J. J. Kavanagh, L. J. Copeland, C. L. Edwards, R. S. Freedman, and J. T. Wharton, “High-dose doxorubicin infusion therapy for disseminated mixed mesodermal sarcoma of the uterus,” *Cancer*, vol. 59, no. 7, pp. 1264–1267, 1987, doi: 10.1002/1097-0142(19870401)59:7<1264::AID-CNCR2820590706>3.0.CO;2-O.
- [179] Z. Peng, C. Wang, E. Fang, X. Lu, G. Wang, and Q. Tong, “Co-delivery of doxorubicin and SATB1 shRNA by Thermosensitive Magnetic Cationic Liposomes for Gastric Cancer Therapy,” *PLoS One*, vol. 9, no. 3, Mar. 2014, doi: 10.1371/journal.pone.0092924.
- [180] H. Shi, L. Li, L. Zhang, T. Wang, C. Wang, D. Zhu, and Z. Su, “Designed preparation of polyacrylic acid/calcium carbonate nanoparticles with high doxorubicin payload for liver cancer chemotherapy,” *CrystEngComm*, vol. 17, no. 26, pp. 4768–4773, Jul. 2015, doi: 10.1039/c5ce00708a.
- [181] B. Yilmaz and F. Yilmaz, “Lab-on-a-Chip technology and its applications,” in *Omics Technologies and Bio-engineering: Towards Improving Quality of Life*, vol. 1, Elsevier Inc., 2018, pp. 145–153.
- [182] G. V. Kaigala, M. Behnam, A. C. E. Bidulock, C. Bargen, R. W. Johnstone, D. G. Elliott, and C. J. Backhouse, “A scalable and modular lab-on-a-chip genetic analysis instrument,” *Analyst*, vol. 135, no. 7, pp. 1606–1617, Jun. 2010, doi: 10.1039/b925111a.
- [183] M. Khan and J.-M. Lin, “Microfluidics for Single-Cell Genomics,” in *Microfluidics*

- for Single-cell Analysis*, 2019, pp. 143–161.
- [184] J. Wang, A. Ibáñez, and M. P. Chatrathi, “On-chip integration of enzyme and immunoassays: Simultaneous measurements of insulin and glucose,” *J. Am. Chem. Soc.*, vol. 125, no. 28, pp. 8444–8445, Jul. 2003, doi: 10.1021/ja036067e.
- [185] D. Huh, W. Gu, Y. Kamotani, J. B. Grotberg, and S. Takayama, “Microfluidics for flow cytometric analysis of cells and particles,” *Physiological Measurement*, vol. 26, no. 3. IOP Publishing, p. R73, Jun. 01, 2005, doi: 10.1088/0967-3334/26/3/R02.
- [186] J. Wang, “From DNA biosensors to gene chips,” *Nucleic Acids Res.*, vol. 28, no. 16, pp. 3011–3016, Aug. 2000, doi: 10.1093/nar/28.16.3011.
- [187] L. Kang, B. G. Chung, R. Langer, and A. Khademhosseini, “Microfluidics for drug discovery and development: From target selection to product lifecycle management,” *Drug Discovery Today*, vol. 13, no. 1–2. Elsevier Current Trends, pp. 1–13, Jan. 01, 2008, doi: 10.1016/j.drudis.2007.10.003.
- [188] L. Seriola, “Centrifugal microfluidics for cell-based assays in flow,” DTU, Technical University of Denmark, 2020.
- [189] J. Ducrée, “Centrifugal Microfluidics,” in *Encyclopedia of Microfluidics and Nanofluidics*, Boston, MA: Springer US, 2008, pp. 234–245.
- [190] S. Smith, K. Land, M. Madou, and H. Kido, “Rapid, low-cost prototyping of centrifugal microfluidic devices for effective implementation of various microfluidic components,” *South African J. Ind. Eng.*, vol. 26, no. 1, pp. 179–190, May 2015, doi: 10.7166/26-1-944.
- [191] O. Strohmeier, M. Keller, F. Schwemmer, S. Zehnle, D. Mark, F. Von Stetten, R. Zengerle, and N. Paust, “Centrifugal microfluidic platforms: advanced unit

- operations and applications,” *Chem. Soc. Rev.*, vol. 44, no. 17, pp. 6187–6229, Sep. 2015, doi: 10.1039/c4cs00371c.
- [192] S. Burger, M. Schulz, F. Von Stetten, R. Zengerle, and N. Paust, “Rigorous buoyancy driven bubble mixing for centrifugal microfluidics,” *Lab Chip*, vol. 16, no. 2, pp. 261–268, Jan. 2016, doi: 10.1039/c5lc01280e.
- [193] I. J. Michael, T. H. Kim, V. Sunkara, and Y. K. Cho, “Challenges and opportunities of centrifugal microfluidics for extreme point-of-care testing,” *Micromachines*, vol. 7, no. 2. MDPI AG, 2016, doi: 10.3390/mi7020032.
- [194] B. S. Lee, J.-N. Lee, J.-M. Park, J.-G. Lee, S. Kim, Y.-K. Cho, and C. Ko, “A fully automated immunoassay from whole blood on a disc †,” doi: 10.1039/b820321k.
- [195] D. King and J. Ducrée, “Optical Detection on Centrifugal Microfluidic Lab-on-a-Disc Platforms,” in *Encyclopedia of Microfluidics and Nanofluidics*, Springer New York, 2015, pp. 2535–2542.
- [196] C. E. Nwankire, G. G. Donohoe, X. Zhang, J. Siegrist *et al.*, “At-line bioprocess monitoring by immunoassay with rotationally controlled serial siphoning and integrated supercritical angle fluorescence optics,” *Anal. Chim. Acta*, vol. 781, pp. 54–62, Jun. 2013, doi: 10.1016/j.aca.2013.04.016.
- [197] Z. Ding, D. Zhang, G. Wang, M. Tang, Y. Dong, Y. Zhang, H.-P. Ho, and X. Zhang, “From chip-in-a-lab to lab-on-a-chip: towards a single handheld electronic system for multiple application-specific lab-on-a-chip (ASLOC),” vol. 16, p. 3604, 2014, doi: 10.1039/c6lc00542j.
- [198] O. Durucan, “Detection of bacterial metabolites through dynamic acquisition from surface enhanced raman spectroscopy substrates integrated in a centrifugal microfluidic platform,” *19th Int. Conf. Miniaturized Syst. Chem. Life Sci.*

Microtas 2015, 2015.

- [199] R. Burger, D. Kirby, M. Glynn, C. Nwankire, M. O’Sullivan, J. Siegrist, D. Kinahan, G. Aguirre, G. Kijanka, R. A. Gorkin, and J. Ducreé, “Centrifugal microfluidics for cell analysis,” *Current Opinion in Chemical Biology*, vol. 16, no. 3–4. Elsevier Current Trends, pp. 409–414, Aug. 01, 2012, doi: 10.1016/j.cbpa.2012.06.002.
- [200] S. Haeberle, T. Brenner, R. Zengerle, and J. Ducreé, “Centrifugal extraction of plasma from whole blood on a rotating disk,” 2006, doi: 10.1039/b604145k.
- [201] S. W. Lee, J. Y. Kang, I. H. Lee, S. S. Ryu, S. M. Kwak, K. S. Shin, C. Kim, H. Il Jung, and T. S. Kim, “Single-cell assay on CD-like lab chip using centrifugal massive single-cell trap,” *Sensors Actuators, A Phys.*, vol. 143, no. 1, pp. 64–69, May 2008, doi: 10.1016/j.sna.2007.06.043.
- [202] M. Madou, J. Zoval, G. Jia, H. Kido, J. Kim, and N. Kim, “Lab on a CD,” *Annual Review of Biomedical Engineering*, vol. 8. Annual Reviews, pp. 601–628, Jul. 11, 2006, doi: 10.1146/annurev.bioeng.8.061505.095758.
- [203] H. Becker and C. Gärtner, “Polymer microfabrication technologies for microfluidic systems,” doi: 10.1007/s00216-007-1692-2.
- [204] R. O. Rodrigues, R. Lima, H. T. Gomes, and A. M. T. Silva, “Polymer microfluidic devices: an overview of fabrication methods,” *U.Porto J. Eng.*, vol. 1, no. 1, pp. 67–79, Sep. 2017, doi: 10.24840/2183-6493_001.001_0007.
- [205] L. Seriola, T. Z. Laksafoss, J. A. J. Haagenzen, C. Sternberg, M. P. Soerensen, S. Molin, K. Zór, and A. Boisen, “Bacterial Cell Cultures in a Lab-on-a-Disc: A Simple and Versatile Tool for Quantification of Antibiotic Treatment Efficacy,” *Anal. Chem.*, vol. 92, no. 20, pp. 13871–13879, Oct. 2020, doi: 10.1021/acs.analchem.0c02582.

- [206] S. E. Birk ‡, L. Seriola ‡, V. Cavallo, J. A. J. Haagensen, S. Molin, L. H. Nielsen, K. Zor, and A. Boisen, “Enhanced Eradication of Mucin-embedded Bacterial Biofilm by Locally Delivered Antibiotics in Functionalized Microcontainers,” *Manuscr. Submitt. to J. Control. Release*, 2020.
- [207] H. Klank, J. P. Kutter, and O. Geschke, “CO₂-laser micromachining and back-end processing for rapid production of PMMA-based microfluidic systems,” 2002, doi: 10.1039/b206409j.
- [208] O. E. Dahl, L. J. Garvik, and T. Lyberg, “Toxic effects of methacrylate monomer on leukocytes and endothelial cells in vitro,” *Acta Orthop.*, vol. 65, no. 2, pp. 147–153, 1994, doi: 10.3109/17453679408995423.
- [209] D. J. Guckenberger, T. E. De Groot, A. M. D. Wan, D. J. Beebe, and E. W. K. Young, “Micromilling: A method for ultra-rapid prototyping of plastic microfluidic devices,” *Lab Chip*, vol. 15, no. 11, pp. 2364–2378, Jun. 2015, doi: 10.1039/c5lc00234f.
- [210] G. S. Fiorini and D. T. Chiu, “Disposable microfluidic devices: Fabrication, function, and application,” *BioTechniques*, vol. 38, no. 3. Eaton Publishing Company, pp. 429–446, May 30, 2005, doi: 10.2144/05383RV02.
- [211] L. Gruzinskyte ‡, L. Seriola ‡, G. Zappalá, T. Z. Laksafoss, E. Te Hwu, K. Zór, and A. Boisen, “Mammalian cell culture on lab-on-a-disc with integrated microscope for real-time optical monitoring,” *Manuscr. Prep.*, 2020.
- [212] S. T. Rajendran, E. Scarano, M. H. Bergkamp, A. M. Capria, C. H. Cheng, K. Sanger, G. Ferrari, L. H. Nielsen, E. Te Hwu, K. Zór, and A. Boisen, “Modular, Lightweight, Wireless Potentiostat-on-a-Disc for Electrochemical Detection in Centrifugal Microfluidics,” *Anal. Chem.*, vol. 91, no. 18, pp. 11620–11628, Sep. 2019, doi: 10.1021/acs.analchem.9b02026.

- [213] M. K. Kim, F. Ingremeau, A. Zhao, B. L. Bassler, and H. A. Stone, “Local and global consequences of flow on bacterial quorum sensing,” *Nat. Microbiol.*, vol. 1, no. 1, pp. 1–5, Jan. 2016, doi: 10.1038/nmicrobiol.2015.5.
- [214] G. Kretzmer and K. Schiigerl, “Response of mammalian cells to shear stress,” 1991.
- [215] A. Park, H. H. Jeong, J. Lee, K. P. Kim, and C. S. Lee, “Effect of shear stress on the formation of bacterial biofilm in a microfluidic channel,” *Biochip J.*, vol. 5, no. 3, pp. 236–241, Sep. 2011, doi: 10.1007/s13206-011-5307-9.
- [216] K. Zór, A. Heiskanen, C. Caviglia, M. Vergani *et al.*, “A compact multifunctional microfluidic platform for exploring cellular dynamics in real-time using electrochemical detection,” *RSC Adv.*, vol. 4, no. 109, pp. 63761–63771, Nov. 2014, doi: 10.1039/c4ra12632g.
- [217] H. J. Kim, D. Huh, G. Hamilton, and D. E. Ingber, “Human gut-on-a-chip inhabited by microbial flora that experiences intestinal peristalsis-like motions and flow{,” doi: 10.1039/c2lc40074j.
- [218] V. dos Santos, R. N. Brandalise, and M. Savaris, *Biomaterials Sterilization Methods*. 2017, pp. 61–73.
- [219] S. Dinicola, S. De Grazia, G. Carlomagno, and J. P. Pintucci, “N-acetylcysteine as powerful molecule to destroy bacterial biofilms. A systematic review,” *Eur. Rev. Med. Pharmacol. Sci.*, vol. 18, no. 19, 2014.
- [220] C. J. R. Sheppard and S. Rehman, “Confocal Microscopy,” doi: 10.1007/978-3-642-28391-8.
- [221] D. A. Boas, C. Pitris, and N. Ramanujam, *Handbook of biomedical optics*. CRC Press, 2016.

- [222] J. R. Lawrence,¹, D. R. Korber, B. D. Hoyle, J. W. Costerton, and A. D. E. Caldwell², “Optical Sectioning of Microbial Biofilms.” Accessed: Nov. 28, 2020. [Online]. Available: <http://jb.asm.org/>.
- [223] A. Bridier, F. Dubois-Brissonnet, A. Boubetra, V. Thomas, and R. Briandet, “The biofilm architecture of sixty opportunistic pathogens deciphered using a high throughput CLSM method,” *J. Microbiol. Methods*, vol. 82, no. 1, pp. 64–70, Jul. 2010, doi: 10.1016/j.mimet.2010.04.006.
- [224] A. Heydorn, “Quantification of biofilm structures by the novel computer program COMSTAT,” *Microbiology-uk*, vol. 146, 2000.
- [225] M. Vorregaard, “Comstat2-a modern 3D image analysis environment for biofilms.” Accessed: Nov. 28, 2020. [Online]. Available: www.imm.dtu.dk.